

5-8 September 2022

Book of Abstracts



Table of contents

.....	1
New possibilities at the high pressure diffraction beamline from the Elettra Synchrotron Facility	6
Neutron total scattering measurements under hydrostatic pressure	7
Dynamic compression of (Mg _x Fe _{1-x})O to Megabar pressures	8
New capabilities for high-pressure experiments at the Large Volume Press end-station P61B.....	9
Recent progress in neutron diffraction studies for ice VII	10
Chemical diversity in simple systems under compression.....	11
Chemical Pressure and Physical Pressure: beyond atomic radii	12
Scale-Free Phase-Field Modeling of Multivariant Martensitic Phase Transformation in Single and Polycrystalline Zirconium and Silicon under Non-hydrostatic Loading.....	13
Potential energy barrier for proton transfer in compressed benzoic acid	14
Effect of a Micro-scale Dislocation Pileup on the Atomic-Scale Multi-variant Phase Transformation and Twinning	15
Potassium from first principles: A case study	16
Insights into the high-pressure behaviour of solid bromine from hybrid DFT calculations.....	17
The Structural Phase Transitions in β , Rutile & Fluorite Crystals of NbO ₂	18
Tensorial stress-plastic strain fields in α - ω Zr mixture, revised phase transformation kinetics, and friction under compression in diamond anvil cell: Coupled Experimental-Analytical-Numerical Approach	20
Random structure generator with fixed environment.....	22
PdH ₂ nanotube: A potential design	23
High-pressure elastic, vibrational and structural study of monazite-type EuPO ₄ from ab initio simulations.	24
Ab Initio study of Ca ₃ Y ₂ Ge ₃ O ₁₂ garnet. Dynamical, elastic properties and mechanical stability under pressure.....	25
Pressure-induced phase transition of fluorine.....	26
Tailored Adamantane derivatives as precursors to Nanodiamonds in mild Pressure and Temperature conditions.....	26
High temperature superconductivity in superhydrides	28
Pressure-enhanced superconductivity in some of the cage-type quasiskuttrudite single crystals	28
New High T _c Superconductors Achieved via High Pressures	30
Search for guidelines for synthesizing low hydrogen affinity alloy hydrides	30
Engineering better superconductors: two-electron models of superconductivity in real space.....	32
Clean-limit superconductivity at 197 K in high-pressure sulfur hydride synthesised using ammonia borane	33
Superconducting properties of AuAgTe ₄ under pressure.....	33
Emergent Magnetic, Electronic and Structural Phases in Pressure-Tuned van der Waals Systems.....	35

Superionicity of H in LaH ₁₀ superhydride.....	35
Metallic Transition in Rhenium Dichalcogenides	36
Structures and Transport Properties of TiZr Alloys with Hydrogen under High Pressure	38
High pressure neutron study on magnetic phases in a Y-type hexaferrite.....	38
Raman study of pure TeO ₂ glass under pressure: interplay between glass network transformations and electronic transitions.....	39
Pressure-induced electronic phase transitions in honeycomb-based transition-metal compounds ..	40
Pressure-driven switching of magnetism in layered CrCl ₃	42
Combined X-ray Raman Scattering Spectroscopy and X-Ray Diffraction on Shock-Compressed Vitreous SiO ₂	42
Influence of PRESSURE and thickness ON SUPERConductivity in high entropy alloys thin films	43
Revealing the mechanisms of the pressure-induced insulator-metal transition in distorted TiNiO ₃ perovskites	44
New type of uniaxial non-magnetic pressure cell	45
Computational Prediction of Planetary Composition from Mass/Radius Data	46
Optimised Spectrum Fitting using Likelihood and Bayes Factor: Carbon Nanotubes under Pressure ..	46
Structural behavior of Copper(I) halide luminescence compounds under High Pressure	48
Elastic properties of dipropylene glycol glasses with different thermobaric histories	48
Structural transformations in Type II Multiferroic and Probable Topological Nontrivial Insulator MnSb ₂ Se ₄ under High Pressure.....	50
Compressibility of chemical compounds.....	51
Universal Hydrogen Bond Symmetrisation Dynamics under extreme Conditions.....	52
Stability of the tetragonal phase of BaZrO ₃ under high pressure	54
High-pressure and high-temperature chemistry of phosphorus and nitrogen: synthesis and characterization of α - and γ -P ₃ N ₅	54
Acoustic wave velocities in Mars' mantle minerals.	56
High-pressure tuning of $d-d$ electronic transitions and bandgap in cobalt iodate, Co(IO ₃) ₂	56
High-pressure polymerisation of CS ₂ : “Bridgman’s black” revisited	57
Melting curve of indium at high pressure measured by picosecond acoustics	58
Formation and stability of dense methane-hydrogen compounds.....	60
Synthesis of van der Waals Ga ₂ S ₃ structures under high pressure.....	61
Elasticity and the post-stishovite transition of eclogitic stishovite: Insights from in-situ XRD and ultrasonic interferometry.....	63
VIPA-based Brillouin spectroscopy: a new tool for exploring the thermodynamics of warm dense molecular system	64
High-pressure behavior of monoclinic (Eu _{1-x} Yb _x) ₂ O ₃ solid solution.....	65
Correlation between spectroscopic and mechanical properties of gold nanocrystals under pressure	66
High Pressure Topological transition of 1T-TiSe ₂	68

Pressure-induced transitions in the [Ru ₂ Cl(Dp-AniF) ₄] molecular unit	69
Moderate Pressure Pasteurisation at Room Temperature on endogenous and inoculated microorganisms of fish soup as a novel nonthermal food pasteurisation methodology	70
Germination and inactivation of <i>Byssochlamys nivea</i> ascospores under hyperbaric storage - dependence on thermal and nonthermal pre-activation steps.....	71
Unravelling the mechanisms of adaptation to high pressure in proteins.....	73
Multi-technical methodological approaches for the study of liquids under extreme conditions of pressure and temperature	74
Room-Temperature Superionic Conduction in Complex Transition Metal Hydrides with High Hydrogen Coordination.....	75
High-pressure synthesis of aluminum-iron alloy hydride	76
The rich structural landscape induced by pressure in multifunctional FeVO ₄	78
Interplay between proton dynamics and Fe valence fluctuation in Fe ₃ (PO ₄) ₂ (OH) ₂	79
General relationship between the bandgap energy and iodine-oxygen bond distance in metal iodates	80
Pressure induced emission enhancement and bandgap narrowing: experimental investigations and first principles theoretical simulations on the model halide perovskite Cs ₃ Sb ₂ Br ₉	82
Pressure driven Phase Transition in NdNiO ₃ Nanostructures	83
Preparation of Confined, Low-Dimensional Boron Nitride in the 1-D Pores of Siliceous Zeolites under High Pressure, High Temperature Conditions.....	85
Resolving puzzles of the deep-focus earthquake mechanism based on plastic strain-induced olivine-spinel transformation and transformation-induced plasticity.....	86
Accurate Crystal Structure of Ice VI from X-Ray Diffraction with HAR.....	87
Rough diamond anvil: Critical microstructure, pressure-dependent yield surface of perfect plasticity, record low pressure for strain-induced α - ω transformation in Zr, and combined strain and time-controlled kinetics	89
The behavior of simple molecule of bromine under high pressure high temperature conditions.....	90
Strain-Induced Phase Transformations under High Pressure: Four-Scale Theory, Experiments, and Phenomena	91
An exploratory study of polymeric matter under high pressure.....	92
Experimental and theoretical study of β -As ₂ Te ₃ under hydrostatic pressure	93
Kinetics of plastic strain induced $\alpha \rightarrow \omega$ phase transition in Zr _{2.5} Nb alloy.....	95
Record Low Transformation Pressure and New Phase Transformation Sequence in Nano-Si under Plastic Compression	96
Far Infrared Study of Pressure-Tunable Fano Resonance and Metallization Transition in semiconducting Transition Metal Dichalcogenides	97
Understanding the behaviour of spin crossover materials for barocaloric applications: (P,T) phase diagrams	99
Boron and Nitrogen Dopants Enhanced Stability of Diamane Induced by High Pressure	100
High pressure Raman study of ternary tin dichalcogenides, Sn _x Se _{2-x}	101

Structural and electronic phase transitions in $Zr_{1.03}Se_2$ at high pressure.....	102
Evidence of Si-II to Si-I reversible phase transformation and retaining of Si-II under ambient pressure after plastic shear under pressure	104
Microstructural evolution across $\alpha \rightarrow \omega$ phase transition in Zr under hydrostatic compression	105

New possibilities at the high pressure diffraction beamline from the Elettra Synchrotron Facility

F.G. Alabarse^{a*}, K.A. Irshad^b, V. Chenda^a, G. Bais^a, G. Skerlj^a, H.K. Poswal^c, I. Cudin^a, R. Borghes^a, M. Polentarutti^a, A. Lausi^{a,d}, D.D. Sarma^e, B. Joseph^a

a. Elettra Sincrotrone Trieste, Italy

b. Gd R IISc-ICTP, Elettra Sincrotrone Trieste, Italy

c. High Press. & Synchr. Rad. Phys. Div., Bhabha atomic research Center, Trombay, India

d. Synchrotron-light for Experimental Science and Applications in the Middle East, Allan, Jordan

e. Solid State and Structural Chemistry Unit, Indian Institute of Science, Bengaluru, India

*e-mail: frederico.alabarse@elettra.eu



Figure 1. He-cryostat and PILATUS3 S 6M detector.

in house developed: 1) a cryogenic loader to permit the loading of a variety of gas media, such as Ar, N₂, O₂, CH₄, CO₂, etc.; and 2) a second vacuum chamber to be used for HP-high *T*

The Indo-Italian high pressure (HP) diffraction beamline, Xpress, at Elettra Sincrotrone Trieste, is increasing its' operational performances by adding new instruments. The beamline utilizes the synchrotron radiation from a superconducting wiggler to produce a 25 keV monochromatic X-ray beam focused on a large area detector for data acquisition in angle dispersive mode. This configuration allows powder and single crystal (SC) diffraction experiments to be performed under HP conditions by using diamond anvil cells (DAC), comprising an online ruby fluorescence spectrometer. The beamline station is equipped with state of the art facilities for HP manipulation: microscope, microdriller, automatic pneumatic pressure controller, etc. The partner institute, IISc Bengaluru, very recently added three new dedicated HP setups compatible to DAC: (i) a very recently commissioned low temperature (*T*) He-cryostat, reaching down to 10 K (Almax easyLab/JANIS), see Fig. 1; (ii) still *on commissioning*: a high *T* vacuum chamber, making use of internal and external heater, reaching up to 1000 K (LOTO-eng); and (iii) a very recently commissioned micro Raman spectrometer (Renishaw, class 4). On the top of this, the beamline team, in collaboration with the Elettra's Research Engineers (RE) group, had *in*

experiments by using an external ring heater (1000 K). The later vessel is on the final assembling stages and compatible for *in situ* synchrotron XRD measurements. Still on new loading possibilities, a commercial gas loading system (Sanchez) is in advanced stages of commissioning, which will permit DAC to be loaded with gases such as He, Ne, *etc.* Beamline data collection and control graphical user interface is being continuously improved by the Elettra's Information Technology group to handle well all these new developments even on *remote mode*. Elettra is currently undertaking an upgrade program, *Elettra 2.0*, to reach an even brighter and coherent synchrotron radiation source. Under this project, Xpress beamline very recently received a new large area detector, DECTRIS PILATUS3 S 6M (see Fig. 1). Which key advances are: direct detection of X-rays; single-photon counting; excellent signal-to-noise ratio and very high dynamic range; short readout time and high frame rates; shutterless operation; modular detectors enabling multi-module detectors with large active area. As a consequence, not only reducing significantly the HP diffraction data collection time, but also increasing the *Q*-range spectra and data quality if compared to the previous detector (MAR345). Xpress developments are *in progress*, perspectives for a near future are powder and SC diffraction under HP (up to megabar pressures) together with variable temperatures from few to several hundred Kelvins. Proposal submission deadline are typically on mid-March and -September. We will present recent scientific highlights from the beamline performed under HP.

Neutron total scattering measurements under hydrostatic pressure

Nicholas Funnell

Total scattering measurements have proved invaluable for in-situ studies on numerous materials, providing structural information over short-range length scales. Though it is now common to explore crystalline samples as, e.g., a function of temperature/flow gas/chemical composition/electric current, it remains challenging to perform local structure studies under pressure. Amorphous substances comprise the majority of total scattering studies under pressure¹ because crystalline materials necessitate the inclusion of a pressure transmitting medium (PTM) in order to avoid sample strain. The PTM has its own local structure scattering signature, and untangling its contribution from that of the sample is non-trivial. This is particularly severe for neutron measurements, where common PTM materials are deuterated, making them significantly more powerful scatterers than their hydrogenous counterparts in X-ray experiments.

This talk describes some of the recent efforts on the PEARL instrument at the ISIS Neutron and Muon Facility toward developing approaches for obtaining pair distribution function data from samples under *hydrostatic* pressure, as well as some early science studies.²⁻⁴

References

1. P. S. Salmon, J. W. E. Drewitt, D. A. J. Whittaker, A. Zeidler, K. Wezka, C. L. Bull, M. G. Tucker, M. C. Wilding, M. Guthrie and D. Marrocchelli, *J. Phys.: Condens. Matter*, (2012), **24**, 415102
2. A. Herlihy, H. S. Geddes, G. C. Sosso, C. L. Bull, C. J. Ridley, A. L. Goodwin, M. S. Senn and N. P. Funnell, *J. Appl. Crystallogr.*, (2021), **54**, 1546–1554
3. A. Herlihy, T. A. Bird, C. J. Ridley, C. L. Bull, N. P. Funnell and M. S. Senn, *Phys. Rev. B*, (2022), **105**, 094114
4. N. P. Funnell, C. L. Bull, S. Hull and C. J. Ridley, *J. Phys.: Condens. Matter*, (2022), **34**, 325401

Dynamic compression of (Mg_xFe_{1-x})O to Megabar pressures

K. Buakor¹, J. Pintor², E. Cunningham³, T. Duffy⁴, A. Gleason³, D. Kim⁴, D. Khaghani³, Z. Konopkova¹, H. J. Lee³, I. Ocampo⁴, C. Plueckthun⁵, M. Schoelmerich⁶, R. Smith⁶, S. Speziale⁷, S. Tracy⁸, H. E. Tsai³, T. Tschentscher¹, M. Harmand² and K. Appel¹

MgO and FeO form a continuous solid solution in a wide range of pressure and temperature conditions. Ferropicriase ((Mg_xFe_{1-x})O, X > 0.5) is the second most abundant mineral of the Earth's lower mantle. It comprises 16-20% of the total mass of this region [1][2], and is considered to be a major component of all rocky planets. Thus, studying the phase diagram of the MgO-FeO system at in-situ conditions may provide unique input to planetary modeling. The phase stability and the structural phase transitions of both end member FeO and the intermediate (Mg,Fe)O solid solutions are currently subject of intense research [3]. The melting curve of FeO has been investigated and determined up to 350 GPa [4][5]. However, the melting processes and structure of liquid FeO at in-situ conditions are still unknown as well as the high-pressure melting behavior across the whole solid solution series.

This study focuses on phase transitions and the melting line of (Mg_xFe_{1-x})O solid solutions along their Hugoniot. We experimentally investigated the effects of Fe-Mg substitution on the phase stability and phase transitions of (Mg,Fe)O solid solutions by measuring X-ray diffraction under shock compression at the Matter in Extreme Conditions instrument of the Linac Coherent Light Source, USA. Samples were either physical vapor deposited FeO or (Mg_{0.4},Fe_{0.6})O single-crystals or (Mg_xFe_{1-x})O slurry powders with X= 1 - 0. Up to 45 J of the long pulse laser available at MEC were used to shock compress the material to up to 140 GPa. The compressed targets were probed with a 13 keV and 17 keV FEL X-ray beam at delay times between -2.4 ns to 350 ns with respect to shock break out spanning shock and release thermodynamic conditions. While no phase transitions could be observed in the

subsolidus, melting of the B1 phase was observed for $(\text{Mg}_x\text{Fe}_{1-x})\text{O}$ in the range of $X= 0.9 - 0.2$. Preliminary analysis will be presented and already provides new insights into the melting conditions in the MgO-FeO system at planetary interior conditions.

[1] T. Irifune, “Absence of an aluminous phase in the upper part of the Earth’s lower mantle” *Nature*, 370, 131-133, (1994)

[2] F.V. Kaminsky, “General physical and chemical models of the Earth’s lower mantle in *The Earth’s lower mantle composition and structure*” in Springer Geology, ch. 2, pp. 5-22 (2017)

[3] F. Coppari, R.F. Smith et al., “Implications of the iron oxide phase transition on the interiors of rocky exoplanets” *Nat. Geosci.*, 14, 121–126 (2021).

[4] R.A. Fischer and A.J. Campbell, “High-pressure melting of wüstite” *Am. Mineral.*, 95, 1473-1477, (2010)

[5] T. Komabayashi, “Thermodynamics of melting relations in the system Fe-FeO at high pressure: Implications for oxygen in the Earth’s core” *J. Geophys. Res. Solid Earth*, 119, 4164–4177, (2014)

Acknowledgments: This work is embedded in the DFG-funded German research unit Matter Under Planetary Interior Conditions hosted at University of Rostock (FOR2440). Sample preparation was performed at DESY, Hamburg, Germany. We acknowledge LCLS for provision of beamtime under proposal LX64 and European XFEL for supporting and hosting the project.

New capabilities for high-pressure experiments at the Large Volume Press end-station P61B

Robert Farla¹, Shrikant Bhat¹, Adrien Neri², Shuailing Ma³, Artem Chanyshv², Kristina Spektor^{1,4}, Christian Lathe^{1,5}, Stefan Sonntag¹, Tomoo Katsura²

¹Deutsches Elektronen-Synchrotron DESY, Hamburg, Germany

²Bayerisches Geoinstitut, University of Bayreuth, Germany

³Institute of High Pressure Physics, School of Physical Scientific and Technology, Ningbo University, Ningbo, China

⁴University of Leipzig, Leipzig, Germany

⁵Deutsches GeoForschungsZentrum Potsdam, Potsdam, Germany

At the end-station P61B of the high-energy wiggler beamline at PETRA III, a Large Volume Press (LVP) ‘Aster-15’ is installed and operational for user experiments at high pressures and temperatures (HPT: 30 GPa, 2300 K) to solve big questions in Earth / Materials sciences and High-P Chemistry. The standard setup features 2 Ge-detectors for energy-dispersive X-ray diffraction (ED XRD) at 30 – 160 keV, and a white-beam microscope for radiography. A dedicated glovebox is available to prepare assemblies in a controlled atmosphere for sensitive materials, such as nitrides and hydrides. Using various anvil-cell assemblies, mm-sized polycrystalline samples can be investigated in the LVP to document phase relations *in*

situ, as well as physical properties such as viscosity. Recently, two additional techniques have been commissioned for the LVP: ultrasonic interferometry (wave speed measurements) and acoustic emissions (AE) detection. The first method features a LiNbO₃ piezo-sensor that transmits pulses and receives echoes at specific ultrasonic sine-wave frequencies (10-60 MHz) to measure the two-way travel time in the sample at HPT. Combined with length measurements of the sample by X-ray radiography, the wave speeds are calculated and compared to seismic wave propagation in the Earth's interior. The second newly available method at HPT and stress conditions uses specialized AE sensors (0.1 – 4 MHz broadband) on 6 anvils to detect and localize events in the sample prone to brittle behavior caused by processes such as dehydration reactions or phase/volume changes. For example, AE detection can be combined with X-ray diffraction and imaging to monitor the sample stress and strain rate history *in situ* during controlled rock deformation. Examples will be shown demonstrating the world-leading capabilities of the P61B LVP station.

Recent progress in neutron diffraction studies for ice VII

Kazuki Komatsu*

Geochemical Research Center, Graduate School of Science, The University of Tokyo, Hongo 7-3-1, Bunkyo-ku, 113-0033 Tokyo, Japan

*kom@eqchem.s.u-tokyo.ac.jp

Ice has a tremendous number of polymorphs, currently at least 20 known. But, most ice polymorphs are found below 2 GPa, and this structural diversity apparently diminished above 2 GPa; basically only two types of structure, body-centred-(pseudo)cubic ices VII, VIII, X and face-centred-cubic ice XVIII. Although these crystal structures appear to be simple, there are many unresolved questions. For instance, it is known that at around 10-15 GPa, various experimental results such as the peak width of Raman spectra and x-ray diffraction, the diffusion coefficient of hydrogen, the x-ray induced dissociation of water molecules etc. show a different trend at lower and higher pressures. These anomalies can be explained by a crossover of two kinds of dynamics, water molecule rotation and hydrogen translation. The dynamics crossover scenario is quantitatively investigated by our neutron study [1] and more directly proven by our dielectric measurement [2]. The most recent single crystal and powder neutron diffraction study reveals detailed atomic distribution in ice VII, which would relate to two kinds of dynamics [3]. Another remained question for ice VII is its phase transition to ice X involving the hydrogen bond (H-bond) symmetrisation. It has been believed that the H-bond symmetrisation would occur at around 60 GPa for H₂O and 70 GPa for D₂O, as suggested by spectroscopic studies a quarter century ago. However, the transition pressure suggested from various experiments has large uncertainties from 40 GPa to above 120 GPa [e.g., 4 and refs therein]. Recently, we developed a nano-polycrystalline

diamond anvil cell (NPDAC) for neutron diffraction experiments exceeding 80 GPa [5,6]. Although detailed structure analyses have still some difficulty due to the contamination of peaks from anvils, the data quality has been significantly improved owing to new devices such as radical collimators.

In this presentation, I will focus on the above two topics for ice VII, 1) anomalies at 10-15 GPa and 2) H-bond symmetrisation with recent technical developments for high-*P* neutron diffraction.

[1] Komatsu K, Klotz S, Machida S, Sano-Furukawa A, Hattori T, Kagi H. *Proc Nat Acad Sci.* 2020;117:6356-61.

[2] Yamane R, Komatsu K, Kagi H. *Phys Rev B.* 2021;104:214304.

[3] Yamashita K. *et al.* in review.

[4] Grande ZM, Pham CH, Smith D, Boisvert JH, Huang C, Smith JS, Goldman N, Belof JL. *Phys Rev B.* 2022;105:104109.

[5] Komatsu K, Klotz S, Nakano S, Machida S, Hattori T, Sano-Furukawa A, Yamashita K, Irifune T. *High Press Res.* 2020;40:184-93.

[6] Komatsu K. *et al.* in preparation.

Chemical diversity in simple systems under compression

Alberto Otero de la Roza

MALTA Consolider Team, Departamento de Química Física y Analítica, Facultad de Química, Universidad de Oviedo, E-33006 Oviedo, Spain;

The application of pressure often causes exotic and unusual phenomena in very simple materials that are alien to our chemical understanding. Computational modeling and bonding analysis methods are an excellent tool to explore these phenomena, although care must be exercised regarding the approximations involved in the method employed and how compression affects the interpretation of bonding indices. This talk focuses on two simple solids that showcase exotic bonding scenarios which are challenging for density functional theory methods: gold sulfide (Au₂S) and silver sulfide (Ag₂S). In Ag₂S, metallophilic interactions between adjacent Ag centers make dispersion effects essential in order to correctly predict its equation of state. The thermodynamic properties of this material are unusual as a consequence of the prevalence of these interactions. In Au₂S, density functional approximations fail at predicting the zero-pressure volumen and bulk modulus and the same time, and this is related to the exotic bonding pattern in this material: The similar electronegativity of gold and sulfur causes a case of strong correlation error in an otherwise simple solid. Novel algorithms and methods for the application of Bader's quantum theory of atoms in molecules, implemented in the open source critic2 program, are

presented and applied to these materials, and the effect of compression on some chemical bonding indices commonly used at ambient conditions are discussed.

Chemical Pressure and Physical Pressure: beyond atomic radii

Álvaro Lobato,¹ Eduardo O. Gomes², Amanda F. Gouveia³, Lourdes Gracia³,
Juan Andrés³ and J. Manuel Recio²

¹MALTA-Consolider Team, Dpto. de Química Física, Facultad de Ciencias Químicas, Universidad Complutense,
28040 Madrid, Spain, a.lobato@ucm.es

² MALTA-Consolider Team and Departamento de Química Física y Analítica, Universidad
de Oviedo, 33006 Oviedo, Spain

³ Departament de Química Física i Analítica, Universitat Jaume I, 12071, Castellón de la
Plana, Spain

Physical and chemical pressure are believed to be connected since the size mismatch produced by the chemical substitutions and compressive effects lead to similar internal strains in a material [1]. However, is this the whole story?

In this work, we outline our latest investigations in relating chemical pressure and physical pressure. We will show that replacing atoms with others of the same atomic size induce the same phase transitions as the physical pressure does, highlighting that the role usually overlooked played by the electronic structure of the guest atom is what mainly determines the equivalence between chemical and physical pressures.

To illustrate our findings, we select the $\text{SnMo}_{(1-x)}\text{W}_x\text{O}_4$ ($x=0-1$) solid solution, where Mo^{6+} and W^{6+} cations have the same ionic radii. By carefully analysing the electronic structure obtained from first principles calculations, we first show how the different response to the stereochemical activity of the Sn^{2+} cation lone pair is key to understand the $\beta \leftrightarrow \alpha$ phase transitions occurring in SnMoO_4 and SnWO_4 at positive and negative pressures, respectively. These results are then compared with the solid solutions, showing that the different electronegativity of the Mo^{6+} and W^{6+} cations alter the behaviour of the lone pair activity inducing also a phase transition between the $\beta \leftrightarrow \alpha$ phases as physical pressure does. The equivalence between chemical and physical pressure is then rationalized in terms of the VSPER and the revised classical lone pair model of Walsh et al. [2,3], allowing us to establish a correlation between physical (p in GPa) and chemical (x in molar fraction) pressure.

Overall, our study defines a versatile chemical approach in which the types of interactions along the formation of solid solutions are clearly differentiated for tuning their properties, providing opportunities in the synthesis and development of new materials.

[1] K. Lin et al, *Chem. Soc. Rev.* 2022, 51, 5351-5364.

[2] A. Walsh et al. *Chem. Soc. Rev.* 2011, 40, 4455–4463.

[3] P.S. Halasyamani, *Chemistry of Materials* 2004, 16, 3586–3592.

Scale-Free Phase-Field Modeling of Multivariant Martensitic Phase Transformation in Single and Polycrystalline Zirconium and Silicon under Non-hydrostatic Loading

Raghunandan Pratoori^a, Hamed Babaei^b, and Valery I. Levitas^c

Iowa State University, Ames, Iowa, USA

^a rnp@iastate.edu

^b hbabaei@iastate.edu

^c vlevitas@iastate.edu

Zirconium is a widely used material in nuclear and other industries owing to its superior mechanical properties. Zr exists in a hcp α phase at low pressure, which transforms to a simple hexagonal ω phase at high pressures. Silicon is the most widely used material for electronic applications. Si exists as cubic Si-I in ambient conditions and transforms first to tetragonal Si-II at high pressure. A scale-free phase field model for phase transformations at large strains developed in [1] is advanced and used to study martensitic phase transformations in Zr and Si under complex nonhydrostatic loadings. The model includes three symmetry related martensitic variants, which can transform to each other or directly from the austenite phase. This model allows for finite strains, lattice rotations, as well as for anisotropic and different elastic properties of phases, which depend on pressure. The gradient energy term is excluded, and the model is applicable for any scale greater than 100 nm. The model tracks finite-width interfaces between austenite phase and the mixture of martensitic variants only, without interfaces between martensitic variants. The volume fractions of martensitic variants are the internal variables rather than order parameters. Model is calibrated using available experimental data, including our own [2]. It is implemented using finite element algorithms based on deal.II for solution of 3D problems. It is applied to study forward and reverse phase transformations in Zr and Si single crystals under different loading conditions and varying strain rates. The model is also modified to include polycrystal analysis and applied to polycrystalline Zr and Si samples generated using Dream3D. The mesh size is also varied to study the microstructure evolution in detail. For most stationary interfaces, local thermodynamic equilibrium conditions (thermodynamic driving force for the interface motion equal to the effective threshold) are satisfied. In the case of Si, we demonstrate the use of a variable athermal threshold dependent on the principal components of Cauchy stress. Kinetics of evolution of volume fraction of each martensitic variant is determined under various loading paths.

1. Babaei H. and Levitas V.I. Finite-strain scale-free phase-field approach to multivariant martensitic phase transformations with stress-dependent effective thresholds. *Journal of the Mechanics and Physics of Solids*, 2020, 144, 104114.
2. Pandey K. K. and Levitas V. I. In situ quantitative study of plastic strain-induced phase transformations under high pressure: Example for ultra-pure Zr. *Acta Materialia*, 2020, 196, 338-346.

Potential energy barrier for proton transfer in compressed benzoic acid

D. Kurzydłowski¹

¹ Faculty of Mathematics and Natural Sciences Cardinal Stefan Wyszyński University, 01-938, Warsaw, Poland

Keywords: proton transfer, DFT modelling, molecular crystals

*e-mail: d.kurzydowski@uksw.edu.pl

Proton transfer (PT) reactions lie at the heart of many chemical transformations, such as acid-base reactions, catalytic processes or hydrogen transport in Earth's mantle. Studying proton dynamics not only gives insight into these transformations, but also leads to a deeper understanding of the quantum effects that are strongly manifested during the PT process. Benzoic acid (BA), with its centrosymmetric dimers bound by strong hydrogen bonds, is considered a model system for studying proton transfer processes.¹

Given that high pressure can greatly alter proton dynamics in solids,² precious experiments were conducted for solid benzoic acid up to 18 GPa.³⁻⁶ However, the challenging nature of these experiments lead to ambiguity in the interpretation of the obtained data. In particular, some studies gave conflicting values of phase transition pressures,^{5,7} while others reported no phase change in compressed BA.^{4,6}

With the aim of elucidating the problems mentioned above we present a computational study on the high-pressure behaviour of benzoic acid.⁸ We model the changes in geometry of BA crystals upon compression up to 15 GPa with the use of the recently proposed SCAN functional, which was shown to correctly reproduce the properties of liquid water, an archetypical hydrogen-bonded system.⁹

We find that pressure-induced shortening of O...O contacts within the BA dimers leads to a decrease in PT barrier, and subsequent symmetrization of the hydrogen bond. However, this effect is obtained only after taking into account zero-point energy differences between BA tautomers and the transition state. The obtained results shed light on previous experiments on compressed benzoic acid, and indicate that a common scaling behavior with respect to O...O distance might be applicable for hydrogen-bond symmetrization in both organic and inorganic systems.²

Acknowledgments: The author acknowledges the support from the Polish National Science Centre (NCN) within the OPUS grant (UMO-2016/23/B/ST4/03250). This research was carried out with the support of the Interdisciplinary Centre for Mathematical and Computational Modelling (ICM), University of Warsaw, within allocation no. GA83-26.

¹ A.J. Horsewill, *Prog. Nucl. Magn. Reson. Spectrosc.* **52**, 170 (2008).

² T. Meier, F. Trybel, S. Khandarkhaeva, D. Laniel, T. Ishii, A. Aslandukova, N. Dubrovinskaia, and L. Dubrovinsky, *Nat. Commun.* **13**, 1 (2022).

³ L. Wang, P.L. Warburton, and P.G. Mezey, *J. Phys. Chem. A* **109**, 1125 (2005).

⁴ W. Cai and A. Katrusiak, *CrystEngComm* **14**, 4420 (2012).

⁵ Y. Tao, Z.A. Dreger, and Y.M. Gupta, *Vib. Spectrosc.* **73**, 138 (2014).

⁶ L. Kang, K. Wang, X. Li, and B. Zou, *J. Phys. Chem. C* **120**, 14758 (2016).

⁷ Z.P. Wang, X.D. Tang, and Z.J. Ding, *J. Phys. Chem. Solids* **66**, 895 (2005).

⁸ D. Kurzydłowski, *RSC Adv.* **12**, 11436 (2022).

⁹ M. Chen, H.-Y. Ko, R.C. Remsing, M.F. Calegari Andrade, B. Santra, Z. Sun, A. Selloni, R. Car, M.L. Klein, J.P. Perdew, and X. Wu, *Proc. Natl. Acad. Sci.* **114**, 10846 (2017).

Effect of a Micro-scale Dislocation Pileup on the Atomic-Scale Multi-variant Phase Transformation and Twinning

Yipeng Peng,¹ Rigelesaiyin Ji,¹ Thanh Phan,¹ Laurent Capolungo,²
Valery I. Levitas,^{1,3,4,+} and Liming Xiong^{1,+}

¹ Department of Aerospace Engineering, Iowa State University, Ames, IA 50011, USA

² Materials Science and Technology Division, Los Alamos National Laboratory, Los Alamos, NM 87545, USA

³ Department of Mechanical Engineering, Iowa State University, Ames, IA 50011, USA

⁴ U.S. Department of Energy, Ames Laboratory, Ames, IA 50011, USA

Dislocations, phase transformations (PTs), and twinning are three most common carriers of plastic flow and can simultaneously be activated when deforming a crystalline media. An understanding of these mechanisms is not only relevant to a broad range of applications, e.g., metal forming, thermomechanical treatments of materials, shape memory alloy processing, elastocaloric applications, high-pressure physics, but also widely spread in nature, e.g., in geophysical processes.

In this work, we aim to probe the mechanisms underlying the interaction between dislocation slip, PTs, reverse PTs, and twinning. Both concurrent atomistic-continuum (CAC) and molecular dynamics (MD) models are constructed to: (i) characterize the internal stress induced by the microscale dislocation pileup at an atomically structured interface; (ii) decompose this stress into two parts, one of which is from the dislocations behind the pileup tip according to the Eshelby model and the other is from the dislocations at the pileup tip according to a super-dislocation model; and (iii) assess how such internal stresses contribute to the atomic-scale phase transformations (PTs), reverse PTs, and twinning.

The main novelty of this work is to unify the atomistic description of the interface and the coarse-grained (CG) description of the lagging dislocations away from the interface within one single framework. Our major findings are: (a) the interface dynamically responds to a pileup by forming steps/ledges, the height of which is proportional to the number of dislocations arriving at the interface; (b) the stress intensity factors are linearly proportional to the number of the dislocations in a nanoscale pileup, but upper bends to a high level when tens of dislocations are involved in a microscale pileup; (c) when the pre-sheared sample is compressed, a direct square-to-hexagonal PT occurs ahead of the pileup tip and eventually grows into a wedge shape. The two variants of the hexagonal phases form a twin with respect to each other; (d) upon a further increase of the loading, part of the newly formed hexagonal phase transforms back to the square phase. The square product phase resulting from this reverse PT forms a twin with respect to the initial square phase. All phase boundaries (PBs) and twin boundaries (TBs) are stationary and correspond to zero thermodynamic Eshelby driving forces; and (e) the stress intensity induced by a pileup consisting of 16 dislocations reduces the stress required for initiating a PT by a factor of 5.5, comparing with that in the sample containing no dislocations.

This work is a first characterization of the behavior of PTs/twinning resulting from the reaction between a microscale dislocation slip and an atomically structured interface. The gained knowledge will advance our understanding on how the multi-phase material behaves in many complex physical processes, such as the synthesis of multi-phase high-entropy alloys or superhard ceramics under high pressure torsion, deep mantle earthquakes in geophysics, and so on, which all involve dislocation slip, PTs, twinning, and their interactions across from the atomistic to the microscale and beyond.

Potassium from first principles: A case study

Andreas Hermann, Victor Naden Robinson, Hongxiang Zong, Gavin Woolman, Long Zhao, Xiangdong Ding, Miriam Marques, Ingo Loa, Sandro Scandolo, Graeme J. Ackland.

It has long been known that the “simple metal” potassium under pressure is anything but simple: a sequence of ever more complicated crystal structures, a turnover of the melting line, substantial drops in electrical conductivity, are all signs of emergent unexpected complexity. Potassium shares this behaviour with the other alkali metals, hinting at a general trend grounded in changes to the electronic structure. This trend is the formation of “electride” compounds under pressure, quasi-binary ionic compounds where the anionic component is an electron pair localized in a suitable interstitial site. In this talk I will show that first principles calculations can capture relatively subtle pressure effects to correctly describe potassium’s phase diagram, including incommensurate phases, partially molten states, and a liquid-liquid crossover.

Potassium takes up an incommensurate host-guest phase between 20 and 54 GPa, and the host-guest ratio has been mapped out in detail experimentally. While inherently impossible to model in periodic boundary calculations, I will show that approximants to this phase are capable of describing the energetics and structural trends accurately, which in turn allows to identify the host-guest phase as a partial electride phase.

The host-guest phase has intriguing high-temperature behaviour, because the guest sublattice was found to melt (or at least, de-correlate) far below the melting line, resulting in a state of matter (the so-called ‘chain melt’) that is partially solid and partially liquid, with the two phases interpenetrating at an atomic scale. To enable simulations of this state beyond the finite size limit of electronic structure calculations, we trained an interatomic potential using machine learning techniques. The potential is able to describe eight different phases and 14 phase transitions in potassium’s phase diagram in quantitative agreement with experiment. I will show that the chain melt is indeed a thermodynamic state and not a transient phenomenon.

The formation of solid electride phases has consequences for the liquid state. Akin to crossing the Widom line above a critical point, pressure can induce a metal-electride crossover in the liquid. We identify this crossover using machine learned molecular dynamics simulations *via* changes to various thermodynamic and transport properties. The liquid-liquid crossover is responsible for the turnover in the melting line, and explains how a liquid can be denser than a close-packed solid. I will discuss a minimal two-state model with general applicability that explains such melt line turnovers.

Insights into the high-pressure behaviour of solid bromine from hybrid DFT calculations

Madhavi H. Dalsaniya,^{1,2} Krzysztof Jan Kurzydłowski,¹ Dominik Kurzydłowski^{2*}

¹ Faculty of Materials Science and Engineering, Warsaw University of Technology, Wółoska 141, 02-507, Warsaw, Poland

madhavi.dalsaniya.dokt@pw.edu.pl, krzysztof.kurzydowski@pw.edu.pl

² Faculty of Mathematics and Natural Sciences, Cardinal Stefan Wyszyński University in Warsaw, 01-038 Warsaw, Poland

d.kurzydowski@uksw.edu.pl

High-pressure research provides fundamental insight into material properties, which is essential for the development and validation of new condensed matter and planetary models [1]. Nowadays high-pressure research has provided a number of new insights into the behavior of molecular crystals, such as H₂, O₂, and NH₃, subject to pressures in the range of hundreds of gigapascal, which corresponds to compressions of about an order of

magnitude [2]. Ab initio modelling within the framework of the density functional theory (DFT) has been established as an important tool for inspiring and guiding these experiments, as well as aiding data interpretation. However, the most commonly used generalized-gradient approximation (GGA) of the density functional theory (DFT) often fails to correctly describe the behavior of molecular systems at high pressure [3,4]. Here we utilize the hybrid DFT approach to model the properties of elemental bromine at atmospheric pressure up to 200 GPa ($\approx 2 \cdot 10^6$ atm) with the Vienna Ab Initio Simulation Package (VASP) [5,6]. The calculations reproduce in very good agreement with experiment the properties of the molecular phase I (*Cmca* symmetry) and its pressure-induced transition into the non-molecular phase II (*Immm*). The experimentally yet unobserved transition into phase III (*I4/mmm*) is predicted to occur at 128 GPa, followed by subsequent formation of an *fcc* lattice at 188 GPa. Analysis of the structure and electronic properties of the modelled phases indicates that the molecular *Cmca* phase becomes metallic just at the borderline of its stability, and that both *Immm* and *I4/mmm* phases are metallic and quasi-2D. Finally, we show that the incommensurate phases of bromine postulated from experiment are transient species which can be viewed as intermediates in the dissociation process occurring at the boundary of the transition from phase I to phase II.

Key words:

High pressure, molecular dissociation, phase transitions, bromine, density functional theory.

References:

1. C. S. Yoo, *Matter Radiat. Extrem*, 2020, 1, 018202.
2. L. Zhang, Y. Wang, J. Lv, and Y. Ma, *Materials Discovery at High Pressures*, *Nat. Rev. Mater*, 2017, 2, 1
3. J. George, C. Reimann, V. L. Deringer, T. Bredow and R. Dronskowski, *ChemPhysChem*, 2015, 16, 728-732.
4. M. Wu, S. T. John and Y. Pan, *Sci. Rep.*, 2016, 6, 1-7.
- A. V. Krukau, O. A. Vydrov, A. F. Izmaylov, and G. E. Scuseria, *Influence of the Exchange*, *J. Chem. Phys.*, 2006, 125.
5. G. Kresse and D. Joubert, *Phys. Rev. B* 59, 1999, 1758.
6. G. Kresse and J. Furthmüller, *Phys. Rev. B* 54, 1996, 11169.

The Structural Phase Transitions in β , Rutile & Fluorite Crystals of NbO₂.

V. Maurya[§] and K. B. Joshi

Department of Physics, M. L. Sukhadia University, Udaipur-313001(India).

[§] Corresponding author: vijaymaurya2414@gmail.com

The NbO₂ exhibits temperature and pressure induced phase transition. Under ambient conditions NbO₂ is found in the semiconducting body-centered-tetragonal (bct) structure. At high temperatures (1080 K) it transforms into a metallic rutile structure and exhibits insulator

to metal transition (IMT) [1,2]. A slightly substoichiometric phase β -NbO₂, was also synthesized using chemical transport reactions [3]. The IMT makes the materials crucial for electronic applications. However, NbO₂ has the advantage of operating over a broad range of temperatures. It is also reported that the bct transforms into β -phase at 5 GPa [4]. So there is enough scope for pressure induced metal insulator phase transition.

In this work, we present the structural properties of rutile (R), fluorite (F) and β -phase (β) of NbO₂. The F is a hypothetical phase. The LAPW code is used for the investigation. Both DFT and DFT+U approaches are applied [5]. The PBE functional is undertaken to solve the Kohn-Sham equation [6]. The valence configuration of Nb and O are $4p^65s^14d^4$ and $2s^22p^4$. The plane wave cut-off parameter $rgkmax$ was set to 7. The energy-volume curves $E(V)$ of three crystals are studied. The $E(V)$ curves using PBE scheme exhibit that R and β have competing ground state. On using PBE+U, the energy of the β reduces. The structural properties of R, F and β crystals deduced from PBE and PBE+U are well accordance with earlier reports. The PBE+U corrects the electronic states beyond PBE, treating $4d$ states of Nb particularly. At $U_{eff}=1$ eV, the lattice constant is very close to the experiment which very well resembles with earlier reports [2,7]. In addition, the bandgap of β -NbO₂ increases as +U increases.

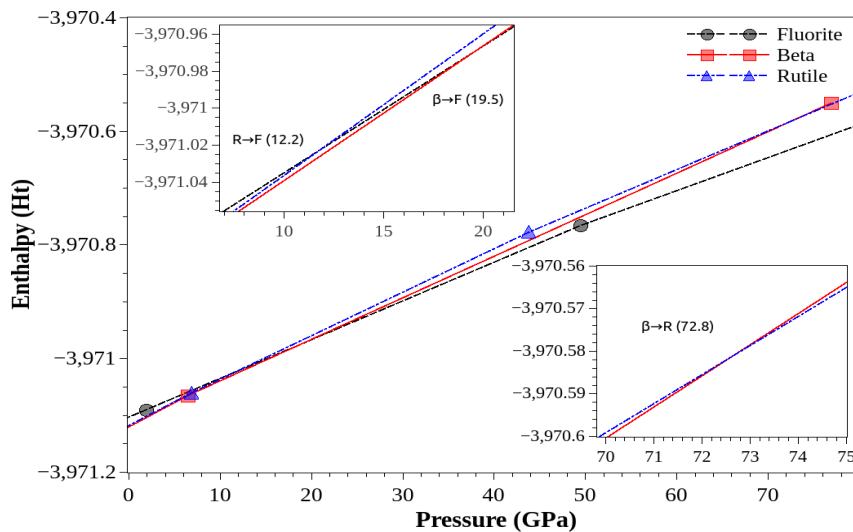


Figure 1.1 The $H(P)$ curves of three NbO₂ crystals using PBE functional. The insets highlight the transition regions.

The pressure induced phase transitions among the R, F and β phases of NbO₂ are investigated by plotting the enthalpy-pressure ($H(P)$) curves. These curves signify the possibilities of the phase transition and point out the transition pressure (PT). Fig. 1.1 signifies $\beta \rightarrow F$, $R \rightarrow F$ and $\beta \rightarrow R$ phase transitions on applying pressure. The transition pressures are listed in Table 1. At ~ 73 GPa the IMT take place from the semiconducting β to the metallic R phase. The PBE and PBE+U calculations give that the bandgap of β -NbO₂ is 0.05 and 0.2 eV .

Table.1 Calculated PT (in GPa) among three NbO₂ crystals two approaches.

	R→F	β→F	β→R
PBE	12.2	19.5	72.8
PBE+U	12.8	14.6	69.8

The structural phase transition accompanied by the IMT makes the NbO₂ crystals important both from physics and technological points of view. Interestingly the effects are pronounced when PBE+U is considered reflecting that 4d band electrons of niobium play significant role in the transitions. In this work electronic properties of β-NbO₂ shall also be discussed.

References

1. K. Seta and K. Naito, *J. Chem. Thermodynamics* **14** 921 (1982).
2. A. O'Hara, T. N. Nunley, A. B. Posadas, S. Zollner and A. A. Demkov, *J. Appl. Phys.* **116** 213705 (2014).
3. H.-J. Schweizer and R. Gruehn, *Zeitschrift für Naturforschung B* **37** 1361 (1982).
4. J. Haines, J. M. Léger, A. S. Pereira, D. Häusermann and M. Hanfland *Phys. Rev. B* **59** 13650 (1999).
5. <http://elk.sourceforge.net/>. ELK-Code.
6. J. P. Perdew, K. Burke and M. Ernzerhof, *Phys. Rev. Lett.* **77** 3865 (1996).
7. W. H. Brito, M. C. O. Aguiar, K.

Tensorial stress-plastic strain fields in α - ω Zr mixture, revised phase transformation kinetics, and friction under compression in diamond anvil cell: Coupled Experimental-Analytical-Numerical Approach

Achyut Dhar¹, K. K Pandey² and Valery I. Levitas^{1*}

¹ Iowa State University, Ames, Iowa, USA

² Bhabha Atomic Research Center, Mumbai, India

(Corresponding author E-mail: vlevitas@iastate.edu)

Various phenomena (phase transformations, chemical reactions, and friction) under high pressures in diamond anvil cell (DAC) are strongly affected by fields of all components of stress and plastic strain tensors [1,2]. However, they could not be measured. Even measured pressure distribution contains a significant error. Here, we suggest a coupled experimental-

analytical-computational approach utilizing synchrotron X-ray diffraction to find all these fields before, during, and after α - ω phase transformation in strongly plastically predeformed Zr, including contact friction. In the proposed approach, inputs from experiments (like in [3]) include radial distribution of the volume fraction of phases and radial and azimuthal elastic strain distributions, all averaged over the sample thickness, variation of lattice parameters of α and ω phases of Zr under hydrostatic conditions, texture, and pressure-dependent elastic moduli of single crystal α -Zr and ω -Zr. XRD peak broadening is used to determine the pressure dependence of the yield strength of phases and X-ray absorption is used to obtain the thickness profile of a sample. The first level of post-processing of these data involves coupling modified Prandtl solution for stress field in polycrystalline Zr with the non-linear elasticity of hydrostatically pre-stressed crystals. This has allowed us to determine the friction-stress distribution at the sample-anvil contact surface, which could not be obtained experimentally, and also the distribution of all stress and elastic strain fields within the sample. At the second level, the finite element method (FEM) algorithm is developed and used for numerical simulations of sample's plastic flow in DAC satisfying contact boundary conditions from the analytical solution [4]. The von-Mises yield condition with pressure-dependent yield strength coupled with Murnaghan elastic potential is used to obtain the elastoplastic response of polycrystalline Zr sample using radial return mapping algorithm.

From the stress and plastic strain fields obtained numerically within the sample, the pressure 2.7 GPa is obtained as the initiation pressure for α -Zr \rightarrow ω -Zr PT, and it is found to be independent of the pressure-shear loading path. This corrected pressure is much higher than 1.4 GPa obtained using hydrostatic EoS for non-hydrostatic loading [3], but still lower than both the phase equilibrium pressure of 3.4 GPa and the PT pressure of 6 GPa under hydrostatic loading. Obtained plastic strain and stress fields will allow us to calibrate, in the future, plastic strain-controlled phase transformation kinetics [2] and to design experiments that would optimize the transformation kinetics in the sample. Obtained results open opportunities for developing quantitative high pressure/stress science, including mechanochemistry, material synthesis, and tribology.

1. V. I. Levitas, *Phys. Rev. B* **70**, 184118 (2004).
2. V.I. Levitas, *Material Transactions*, **60** (2019), 1294.
3. K. K. Pandey and V. I. Levitas, *Acta Materialia*, **196** (2020), 338-346.
4. B. Feng, V.I. Levitas, and W. Li, *International Journal of Plasticity*, **113** (2019), 236-254.

Random structure generator with fixed environment

Yana V. Propad¹, Ivan A. Kruglov^{1,2}

¹ *Moscow Institute of Physics and Technology, 9 Institutsky lane, Dolgoprudny 141700, Russia*

² *Dukhov Research Institute of Automatics (VNIIA), Moscow 127055, Russia*

Keywords: crystal structure prediction, random generator

*e-mail: propad@phystech.edu

The generation of crystal structures is a big problem for crystallography and crystal structure prediction [1]. The creation of random crystal structures (in which the positions of some of the structural elements are known) is still an open question. This problem arises when the positions of some atoms can be determined using experimental techniques. Important example is superconducting hydrides, where positions of heavy atoms can be determined using the X-ray, yet hydrogen positions remain unknown. Another example is molecular crystals and cocrystals of solvates, where positions of solvent molecules can also be unknown. Crystal structure generators that exist today do not allow adding and fixing known structural information (i.e., environment).

In this work we present a new random structure generator that allows one to specify known structural information such as the size of a cell and the position of certain atoms or molecules in it. The input of the algorithm is the crystal structure parameters, the positions of fixed atoms or molecules, and the types and number of structural elements that need to be added in the cell. We illustrate this method by applications to uranium, lanthanum and sulfur hydrides at different pressures. In the case of hydrides, in a cell with heavy atoms (which positions were previously determined using the powder X-ray diffraction) hydrogen atoms were placed with randomly generated positions. Generated structures were used as seeds in the evolutionary algorithm USPEX [2], where they were relaxed with VASP at given pressures. Using our method, we found stable phases for uranium, lanthanum, and sulfur hydrides, which correspond to experimental results from [3], [4], and [5] respectively. Using the developed method we also found stable structures of CL₂₀-N₂O molecular crystal, which can be used as energetic materials.

References:

- [1] A.R. Oganov, C.W. Glass, *The Journal of Chemical Physics*, V. 124, Is. 4, 2006
- [2] A.O. Lyakhov, A.R. Oganov, H.T. Stokes, Q. Zhu, *Computer Physics Communications*, V. 184, pp. 1172 – 1182, 2013
- [3] I.A. Kruglov, A.G. Kvashnin, A.F. Goncharov, A.R. Oganov, *Science Advances*, V. 4, I. 10, 2018
- [4] I.A. Kruglov, D.V. Semenov et. al, *Phys. Rev. B* 101, 024508, 2020
- [5] A.P. Drozdov, M.I. Erements, I.A. Troyan, V.Ksenofontov, S.I. Shylin, *Nature*, V. 525, pp. 73 – 76, 2015

PdH₂ nanotube: A potential design

Zeliang Liu^{1,2}, Wei Luo²

¹Key Laboratory of Mechanical Reliability for Heavy Equipments and Large Structures of Hebei Province,
Yanshan University, Qinhuangdao, 066004 China

²Department of Physics and Astronomy, Uppsala University, Uppsala, S75121, Sweden

Since the discovery of carbon nanotubes by Iijima^[1], nanotubes as a kind of nanostructures have attracted researchers' attention for decades. Studies have shown that nanotubes have more superior properties. For example, the high tensile strength and elastic modulus of nanotubes, combined with a low density which makes them act as nanoscale fillers to improve the elastic properties of composites^[2]. Nanotubes were used as electrically conductive fillers in plastics due to the conductivity properties^[3]. In addition, the size and chirality dependence of elastic and electronic properties in nanotubes leads to a range of potential applications^[4].

As is well known, nanotubes structure can be constructed by rolling a two-dimensional material in a certain direction. Such as carbon nanotube^[5], boron nanotubes^[6] and TiO₂ nanotube^[7]. The recent study shown that high hydrogen content in monolayer PdH₂ is stability. This makes the PdH₂ nanotube possible by rolling the monolayer PdH₂.

A size dependence of stability, elastic and electronic properties in PdH₂ nanotube are studied using first principle calculations based on density function theory. Both zigzag ($n \times 0$) and armchair ($m \times n$) of PdNTs with $n = 8 \sim 24$ and $m = n = 5 \sim 16$ were considered. All the calculations are performed based on density functional theory (DFT) as implemented in the Vienna Ab initio Simulation Package (VASP) code.

It is found that the zigzag form is more stable than the armchair form. While, there is a singularity of strain energy at around 10 Å in zigzag form leads to armchair form is more stable than zigzag form. The Young's modulus of zigzag and armchair PdNTs converges to a constant value of approximate 421 GPa and 393 GPa when the tube diameter larger than 20 Å. They are close to the calculated monolayer PdH₂ Young's modulus of 403 GPa. The electronic calculations revealed that both of zigzag and armchair PdNTs present a metallic property. The electronic density of states points the narrow states at around Fermi energy level for the (10×0), (14×0), (22×0) and (8×8) nanotubes which predicts the appearance of quantum states. The band structures PdNTs are degenerated along the tube axial direction and highly dispersive.

Reference

[1] Iijima S. *Helical microtubules of graphitic carbon*. *Nature*, 1991, 354(6348): 56.

[2] Yu MF, Lourie O, Dyer MJ, et al. *Strength and breaking mechanism of multiwalled carbon nanotubes under tensile load*. *Science*, 2000, 287(5453): 637-640.

- [3] Bauhofer W, Kovacs JZ. A review and analysis of electrical percolation in carbon nanotube polymer composites. *Compo. Sci. Technol.*, 2009, 69(10): 1486-1498.
- [4] Yang X, Li HJ, Hu MZ, et al. Elastic properties investigation on single-wall ZrO₂ nanotubes: A finite element method with equivalent Poisson's ratio for chemical bonds. *Physica E*, 2018, 98: 23-28.
- [5] Machón M, Reich S, Thomsen C, et al. Ab initio calculations of the optical properties of 4-Å-diameter single-walled nanotubes. *Phys. Rev. B*, 2002, 66(15): 155410.
- [6] Kochaev A. Elastic properties of noncarbon nanotubes as compared to carbon nanotubes. *Phys. Rev. B*, 2017, 96(15): 155428.
- [7] Ma R, Bando Y, Sasaki T. Directly rolling nanosheets into nanotubes. *J. Phys. Chem. B*, 2004, 108(7): 2115-2119.

High-pressure elastic, vibrational and structural study of monazite-type EuPO₄ from ab initio simulations.

P. Rodríguez-Hernández, and A. Muñoz

Instituto de Materiales y Nanotecnología, Departamento de Física, MALTA Consolider Team, Universidad de La Laguna, San Cristóbal de La Laguna, E-38205 Tenerife, Spain

The APO₄ orthophosphates compounds (A= trivalent material) are analogous materials to orthoarsenates, orthovanadates, and orthosilicates. They are basically formed by AO₃ or AO₉ polyhedral and PO₄ tetrahedra. The size of the ionic radius of the A cation defines the two different structures where this family compounds crystallizes. APO₄ compounds with the ionic radius lower than Gd crystallize in the tetragonal zircon structure (*I4₁/amd*, space group 141 with Z=4). The rest of orthophosphates crystallize in a monoclinic lower symmetry phase, monazite structure (*P2₁/n*, space group 14 with Z=4). Monazite structure is isostructural to cerium phosphate mineral (monazite). The structure can be viewed as being composed by alternating edge-sharing AO₉ polyhedra, with a structural distortion derived from a rotation of the PO₄ tetrahedra and a lateral shift of the (100) planes that reduces symmetry from tetragonal to monoclinic.

In this work EuPO₄ monazite-type has been studied under high pressure by first principles calculations in the framework of density functional theory. The work focuses on the analysis of the structural, dynamical and elastic properties of this material. Results about the structure and its evolution under pressure, the equation of state and the compressibility are reported. The evolution of the Raman and Infrared frequencies, and their pressure coefficients are also presented. Finally, the study of the elastic constants allows to provide information related with the elastic properties of this compound and their mechanical stability. The system becomes mechanically unstable over 48.5 GPa.

ACKNOWLEDGEMENTS

This work was supported by MCIN/AEI/10.13039/501100011033 under Project PID2019-106383GB-43, and the MALTA Consolider Team network RED2018-102612-T, financed by MINECO/AEI/10.13039/501100003329.

Ab Initio study of $\text{Ca}_3\text{Y}_2\text{Ge}_3\text{O}_{12}$ garnet. Dynamical, elastic properties and mechanical stability under pressure

A. Muñoz¹, P. Rodríguez-Hernández¹,

¹ *Instituto de Materiales y Nanotecnología, Departamento de Física Universidad de la Laguna and MALTA Consolider Team, La Laguna, 38205, Tenerife, Spain*

Nowadays, oxide garnets are being used for technological application in the field of optical materials and solar energy as well as active elements for solid-state laser. Their high thermal conductivity, hardness and chemical and mechanical stability make them good host matrices for rare ions with interesting luminescence properties.

In this work, bulk properties at equilibrium and under hydrostatic pressure of yttrium gallium garnet, $\text{Ca}_3\text{Y}_2\text{Ge}_3\text{O}_{12}$, are studied by ab initio calculations in the framework of the density functional theory using plane-waves and the pseudopotential theory. The evolution of phonon frequencies and their pressure coefficients are presented, and the dynamical stability analyzed. The variation of elastic constants with pressure is also analyzed and the Born stability criteria are applied to determine the mechanical stability of this garnet under hydrostatic pressure.

ACKNOWLEDGEMENTS

This work was supported by MCIN/AEI/10.13039/501100011033 under Project PID2019-106383GB-43, and the MALTA Consolider Team network RED2018-102612-T, financed by MINECO/AEI/10.13039/501100003329.

Pressure-induced phase transition of fluorine

Giovani L. Rech, André L. Martinotto, Janete E. Zorzi, and Cláudio A. Perottoni

Universidade de Caxias do Sul, Brazil

Fluorine is the most reactive element of the periodic table, thus rendering its empirical investigation challenging to perform while making it an interesting problem for computer simulations. In this work, we searched for crystalline structures of fluorine at 0 and 100 GPa using an evolutionary search algorithm. The energy calculations and structure relaxations were performed using Density Functional Theory at the PBE0+D3(ABC)/TVZP level of theory. The best candidate structures at each pressure were selected for further investigation. In particular, the static energy difference between two phases, space group C2/c (experimentally observed α -F₂) and a hypothesized high-pressure phase, space group Cmce, was assessed by Quantum Monte Carlo calculations. Furthermore, besides the energy difference favoring the C2/c structure, the Cmce phase exhibits dynamical instability near the Γ -point, which disappears with increasing pressure. The unstable vibrational mode can be related to the absence of σ -holes in the fluorine molecule, which renders a repulsive head-to-head interaction between molecules, as opposed to heavier halogens, in which the presence of σ -holes stabilizes the orthorhombic Cmce structure. Evidence suggests a pressure-induced, second-order phase transition C2/c \rightarrow Cmce, whose order parameter goes to zero at about 2.5 GPa under static conditions (0 K, no zero-point energy contribution).

Tailored Adamantane derivatives as precursors to Nanodiamonds in mild Pressure and Temperature conditions

Maxime Bonsir, Yves H. Geerts

Laboratory of Polymer Chemistry, Université Libre de Bruxelles, Boulevard du Triomphe, CP 206/1, Brussels, Belgium

Nanodiamonds (NDs) are promising nanomaterials for cutting-edge technologies such as quantum computing, pharmaceutical vectoring or biomedical sensing and imaging. These applications are rooted in the NDs biocompatibility, spin and fluorescence properties. In particular, specific defects, such as Nitrogen-Vacancy centers (NV⁻ centers) are responsible for their fluorescence properties. However, current synthetic methods towards NDs are showing their limitations to produce NDs of controlled size, structure and desirable defects due to the harsh conditions of high pressure and temperature needed to convert precursors

to NDs. To this end, the use of well-designed molecular precursors could allow the synthesis of NDs in milder pressure and temperature conditions, which will result on a better control on the conversion and ultimately lead to enhanced properties.

The design of these molecular precursors is based on the adamantane molecule, the smallest molecular component of the diamond family. Multiple designs of these precursors can be obtained by organic chemistry synthesis, allowing the obtaining of a wide variety of functionalized adamantanes of tailored structure and composition. Multiple preliminary structural criteria for these precursors are considered, such as steric strain, similarity with the diamond unit cell or incorporation of defect-generating atoms. The precursors are studied regarding their structural and thermal properties by X-ray diffraction (crystal packing, bond lengths and angles), dynamic NMR experiments and thermogravimetric analyses.^[1,2] The goal is to rationalize the chemical structure and properties of the precursors to the conversion parameters and find the most optimal precursors for the synthesis of NDs in mild conditions of temperature and pressure.

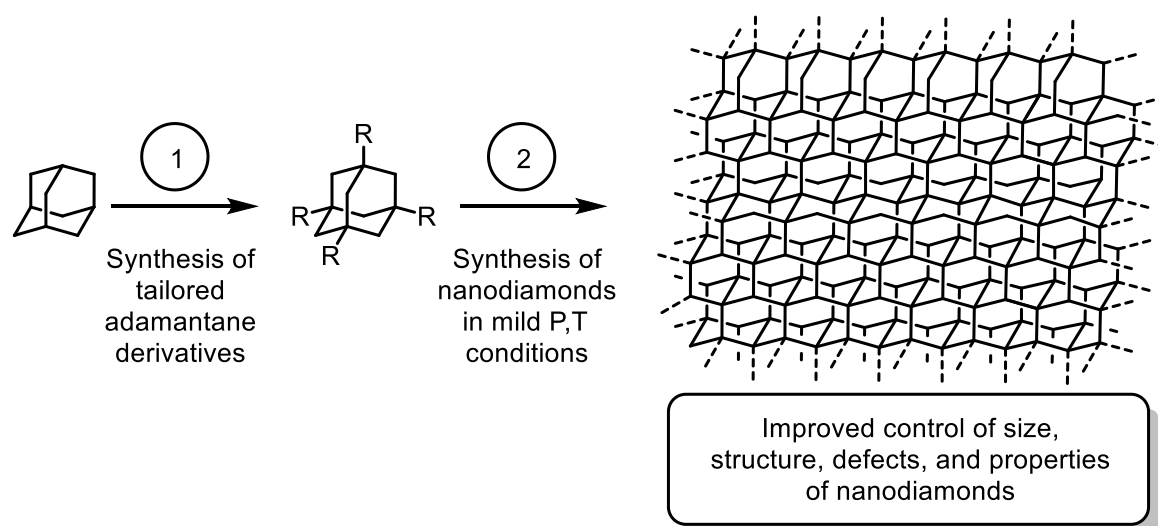


Figure 1. Overview of the steps towards nanodiamonds of controlled properties using adamantane derivatives as precursors

[1] M. Bonsir, C. Davila, A. R. Kennedy, Y. Geerts, *Eur. J. Org. Chem.* **2021**, 2021, 5227–5237.

[2] M. Bonsir, A. R. Kennedy, Y. Geerts, *ChemistryOpen* **2022**, e202200031.

High temperature superconductivity in superhydrides

M. I. Eremets

Max-Planck-Institut fuer Chemie, Hahn-Meitner-Weg 1, 55128 Mainz, Germany

Since the discovery of superconductivity at ~ 200 K in H₃S [1], similar or higher transition temperatures, T_C s, have been reported for various hydrogen-rich compounds under ultra-high pressures [2]. Superconductivity was experimentally proved by different methods, including electrical resistance, magnetic susceptibility, optical infrared, and nuclear resonant scattering measurements. The crystal structures of superconducting phases were determined by X-ray diffraction. The pronounced isotope effect in electrical transport and magnetization measurements indicates a conventional phonon-mediated superconductor. The results are in good agreement with the theoretical predictions, which describe superconductivity in hydrides within the framework of the conventional BCS theory.

Magnetic properties, one of the most important characteristics of a superconductor, have not been satisfactorily defined. We develop SQUID magnetometry under extreme high-pressure conditions [3] and report characteristic superconducting parameters for H₃S and LaH₁₀—the representative members of two families of high-temperature superconducting hydrides. In particular, we determine a London penetration depth λ_L of ~ 20 nm in H₃S and ~ 30 nm in LaH₁₀. These compounds have the values of the Ginzburg-Landau parameter $\kappa \sim 12$ – 20 and thus create a group of “moderate” type II superconductors. Recently we further developed magnetic measurements with the trapped magnetic flux. This technique provides a strong magnetic response but eliminates the huge background of a bulky diamond anvil cell.

A part of the report will be a discussion of possibilities of further increasing of T_C to room temperature and above, with emphasis on experimental expectations.

References

Drozdov, A.P., et al., Conventional superconductivity at 203 K at high pressures.

Nature 2015. **525**: p. 73.

Flores-Livas, J.A., et al., A perspective on conventional high-temperature superconductors at high pressure: Methods and materials. Phys. Rep., 2020. 856: p. 1-78.

Minkov, V.S., et al., Magnetic field screening in hydrogen-rich high-temperature superconductors. Nature Communications, 2022.

Pressure-enhanced superconductivity in some of the cage-type quasiskuttrudite single crystals

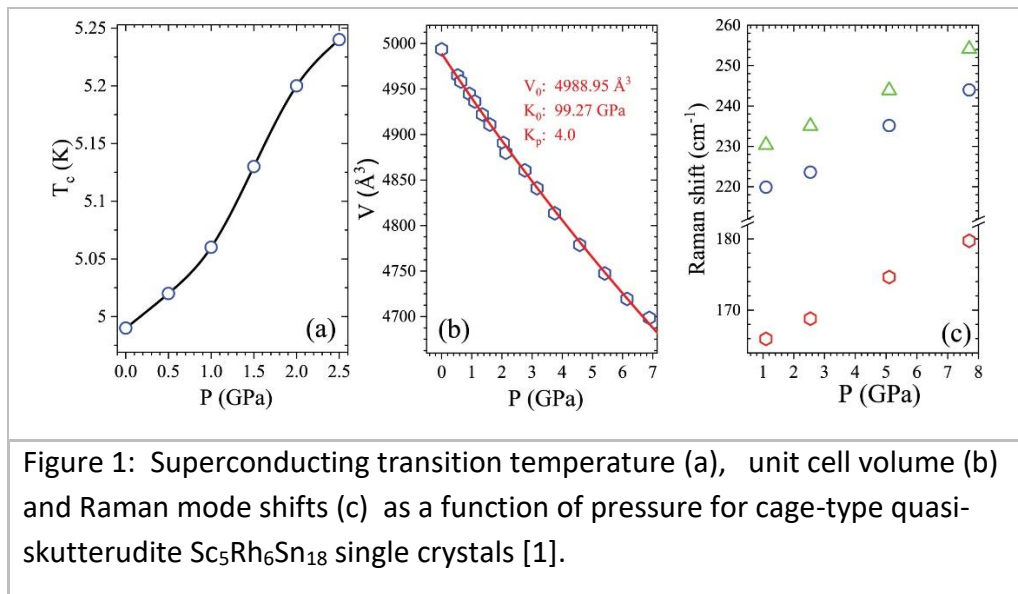
Govindaraj Lingannan^a, Muthukumaran Sundaramoorthy^{a,b}, Sonachalam Arumugam^a, Boby Joseph^{b*}

a. Center for High Pressure Research, School of Physics, Bharathidasan University, Tiruchirappalli, 620024, India.

b. Elettra-Sincrotrone Trieste S.C. p. A., S.S. 14, Area Science Park, Basovizza 34149, Italy.

*e-mail: boby.joseph@elettra.eu

Several cage-type quasiskutterudite crystal lattice systems show type II superconductivity with moderate superconducting transition temperature (T_c). High-pressure studies on such systems are important to understand the superconducting electron pairing mechanism in these class of materials. Recently we have been involved in systematic high-pressure studies of several of such systems [1,2]. In few of the investigated systems, there is a continuous increase in T_c with pressure. For example, the $\text{Sc}_5\text{Rh}_6\text{Sn}_{18}$ system show a continuous increase in T_c from 4.99 K at ambient conditions to 5.24 K at 2.5 GPa [1]. The rattling atom in the quasiskutterudite lattice is found to lead to Raman modes which can contribute to the understanding of pressure dependence of the phonon modes, eventually contributing to the understanding of electron-phonon coupling in these systems. Raman investigations of $\text{Sc}_5\text{Rh}_6\text{Sn}_{18}$ ambient pressure revealed the presence of three weak modes at 165.97, 219.86 and 230.35 cm^{-1} . In this system. the lattice parameters and volume exhibited a smooth decrease without any anomalies as a function of pressure in this system in below 8 GPa where HP Raman investigations revealed a linear shift of all the three Raman modes to higher wavenumbers with increasing pressure [1]. Similar pressure dependence are seen in several members of the quasiskutterudite crystal lattice systems, indicating the possibility to obtain a universal picture on the pressure effect in these class of materials.



Reference: [1] G. Lingannan et al 2022 *J. Phys.: Condens. Matter* 34 245601

<https://doi.org/10.1088/1361-648X/ac61b6>; [2] M. Sundaramoorthy et al in-preparation

New High Tc Superconductors Achieved via High Pressures

Changqing JIN¹

¹Institute of Physics, Chinese Academy of Sciences(IOPCAS), Beijing 100190, China

Corresponding author: Changqing JIN

Email: Jin@iphy.ac.cn

Key words: New Superconductor Materials; High Tc; High Pressure Effects

New high Tc superconductors by design are synthesized including Ba₂CuO_{3+y} cuprates with compressed copper oxygen octahedron showing unexpected superconductivity yet with very high Tc above 73K^[1], the superhydrides of calcium with Tc above 200K^[2], the superhydrides of zirconium showing Tc above 70K^[3] by using synergetic high pressure techniques.

References

- W. M. Li, J. F. Zhao, C. Q. Jin et al., "Superconductivity in a unique type of copper oxide", *PNAS* **116**, 12156(2019);
Z. W. Li, X. He, C. Q. Jin et al., "Superconductivity above 200K Observed in Superhydrides of Calcium", *Nature Commun.* **13**, 2863 (2022);
C. L. Zhang, X. He, C. Q. Jin et al., "Superconductivity in Zirconium Polyhydrides with Tc above 70 K". *Sci. Bull.* **67**, 907(2022)
-

Search for guidelines for synthesizing low hydrogen affinity alloy hydrides

R. Utsumi^{1,2}, M. Morimoto^{1,2}, H. Saitoh^{1,2}, T. Watanuki^{1,2}, T. Sato³, S. Takagi⁴, and S. Orimo⁴

National Institutes for Quantum Science and Technology¹, University of Hyogo², Shibaura Institute of Technology³, Tohoku University⁴

Backgrounds and Objects

We have synthesized novel metal hydrides with hydrogen storage properties by using a high-pressure and high-temperature method. Conventional hydrides are made from combinations of two kinds of metals: one is a metal reacts easily with hydrogen near ambient pressure, and the other is a metal with low hydrogen affinity, which does not react with hydrogen below 1 GPa. The problem is that metals that easily react with hydrogen are expensive. We are attempting to synthesize novel hydrides containing only metals with low hydrogen affinities to

synthesize low-cost hydrides. We have obtained several hydrides consisting of aluminum and transition metals. These results have shown that even combinations of metals with low hydrogen affinities can be used to produce hydrides. To broaden the variety of hydrides consisting of metals with low hydrogen affinities, we have tried to obtain a guideline to search such hydrides.

The purpose of the present study is to clarify the hydrogenation mechanism of alloys consisting of metals with low hydrogen affinities. We have investigated hydrogenation reactions of Fe–Mo alloys.

Methods

$\text{Fe}_x\text{Mo}_{1-x}$ ($0.41 \leq x \leq 0.88$) alloys were hydrogenated at a hydrogen pressure of 6 GPa and 1025 K for 2 h using a cubic-type multi-anvil press. We investigated crystal structures of the samples during hydrogenation and dehydrogenation reactions by in-situ synchrotron radiation X-ray diffraction measurement system at BL14B1, SPring-8.

Results

Fe–Mo alloys before hydrogenation have five different crystal structures depending on their compositions and thermal treatment temperatures. Those after hydrogenation reactions are solid solution phases of FeH_x and MoH, and the Fe–Mo alloy hydrides have two structures. One of the Fe–Mo alloy hydrides was the $\text{Fe}_x\text{Mo}_{1-x}$ ($0.66 \leq x \leq 0.73$) hydride with hexagonal close-packed (hcp) structure. The hcp $\text{Fe}_{0.67}\text{Mo}_{0.33}\text{H}_{\sim 1}$ was formed a few minutes after $\text{Fe}_{0.67}\text{Mo}_{0.33}$ alloy was heated to 1025 K at 6 GPa in fluid hydrogen, according to in-situ powder X-ray diffraction profiles. The structure was isomorphous to the hcp MoH and similar to the double hexagonal close-packed (dhcp) FeH. Another can be explained as a solid solution phase of face-centered cubic (fcc)- FeH_x and hcp-MoH. We have found a search guideline based on these results. The guideline is that even if the structures of alloys before hydrogenations are different, they form hydrides with similar structures to FeH_x and MoH when reacted with hydrogen. In other words, formed hydrides tend to be solid solution phases of FeH_x and MoH.

Conclusions

We have clarified the hydrogenation reaction process of Fe–Mo alloys, which gives us a search guideline of hydrides consisting of metals with low hydrogen affinities only

Engineering better superconductors: two-electron models of superconductivity in real space

T. Novoa^{1,*}, F. Belli², I. Errea², J Contreras-García^{1,*}

¹Laboratoire de Chimie Théorique, Sorbonne Université/CNRS, 4 Pl. Jussieu, Paris, France

*Presenting author e-mail address: contrera@lct.jussieu.fr

Necessary and sufficient conditions for the design of high temperature (T_c) superconductors are crucial for the inverse design of new compounds with improved T_c .

We have recently shown that the underlying chemical structure and bonding need to be characterized for a good comprehension of the chemical composition-superconductivity relation. More specifically, we have shown that the Electron Localization Function [2] can be used to define a quantity called the networking value, which correlates well with the predicted critical temperature, much better than any other descriptor analyzed thus far. And this, for all bonding types [3]. Nevertheless, a deeper understanding of its working mechanism was still missing.

We have constructed pair densities for 2 valence electrons on simple metal and a Cooper pair in real space using a local density approximation model. This has allowed us to show how the networking value is affected by pressure and how the superconducting and metallic states are related. Investigations using superconducting DFT (SC-DFT) have further enabled to formalize this result. Finally, a code for the automatic determination of the networking value has been developed making use of the properties of periodic graphs.

These developments set clear paths for the automatic engineering of better superconductors,

References

- [1] A. P. Drozdov, M. I. Eremets, I. A. Troyan, V. Ksenofontov, and S. I. Shylin. *Conventional superconductivity at 203 kelvin at high pressures in the sulfur hydride system. Nature* 2015, 525, 73
- [2] A. D. Becke and K. E. Edgecombe. *A simple measure of electron localization in atomic and molecular systems. The Journal of Chemical Physics* 1990, 92, 5397
- [3] F. Belli, T. Novoa, J. Contreras-Garcia and I. Errea, *Strong correlation between electronic bonding network and critical temperature in hydrogen-based superconductors. Natur. Comm.* 2021, 12, 5381

Clean-limit superconductivity at 197 K in high-pressure sulfur hydride synthesised using ammonia borane

Israel Osmond¹, Owen Moulding¹, Sam Cross¹, Takaki Muramatsu¹, Annabelle Brooks¹, Oliver Lord², Timofey Fedotenko³, Jonathan Buhot¹, Sven Friedemann¹

¹*H.H. Wills Physics Laboratory, University of Bristol, United Kingdom*

²*School of Earth Sciences, University of Bristol, United Kingdom*

³*Photon Science, DESY, Germany*

The search for room temperature superconductivity in hydrogen rich compounds has accelerated since the discovery of superconductivity in compressed sulfur hydride, H₃S, in 2015 [1]. Controlled synthesis of hydrides remains a challenge, and further work on the formation pathways will prove vital in the search for room temperature superconductivity in such compounds. Here we confirm the synthesis of cubic Im-3m H₃S by laser heating elemental sulfur and hydrogen donor ammonia borane, NH₃BH₃. Superconductivity is characterised using electrical transport measurements in a diamond anvil cell, confirming a transition temperature T_c = 197 K at 153 GPa, in good agreement with previous studies. The coherence length extracted from measurements of the upper critical field H_{c2} together with estimations of the carrier mean free path from the normal state resistance suggest that H₃S follows clean-limit behaviour. The work further highlights the potential for in situ synthesis of clean high-T_c hydrides using ammonia borane, a more accessible synthesis alternative to pure hydrogen.

[1] A.P. Drozdov *et al.*, *Nature* 525, 73 (2015).

Superconducting properties of AuAgTe₄ under pressure

Y. Amiel^{1*}, E. Greenberg², S. Chariton², Y. Ponosov³, G. Kafle⁴, E. Komleva³, P. Becker-Bohatý⁵, L. Bohatý⁵, S. Streltsov³, I. Mazin⁶, E. Margine⁴, D. Khomskii⁵, A. Palevski¹, G. Kh. Rozenberg¹

¹*School of Physics and Astronomy, Tel Aviv University, 69978 Tel Aviv, Israel.*

²*Center for Advanced Radiation Sources, University of Chicago, 5640 South Ellis Avenue, Chicago, Illinois 60637, USA*

³*M.N. Miheev Institute of Metal Physics of Ural Branch of Russian Academy of Sciences, 620108 Ekaterinburg, Russia*

⁴*Department of Physics, Applied Physics, and Astronomy, Binghamton University-SUNY, Binghamton, New York 13902, USA*

⁵*Universitaet zu Koeln, Zuelpicher str. 77, 50937 Koeln, Germany*

⁶*Department of Physics and Astronomy and Quantum Science and Engineering Center, George Mason University, Fairfax, Virginia 22030, USA*

Gold is one of the most inert metals, it forms very few compounds. The known compounds have sometimes rather interesting properties. Thus, AuTe₂ (mineral calaverite) is the rare example of incommensurate crystal structure in natural minerals [1]. It is a metal, and when doped by Pd or Pt, and also under pressure, it becomes superconducting [2]. This is a rare case since superconducting compounds made of Au and non-metallic elements are extremely rare. Besides AuTe₂, we are aware only of one more, the recently synthesised under high pressure SrAuSi₃ [3]. Similar to Au, another noble element, Ag, gives only few compounds, and very few of them are superconducting [4]. Finding new superconducting compounds of gold (and silver) is a challenge – especially having in mind that the rather close “relative” of those, Cu, one row higher in the Periodic table, gives the best High-T_c superconductors. Thus, besides its own interest, finding novel Au and Ag superconductors could help to understand why they behave so differently.

Here we undertook the search of novel Au-containing superconductors and found superconductivity in a “close relative” of calaverite AuTe₂ – in a mineral sylvanite AgAuTe₄, which can be considered as calaverite in which half of gold ions are substituted by silver. We investigated AuAgTe₄ under compression using single crystal X-ray diffraction, Raman spectroscopy combined with first-principles calculations and found in accord with previous prediction [5] a structural phase transition from the low-pressure (LP) monoclinic *P2/c* to the high-pressure (HP) *P2/m* structure around 5 GPa. Resistance *R(T)* and *R(H)* measurements at various pressures and external magnetic fields, show that the HP phase is superconducting with a critical temperature of superconductivity $T_c \approx 3.5$ K and $H_c \approx 1.2$ T at $P \approx 5$ GPa. We further examined the superconducting properties of the *P2/m* phase using the EPW package and identified that the main contribution to the electron-phonon coupling arises from the low-energy phonon modes. We note also an onset of superconductivity even in the LP dimerized phase at $P \approx 1.4$ GPa with $T_c \approx 0.8$ K. With further pressure increase, T_c increases almost linearly up to ≈ 2.7 K at 4.4 GPa ($H_c \approx 0.5$ T) and then hardly changes in the LP phase.

Thus, we managed to find yet one more real chemical compound of gold (and silver) which is superconducting. Theoretical analysis carried out demonstrated that most probably the superconductivity here is of a conventional type, predominantly due to electron-phonon interaction.

Acknowledgments: This research was supported by the Israel Science Foundation (Grant No. 1748/20) and by National Science Foundation Grant No. DMR-2132586.

1. S. V. Streltsov *et al.*, *PNAS* 2018, **115**, 9945.
2. Sh. Kitagawa, *et al.*, *J. Phys. Soc. Jpn.* 2013, **82**, 113704.
3. M. Isobe, *et al.* *Chem. Mater.* 2014, **26**, 2155
4. K. Andres, N.A. Kuebler, M.B. Robin, *J. Phys. Chem. Solids* 1966, **27**, 1747
- A. V. Ushakov *et al.*, *J. Phys.: Condens. Matter* 2019, **31**, 235601.

Emergent Magnetic, Electronic and Structural Phases in Pressure-Tuned van der Waals Systems

S. S. Saxena¹

¹*Cavendish Laboratory, University of Cambridge, J. J. Thomson Avenue, Cambridge, CB3 0HE, United Kingdom*

We report discovery of new metallic and magnetic phases in the van-der-Waals antiferromagnets MPS_3 , where M = Transition Metal, form an ideal playground for tuning both low-dimensional magnetic and electronic properties[1-4]. These are layered honeycomb antiferromagnetic Mott insulators, long studied as near-ideal 2D magnetic systems with a rich variety of magnetic and electric properties across the family. We will present magnetic, structural and electrical transport results and compare the behaviour of Fe-, V-, Mn- and $NiPS_3$ as we tune them towards 3D structures – and Mott transitions from insulator to metal. I will show recent results on record high-pressure neutron scattering, which has unveiled an enigmatic form of short-range magnetic order in metallic $FePS_3$. We have mapped out the full phase diagram - a first in this crucial family of materials. We observe multiple transitions and new states, and an overall increase in dimensionality and associated changes in behaviour.

[1] G. Ouvrard *et al.*, *Mat. Res. Bull.*, 1985, 20, 1181.

[2] C.R.S. Haines *et al.*, *Phys. Rev. Lett.* 2018, 121, 266801.

[3] M.J. Coak *et al.*, *J.Phys.:Cond. Mat.* 2019, 32, 124003.

[4] M.J. Coak *et al.*, *Phys. Rev. X*, 11, 011024 (2021)

Superionicity of H^- in LaH_{10} superhydride

Maélie Caussé, Grégory Geneste and Paul Loubeyre

CEA

Computational studies have successfully predicted the dramatic uptake of hydrogen by metals under pressure leading to the formation of superhydrides. They can be viewed as additive volume alloys between metal hydrogen and a metal [1]. LaH_{10} exemplifies the properties of these novel H-rich compounds which form a novel class of superconducting materials, since it displays a very high superconducting critical temperature (T_c) of 250K [2,3].

We show here another remarkable property for superhydrides, namely H^- superionicity. In particular we will answer the following questions: can the H diffusion constant reach the high value needed for qualifying a superionic phase? If the fluid-like H atoms diffusion associated to a melting of the H sublattice and can LaH_{10} be stable under such conditions ? How do the

hydride ions (H⁻) conductivity in LaH₁₀ compare to those of the recently discovered hydridic ionic conductors?

Superionic conductors are solid materials that display very high ionic conductivities, about 1 (Ω . cm)⁻¹ and associated to a diffusion coefficient about $D \sim 10^{-5}$ cm²/s, as those typically found in molten salts [4]. Recently, the stability of a hydride (H⁻) superionic phase was predicted by *ab initio* molecular dynamics in sodium silicon hydride Na₂SiH₆ [5]. The current strategy to rational design of superhydrides at low pressure [6] could lead to an hydrogen energy material use of superionicity in superhydrides.

By means of *ab initio* molecular dynamics simulations in LaH₁₀, an exceptionally high hydride (H⁻) diffusion coefficient is calculated at high temperature ($D = 1.7 \cdot 10^{-4}$ cm²/s at 163GPa, 1500K, corresponding to an ionic conductivity of $\sigma = 0.9$ Scm⁻¹). The connected path for the hydride ionic diffusion is disclosed, with the H-sublattice keeping its clathrate structure. LaH₁₀ compound remains remarkably stable under temperature in its superionic phase up to a melting temperature similar to that of pure La. The conductivity properties of LaH₁₀ are discussed in relation with the recently discovered family of compounds showing fast pure hydride ions transport.

References :

- B. Guigue, A Marizy, and P. Loubeyre, Phy. Rev. B 102, 014107 (2020)*
M. Somayazulu, M. Ahart, A. K. Mishra, Z. M. Geballe, M. Baldini, Y. Meng, V. V. Struzhkin, and R. J. Hemley, Phy. Rev. Letters 122,027001 (2019)
A. P. Drozdov, P. P. Kong, V. S. Minkov, S. P. Besedin, M. A Kuzovnikov, S. Mozaffari, D. A. Balicas, M. Tkacz and M. I. Eremets, Nature 569, 528 (2019)
J. Boyce and B. Huberman, Physics Reports 51,198 (1979)
T. Liang, Z. Zhang, H. Yu, T. Cui, C. J. Pickard, D. Duan, and S. A. T. Redfern, The Journal of Physical Chemistry Letters 12,7166 (2021)
Z. Zhang, T. Cui, M. J. Hutcheon, A. M. Shipley, H. Song, M. Du, V. Z. Kresin, D. Duan, C. J. Pickard and Y. Yao, Phys. Rev. Letters 128, 047001 (2022)

Metallic Transition in Rhenium Dichalcogenides

Md. Nur Hasan¹, Felix Sorgenfrei², Patrik Thunstrom², Samir Kumar Pal¹, D. D. Sarma^{3,4}, Olle Eriksson^{2,5*} and Debjani Karmakar^{2,6,*}

¹ S. N. Bose National Centre for Basic Sciences, India, ² Uppsala University, Sweden,

³ Indian Institute of Science, India, ⁴ CSIR-NIIST, India,

⁵ Örebro University, Sweden, ⁶ Bhabha Atomic Research Centre, India

olle.eriksson@physics.uu.se (O.E.), debjani.karmakar@physics.uu.se (D.K.)

Rhenium dichalcogenides (ReS_2 and ReSe_2) with distorted $1T'$ structures and triclinic symmetry group $P-1$ ¹, constituted the centre of debates due to their contradicting theoretical and experimental results. Using a comparative analysis of the formation energies, we predict the correct structures of these two compounds, capable of minimizing the contradictions. In existing literature, the compression behaviour of these two systems is studied for the structures of ReS_2 and ReSe_2 , predicted by Murray *et al.*² and Wildervanck *et al.*³ respectively. Our work points out that the rectification of these two structures, as predicted by Lamfers *et al.*¹ results into the structures with the lowest formation energy. For these newly predicted structures of ReS_2 and ReSe_2 , with the help of first-principles investigations, we explored the effects of high-pressure by using a GGA-PBE exchange-correlation functional and including van der Waals correction. The effects on electronic band structures with isotropic reduction of volume are investigated and both of them are observed to undergo a semiconductor to metallic transition. The variations of the total energy versus the volume for the unit cells of ReS_2 and ReSe_2 are fitted with the Birch-Murnaghan equation of state and the values of the bulk moduli for ReS_2 and ReSe_2 are calculated to be 73.4 and 53.4 GPa respectively. The percentages of volume reduction corresponding to the metallic transition in ReS_2 and ReSe_2 are 4.6% and 18.2% and the estimated pressures needed to obtain this transition are 3.4 and 9.7 GPa respectively. We have also analysed the nature of band-overlaps under higher pressures beyond metallic transition. In ReS_2 , with higher pressure, there is an increase of metallic overlap. In ReSe_2 , due to the flatness of the bands at the band-edges of the ambient structure, there is a reentrant semiconducting transition under higher pressure. The orbital projection analysis near the metallic transition implies that in ReS_2 , there is a larger contribution of the out-of-plane orbitals than the in-plane ones due to higher interlayer electronic hybridization. ReSe_2 , on the other hand, have higher in-plane contribution due to its more 2D-like nature with lesser interlayer coupling. Next, with the help of a combined full-potential density functional theory and multiplet ligand field theory (DFT+MLFT), the X-ray spectral properties of these two systems are analysed in the light of their intricate differences of high pressure optimized structures after metallic transition.

References

- Lamfers, H. J.; Meetsma, A.; Wiegers, G. A.; de Boer, J. L., *J. Alloys Compd.* 1996, 241 (1), 34-39.
Murray, H. H.; Kelty, S. P.; Chianelli, R. R.; Day, C. S., *Inorg. Chem.* 1994, 33 (19), 4418-4420.
Wildervanck, J. C.; Jellinek, F., *J. less-common met.* 1971, 24 (1), 73-81.
-

Structures and Transport Properties of TiZr Alloys with Hydrogen under High Pressure

Bin Li¹, Soonbeom Seo², Dongzhou Zhang³, Tuson Park², and Jaeyong Kim^{1,*}

¹*Department of Physics, Institute for High Pressure, Hanyang University, Seoul, 04763, Republic of Korea*

²*Department of Physics, Center for Quantum Materials and Superconductivity (CQMS) and Sungkyunkwan University, Suwon, 16419, Republic of Korea*

³*Advanced Photon Source, Argonne National Laboratory, IL, 60439, USA*

*kimjy@hanyang.ac.kr

Effects of pressure on the structure, electronic resistance, and the critical magnetic field values for superconductivity of pristine and hydrogenated TiZr alloys were investigated. With increasing pressure from ambient to 55 GPa, structures of pure TiZr alloys at equiatomic composition changed from an hcp to a bcc through an hcp-omega phase, while hydrogenated ones exhibit various intermediate phases, including bcc-H and tetragonal phases. Superconducting transition temperature, T_c , of pure TiZr alloys significantly increased from 2.7 K to 11.7 K with increasing pressure from 5.4 GPa, and 50 GPa, respectively. Interestingly, the T_c values for hydrogenated samples increased from 3.4 K to 9.4 K at 6 GPa and 32 GPa, respectively, but decreased to 8 K with increasing pressure further to 55 GPa. Applying the external magnetic field suppressed T_c value. Our combined results with the structure and transport measurements demonstrated that applying pressure increases the T_c while hydrogen atoms contribute to decreasing the values.

High pressure neutron study on magnetic phases in a Y-type hexaferrite

Yan Wu¹, Kun Zhai², Young Sun², Bianca Haberl¹, Huibo Cao¹

¹*Neutron Scattering Division, Neutron Science Directorate, Oak Ridge National Laboratory, Oak Ridge, Tennessee 37831, USA*

²*Beijing National Laboratory for Condensed Matter Physics, Institute of Physics, Chinese Academy of Sciences, Beijing 100190, China*

Multiferroics have attracted tremendous research interests with their rich physics and potential in constructing next-generation multifunctional devices. Y-type hexaferrite $\text{Ba}_2\text{Mg}_2\text{Fe}_{12}\text{O}_{22}$ is a particularly interesting materials in the type-II multiferroics due to its large magnetoelectric effect, rich magnetic phase transitions and easy tunable magnetic phases. The magnetic structure of $\text{Ba}_2\text{Mg}_2\text{Fe}_{12}\text{O}_{22}$ consists of two groups of L- (large moment) and S- (small moment) blocks alternating stacked along the c-axis direction. Due to

the convolution of the magnetic moments between different blocks and their correlation of lattice, the material yields a longitudinal cone ground state. Specifically, heavily Sr-doped samples exhibit an alternating longitudinal conical ground state. In our earlier work, we found that tuning the ground state spin cone symmetry with Sr doping level can improve the magnetoelectric (ME) effects in the $\text{Ba}_{2-x}\text{Sr}_x\text{Mg}_2\text{Fe}_{12}\text{O}_{22}$ family and achieved a record high ME coefficient in $\text{Ba}_{0.4}\text{Sr}_{1.6}\text{Mg}_2\text{Fe}_{12}\text{O}_{22}$ through systematically increasing the Sr-doping level. The idea of further confining the interacting magnetic/ ferroelectric (FE) blocks to smaller units with pressure is expected to lead to more interesting changes in ME coupling and magnetic/FE polarization behaviors.

Here, we used neutron scattering techniques to investigate the pressure effects on $\text{Ba}_{0.4}\text{Sr}_{1.6}\text{Mg}_2\text{Fe}_{12}\text{O}_{22}$ via a combination of experiments using piston cylinder clamp cells and diamond anvil cells up to a pressure of 8.3 GPa. We found that $\text{Ba}_{0.4}\text{Sr}_{1.6}\text{Mg}_2\text{Fe}_{12}\text{O}_{22}$ goes through a series of interesting magnetic phases under pressure and the T_c of the ground state is greatly elevated with high pressure. The spin cone symmetry, which is closely related with FE properties in this system, is however, changing in a way not favoring the polarization under pressure. Overall, our systematic study of pressure effect on the magnetic phases in $\text{Ba}_{0.4}\text{Sr}_{1.6}\text{Mg}_2\text{Fe}_{12}\text{O}_{22}$ gives important insights for understanding the mechanisms behind ferroelectricity and magnetism in hexaferrites and similar magnetic systems.

This research used resources at High Flux Isotope Reactor, a DOE Office of Science User Facility operated by the Oak Ridge National Laboratory.

Raman study of pure TeO₂ glass under pressure: interplay between glass network transformations and electronic transitions

Elissaios Stavrou

The effect of pressure on network glasses has attracted extensive experimental and theoretical research efforts, aiming to elucidate their structure and dynamics under thermodynamic stimuli. In network glasses pressure often induces structural modifications of the short-range order (SRO), resulting to changes in the connectivity of the structural units and/or increase of the coordination number. In contrast to their crystalline counterparts, in glasses such changes are happening gradually over a pressure range instead of first-order like transition. In addition to changes in the SRO, transformations of the medium range order (MRO), which represents a beyond the atomic scale order of few nm, were also observed. Thus, most of such glasses are known to exhibit a series of glass-to-glass transitions (polyamorphism) under pressure. The particular case of the MRO has attracted additional

interest due to its uniqueness in glasses, i.e., it is absent in the crystalline counterparts. MRO is traditionally probed using either static probing techniques, X-ray diffraction first sharp diffraction peak (FSDP), or dynamic techniques such as Raman spectroscopy and inelastic neutron-scattering. In the latter case, the so-called Boson peak (BP) is a characteristic low-frequency feature in the spectra of glasses. It is broadly accepted that the BP is due to vibrations of the disordered medium beyond the atomic distance scale and, consequently, related to the MRO. In this context, the use of thermodynamic stimuli, such as temperature and pressure, looks appealing for understanding the nature and the origin of the Boson peak at the microscopic level.

In this work, a network glass (pure TeO₂) was studied, for the first time, up to the record pressure of 70 GPa using Raman spectroscopy. The Boson peak frequency (ω_b) exhibits a decrease of the $\partial\omega_b/\partial P$ slope at 5-6 GPa, indicating a modification towards a more compact tellurite network. Above 30 GPa, ω_b reaches a “saturation” with a practically constant value up to 70 GPa. In the short-range order, both our experimental and theoretical results indicate that pressure up to 15 GPa induces the transformation of single Te-O-Te bridges to double Te-O₂-Te bridges, leading to a more compact tellurite network. At higher pressures, a new Raman activity develops around 580 cm⁻¹ and is associated with the increase of Te coordination to six-fold. Natural bond orbital analysis showed that the formation of double Te-O₂-Te bridges favors the $s \rightarrow d$ transition, which promotes the increase of Te coordination number at higher pressures through a d^2sp^3 hybridization. This results to the formation of a practically canonical TeO₆ octahedron, in strict difference with crystalline TeO₂ at the same pressure range, and the development of a 3D network that freezes the medium range order. Our study highlights the interplay between pressure-induced electronic transitions and the increase in Te coordination number in the flexible tellurite glass network. Given that our study is the first to record the BP at such pressures, it paves the way for further exploration of this unique in glasses feature at high pressures.

Pressure-induced electronic phase transitions in honeycomb-based transition-metal compounds

Tomohiro Takayama

Max Planck Institute for Solid State Research

Heavy transition compounds including $4d$ and $5d$ elements have been attracting attention as a playground for novel electronic phases. The interplay between moderate electron correlation and strong spin-orbit coupling yields spin-orbit-entangled states in these

systems, and their interactions may lead to exotic phenomena such as Kitaev spin liquid, multipolar ordering and topological semimetals.

In these $4d$ and $5d$ transition-metal compounds, their ground states are often determined by a delicate balance of relevant parameters such as spin-orbit coupling, inter-site hopping and crystal field. Small change of these parameters may give rise to a drastic change of their electronic properties. Application of pressure is thus expected to be a valuable tool to control their ground states.

We have focused on two honeycomb-based compounds, hyperhoneycomb iridate $b\text{-Li}_2\text{IrO}_3$ and a honeycomb ruthenate $\text{Ag}_3\text{LiRu}_2\text{O}_6$, and found their pressure-induced electronic phase transitions. The former compound is one of the candidates of Kitaev spin liquid [1] but in fact shows a long-range magnetic order at ambient pressure due to the presence of magnetic interactions other than the Kitaev-type [2]. We attempted to modify the magnetic interactions by applying pressure. For the high-pressure neutron diffraction and resonant inelastic x-ray scattering, we found a pressure-induced Ir-Ir dimerization where the spin-orbit-entangled states are altered to a molecular orbital state [3]. This indicates the appearance of competing dimer phase instead of spin-liquid state, and the competition between spin-orbital entanglement and molecular orbital formation is likely present in other Kitaev materials and $4d/5d$ compounds as well.

The honeycomb ruthenate $\text{Ag}_3\text{LiRu}_2\text{O}_6$ possesses spin-orbit-entangled singlet states at ambient pressure. A honeycomb lattice of such singlet states is expected to show a quantum phase transition to exotic magnetic ground state called excitonic magnetism when exchange interactions are sufficiently strong. In order to realize the excitonic magnetism, we investigated the pressure effect on $\text{Ag}_3\text{LiRu}_2\text{O}_6$ to enhance the exchange interactions. Instead of driving excitonic magnetism, we found two pressure-induced phase transitions, first to a weak dimer state of Ru atoms, and eventually to a strong Ru-Ru dimer phase with molecular orbital formation. Although the high-pressure phase is analogous to that found in $b\text{-Li}_2\text{IrO}_3$, the intermediate phase represents a unique spin-orbit-coupled dimer state produced by an intricate balance of spin-orbit coupling, exchange interaction and lattice distortion [4].

Therefore, our works point to rich electronic phases of $4d/5d$ transition-metal compounds induced by pressure. Because of various competing parameters and interactions in those materials, we believe that we can realize further exotic electronic phases with the aid of high-pressure techniques.

[1] H. Takagi, T. Takayama, G. Jackeli, G. Khaliullin, and S.E. Nagler, *Nat. Rev. Phys.* **1**, 264 (2019).

[2] T. Takayama et al., *Phys. Rev. Lett.* **114**, 077202 (2015).

[3] T. Takayama et al., *Phys. Rev. B* **99**, 125127 (2019).

[4] T. Takayama et al., *arXiv:2205.12123*

Pressure-driven switching of magnetism in layered CrCl₃

Azkar Saeed Ahmed

Layered transition-metal compounds with controllable magnetic behaviors provide many fascinating opportunities for the fabrication of high-performance magneto-electric and spintronic devices. The tuning of their electronic and magnetic properties is usually limited to the change of layer thickness, electrostatic doping, and the control of electric and magnetic fields. However, pressure has been rarely exploited as a control parameter for tailoring their magneto-electric properties. Here, we report a unique pressure-driven isostructural phase transition in layered CrCl₃ accompanied by a simultaneous switching of magnetism from a ferromagnetic to an antiferromagnetic ordering. Our experiments, in combination with ab initio calculations, demonstrate that such a magnetic transformation hinders the band-gap collapse under pressure, leading to an anomalous semiconductor-to-semiconductor transition. Our findings not only reveal high potential of CrCl₃ in electronic and spintronic applications under ambient and extreme conditions but also establish the basis for exploring unusual phase transitions in layered transition-metal compounds.

Combined X-ray Raman Scattering Spectroscopy and X-Ray Diffraction on Shock-Compressed Vitreous SiO₂

L. Bussmann^{1*}, M. Elbers³, C. Albers², J. Kaa^{2,4}, N. Thiering², M. Sundermann⁵, H. Gretarsson⁵, T. Schlothauer¹, G. Heide¹, C. Sternemann², S. Fuhrmann¹

¹TU Bergakademie Freiberg, Freiberg High Pressure Center (FHP), D-09599 Freiberg, Germany ²Technische Universität Dortmund, Fakultät Physik/DELTA, D-44221 Dortmund, Germany ³Universität Potsdam, Institut für Geowissenschaften, D-14467 Potsdam-Golm, Germany ⁴European XFEL, D-22869 Schenefeld, Germany

⁵Deutsches Elektronen-Synchrotron DESY, D-22607 Hamburg, Germany

*lena.bussmann@igt.tu-freiberg.de

The university of Freiberg is one of the few institutions with access to an underground mine research and teaching purposes. Since 2006 it is equipped with a shock wave laboratory (SWL) mainly dedicated to conducting research in materials synthesis. Vitreous SiO₂, or silica glass, is a suitable material for gaining deeper understanding on impact processes within this experimental frame since the pressure-related properties of silica glass have been vastly investigated and are fairly well known. At the same time, many questions remain unsolved,

and silica glass is still of high interest due to its significance in several scientific disciplines such as geosciences or material sciences.

A series of silica glass powder samples have been shock-compressed in the SWL, and subsequently investigated at the P01 beamline of PETRA III at DESY, Hamburg, using a combination of X-ray Raman scattering spectroscopy (XRS) and X-ray diffraction (XRD). Studying both the Si L-edge and O K-edge via XRS allows to classify the effects of shock-compression on the short-range structure, while the simultaneous analysis of the position of the first sharp diffraction peak in the X-ray diffractograms yields information on intermediate-range correlations. The combination of both methods hence allows to analyse the sample series in terms of the effective shock pressure achieved in the shock laboratory.

Furthermore, time-resolved recording of X-ray diffraction patterns revealed a structural 'relaxation' process in the shock-compressed samples induced by the X-ray irradiation. This process is set in comparison to an *ex-situ* thermal relaxation study of heat-treated glass samples and characterized by collating the complementary XRD and XRS results.

Influence of PRESSURE and thickness ON SUPERConductivity in high entropy alloys thin films

G. Pristáš^{1,*}, J. Bačkai^{1,2}, M. Orendáč¹, S. Gabáni¹, F. Košuth^{1,3}, M. Kuzmiak^{1,2}, P. Szabó¹, R. Franz⁴, S. Hirn⁴, Ch. Mitterer⁴, S. Vorobiov³, K. Flachbart¹

¹*Institute of Experimental Physics SAS, Watsonova 47, 04001 Košice, Slovakia*

²*Faculty of Electrical Engineering and Informatics, Technical University, Letná 9, 04200 Košice, Slovakia*

³*Institute of Physics, P. J. Šafárik University, Park Angelinum 9, 040 01 Košice, Slovakia*

⁴*Department of Materials Science, Montanuniversität Leoben, Franz-Josef-Straße 18, 8700 Leoben, Austria*

*gabriel.pristas@saske.sk

High entropy alloys (HEA) Nb₆₇Hf₁₁Ti₁₁Zr₁₁ and Ta₃₅Nb₃₅Hf₁₀Ti₁₀Zr₁₀ in bulk form exhibit a transition to superconducting state at $T_c = 9.2$ K and $T_c = 8$ K, respectively and belongs to the highest values of critical temperature among HEAs. In this study we have prepared and investigated superconducting Nb₆₇Hf₁₁Ti₁₁Zr₁₁ and Ta₃₅Nb₃₅Hf₁₀Ti₁₀Zr₁₀ high entropy alloys in form of thin films with thicknesses of 600, 100 and 30 nm, and compared their properties with bulk counterparts. We have shown that the superconducting transition temperature T_c as well as the upper critical magnetic field $B_{c2}(0)$ decrease with decreasing thickness. Application of hydrostatic pressure up to 33 kbar on the 600 nm Ta₃₅Nb₃₅Hf₁₀Ti₁₀Zr₁₀ film shows a decrease of T_c with pressure, which differs from that observed on bulk sample. However, no clear T_c dependence was observed if pressure was applied on the 100 nm film. This result is most likely related to increasing disorder (tendency to structure amorphization) in thinner films.

Moreover, we performed point-contact spectroscopy measurements on the 600 nm $\text{Nb}_{67}\text{Hf}_{11}\text{Ti}_{11}\text{Zr}_{11}$ film and were able to observe directly the temperature development of the superconducting energy gap $\Delta(T)$, which is consistent with that of conventional phonon mediated Bardeen–Cooper–Schrieffer superconductors.

Revealing the mechanisms of the pressure-induced insulator-metal transition in distorted TlNiO_3 perovskites

J. E. Rodrigues^{1,*}, A. D. Rosa¹, T. Irifune², G. Garbarino¹, J. A. Alonso^{3,*}, O. Mathon¹

⁽¹⁾ European Synchrotron Radiation Facility (ESRF), 71 Avenue des Martyrs, 38000 Grenoble, France.

⁽²⁾ Geodynamics Research Center (GRC), Ehime University, Matsuyama, 790-8577, Japan.

⁽³⁾ Instituto de Ciencia de Materiales de Madrid (ICMM), CSIC, Sor Juana Inés de la Cruz 3, E-28049 Madrid, Spain.

Rare-earth perovskite nickelates $R\text{NiO}_3$ (R stands for a rare-earth element) have attracted large attention in the past few decades, because of their unique electronic properties that emerge with the insulator-to-metal transition. Such a property can be easily tuned *via* chemical substitution or external variables. Yet the underlying mechanism of this transition remains little understood, hindering a generic descriptive formalism of such transitions and to exploit these compounds fully for industrial applications. While most previous studies focused on nickelates with partially filled $4f$ cations on the R site, we studied the mechanism of this transition on a rare nickelate with Tl^{3+} (thallium) on the R site, that comprises fully filled orbitals. This compound exhibits a simplified electronic structure and presents therefore an ideal system to untangle the electronic and structural origin of this transition. We studied first the pressure-induced and temperature-induced insulator-metal transition in TlNiO_3 at different atomic and electronic length scales by employing synchrotron X-ray diffraction and X-ray absorption spectroscopy. We found that the structural phase transition $P2_1/n \rightarrow Pbnm$ that takes place at 10.8 GPa is driven by a collective $[\text{NiO}_6]$ octahedral rearrangement. These collective movements resulted in an increased bond-angle Ni–O–Ni of 159° which moved the electron charge away from the Tl cations towards the Ni. In a second step, the temperature-driven insulator-metal transition was studied by X-ray absorption spectroscopy that occurred at 550 K under ambient pressure.

New type of uniaxial non-magnetic pressure cell

J. Kaštil¹, D. Tichý², J. Kamarád¹

¹*Institute of Physics, AS CR, Czech Republic,*

²*Titan Machinery s.r.o., Czech Republic*

In contrast to isotropic effects of hydrostatic pressure, the uniaxial compression of solids can be applied to study directly an anisotropic character of physical properties. The presented non-magnetic uniaxial pressure CuBe cell that is tailored for SQUID magnetometers makes possible to study magnetic anisotropy of solids under uniaxial stress at wide range of magnetic field and temperatures. The cell ensures compression of samples by uniaxial stress in direction perpendicular (transversal stress) or parallel (axial stress) to the cell axis, which is the direction perpendicular or parallel to magnetic field, respectively.

The original design of the cell comes out from a new type of the squeezer that consists of two prisms and their holder with a square conical orifice. The axial force up to 3000 N acting on the squeezer is produced by the calibrated CuBe tube-springs. A transfer of the axial force into transversal direction in the precise fabricated squeezer was carefully tested and calibrated. The relevant calibration procedures will be presented.

A usefulness of the cell in the high-pressure research was verified by a study of magnetic properties and structural transition of the Heusler Ni₂MnSn-based alloys. The diffusion-less structural transformation of the alloys from high-temperature cubic structure (austenite) into low-temperature orthorhombic structure (martensite) is accompanied by a decrease of volume, by a strong decrease of magnetization due to an up-rise of antiferro-magnetic interactions and by an occurrence of both, the exchange-bias and the exchange-spring effects. The isotropic action of hydrostatic pressure leads to a support of presence of the martensite phase of the alloys and to an increase of the transition temperature, but a microscopic mechanism of the transition that is dependent on a twin-structure creation is almost unaffected. However, anisotropic magnetostriction and magneto-crystalline anisotropy play an important role in the twin-structure creation. This is the reason of interest in the study of the alloys under anisotropic uniaxial compression. A comparative study of effects of hydrostatic and uniaxial pressure on all these volume-sensitive phenomena helps to understand an origin of their microscopic mechanisms. The first results of the comparative study will be presented.

Computational Prediction of Planetary Composition from Mass/Radius Data

J. Manuel Recio¹, Alberto Otero-de-la-Roza¹, David Sánchez², and Fernando Izquierdo-Ruiz³

¹MALTA-Consolider Team and Departamento de Química Física y Analítica, Universidad de Oviedo, 33006 Oviedo, Spain

³Facultad de Ciencias, Universidad de Oviedo, 33006 Oviedo, Spain

³MALTA-Consolider Team, Dpto. de Química Física, Facultad de Ciencias Químicas, Universidad Complutense, 28040 Madrid, Spain

We present a new program that proposes multiple compositions for differentiated planetary interiors that are compatible with the observed mass and radius of the planet. The program uses an internal database of equations of state for candidate planetary materials based on available knowledge of solar system planets and chondrite meteorites. After numerical integration of the hydrostatic equilibrium differential equations and requiring a zero pressure value at the planet surface, the code provides the pressure-density-radius profile for the planet. The program generates a number of likely candidate compositions that can be used to constrain our knowledge of the planet's internal structure. The equation of state database contains Earth-like materials like iron-nickel alloys and silicates but also other materials found in these chondrite meteorites like silicon carbide, Mg/Al spinel, water, and others. We have analyzed four planet models: i) super-Earths and super-Mercuries, formed mainly by iron and silicates, ii) gaseous planets such as Jupiter and Neptune, composed of gases that, in our model, are represented by helium and hydrogen, iii) oceanic planets (hycean), which contain a significant amount of water in their composition and iv) carbon-rich planets, for which we consider pure carbon (graphite and diamond) and silicon carbon as main components. We apply the mass-radius relationships to the planet models developed to several particular exoplanets such as those of the Trappist-1 system, HD 149026b and the Gliese 436-b. In addition, we examine planets that are believed to be rich in carbon as CoRoT-7b, Kepler-9d, Kepler-10d and 55Cnc-e. We show that the method used in combination with the developed planetary models allow to obtain information about these planets from only their observed radius and mass.

Optimised Spectrum Fitting using Likelihood and Bayes Factor: Carbon Nanotubes under Pressure

David J. Dunstan

School of Physical and Chemical Sciences, Queen Mary University of London, London E1 4NS, UK.

Bayesian methods combine well with least-squares fitting of spectra. The Likelihood L , the Occam Factor OF and the Marginal Likelihood Integral $MLI = \int L \cdot OF$ are readily evaluated after each least-squares fit [1, 2]. Increases in $\ln L$ show improved fit to the data. The MLI exposes over-fitting. The Bayes Factor BF, the ratio of MLI between models, guides the choice of the best model.

These methods are demonstrated on a set of Raman spectra of radial breathing modes (RBM) of carbon nanotubes at pressures up to 12 GPa [3]. These spectra were previously fitted in the traditional way, with Voigt lineshapes for the Raman peaks and with broad peaks introduced to describe the background [4]. Recently, we used Bayesian methods to study the largest peaks of one of these spectra. In the better model, the background is replaced by stronger tails on the peak lineshapes [5]. Here we extend this analysis to the full set of spectra.

The Bayesian method demands full use of prior knowledge, and avoidance of any other constraints on the model. The most dramatic improvement we obtained came from removing the constraint which relates the widths of the Lorentzian and Gaussian contributions to the pseudo-Voigt peak function. The resulting better fit enabled the identification of many previously unobserved weak peaks in the spectra. Some of these could be identified as further RBM peaks, while others are independent of pressure (such as laser ghosts).

Overall, these improvements in the models gave increases in $\ln L$ up to 200, which corresponds to an increase of $e^{200} \sim 10^{87}$ in the relative probability of the final model to the initial model of Ref.3. Moreover, it permitted more accurate tracking of the peak parameters of some of the RBM peaks at pressures above their collapse pressures. They are found to stop moving (within uncertainty) with pressure, as previously reported for the G-band Raman peaks [1].

These refined outcomes will contribute to an understanding of the mechanical properties of graphene, in particular as they relate to nanotubes and their response to pressure.

1. S.F. Gull, *Bayesian inductive inference and maximum entropy*, in *Maximum Entropy and Bayesian Methods in Science and Engineering* (Kluwer Academic Publishers, 1988), ed. Erickson G.J. and Smith C.R., vol.1, pp 53-74.
2. D.J.C. MacKay, 1992, *Bayesian interpolation*, *Neural Computation* **4**, 448-472.
3. A.C. Torres-Dias, S. Cambré, W. Wenseleers, D. Machon and A. San-Miguel, 2015, *Chirality-dependent mechanical response of empty and water-filled single-wall carbon nanotubes at high pressure*, *Carbon* **95**, 442-451.
4. A.C. Torres-Dias, T.F.T. Cerqueira, W. Cui, M.A.L. Marques, S. Botti, D. Machon, M.A. Hartmann, Y.W. Sun, D.J. Dunstan and A. San-Miguel, 2017, *From mesoscale to nanoscale mechanics in single-wall carbon nanotubes*, *Carbon* **123**, 145-150.
5. D.J. Dunstan, J. Crowne and A.J. Drew, 2022, *Easy computation of the Bayes Factor to fully quantify Occam's razor*, *Scientific Reports* **12**:993.

Structural behavior of Copper(I) halide luminescence compounds under High Pressure

Gonzalez-Platas, J., Rodriguez-Mendoza, U.R., Molina-Hernández, R., Murillo, M. and Amo-Ochoa, P.

Departamento de Física. Instituto Universitario de Estudios Avanzados en Física Atómica, Molecular y Fotónica (IUDEA) and MALTA Consolider Team, Universidad de La Laguna, Tenerife, Spain.

Departamento de Física. Instituto de Materiales y Nanotecnología (IMN) and MALTA Consolider Team, Universidad de La Laguna, Tenerife, Spain.

Departamento de Química Inorgánica. Universidad de La Laguna, Tenerife, Spain. Departamento de Química Inorgánica. Universidad Autónoma de Madrid, Madrid, Spain.

Copper(I) halide compounds exhibit interesting mechanochromic and thermochromic luminescent properties with critical technological applications. Mainly due to their large variety of structural configurations where Cu-X has the capability to form clusters with different dimensionality as rhomboid dimers, cubane, or staircase ladders [1-2]. It does a large variety of Cu...Cu interactions give attractive photoluminescence properties. Therefore, it could be interesting to explore new properties if we could control these interactions by applying external stimuli as temperature, or pressure. We'll present the most relevant results about the structural changes with their different types of phase transitions that occurred together with luminescence studies under pressure as well as the determination at room temperature of the compressibility behaviour (EoS) of these compounds.

References

Q. Benito, I. Maurin, T. Cheisson, G. Nocton, A. Fargues, A. Garcia, C. Martineau, T. Gacoin, J.-P. Boilot, and S. Perruchas Chem. - A Eur. J., 2015, 21, pp. 5892–5897

A. Aguirrechu-Comerón, R. Hernández-Molina, P. Rodríguez-Hernández, A. Muñoz, U. R. Rodríguez-Mendoza, V. Lavín, R. J. Angel, and J. Gonzalez-Platas, Inorg. Chem. 2016, 55, 7476-, vol. 55, no. 15, pp. 7476–7484.

J. Gonzalez-Platas, M. Alvaro, F. Nestola, and R. Angel, J. Appl. Crystallogr., 2016, 49, 1377–1382.

Elastic properties of dipropylene glycol glasses with different thermobaric histories

Igor Danilov, Elena Gromnitskaya, Vadim Brazhkin

Institute for High Pressure Physics, Russian Academy of Sciences, Troitsk, Moscow, Russia

idanilov@hppi.troitsk.ru

Unlike liquids and crystals, glasses are non-ergodic nonequilibrium systems, which means that their state is not an unambiguous function of external PT parameters, but depends on the time and protocol of their production. A striking proof of non-ergodicity is the existence

of the phenomenon of pressure densification of glass. Densified glass is obtained by cooling a liquid at high pressure and then releasing the pressure. Its density is greater than that of glass obtained under normal pressure. Earlier we showed that high-pressure densified propylene carbonate had higher elastic moduli than low-pressure glass [1]. We have studied the influence of thermobaric history on the elastic properties of dipropylene glycol (C₆H₁₄O₃) glasses: high pressure glasses (densified) and low pressure glasses (ordinary). To create high-pressure glasses, we compressed the liquid to 1 GPa, quickly quenched it to a temperature of 77 K, and then released the pressure to 0.1 GPa. Low-pressure glasses were created at

0.1 GPa by cooling to 77 K.

The studies were carried out using a piston-cylinder high-pressure apparatus [2]. Since dipropylene glycol is liquid under normal conditions, we used thin-walled Teflon capsules with copper caps to contain the substance. Capsule diameter 18 mm, height 8-10 mm. To measure the ultrasound velocity, transverse waves with a frequency of 5 MHz and longitudinal waves with a frequency of 10 MHz were passed through the sample. The transit time was measured with an accuracy of 1 ns, and the change in the sample length with an accuracy of 1 μm. Bulk modulus *B* and shear modulus *G* were calculated in the approximation of a homogeneous isotropic medium.

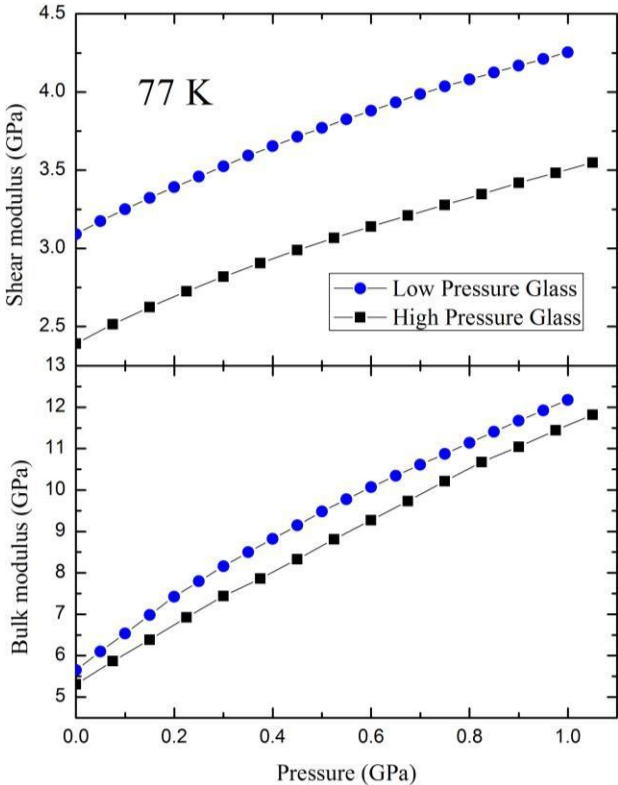


Fig. 1 Pressure dependences of the shear and bulk modulus at 77 K for dipropylene glycol glasses with different thermobaric histories

High-pressure densified dipropylene glycol had higher elastic moduli than low-pressure glass. While the difference in the densities of glasses obtained at 0.1 GPa and 1 GPa turned out to be only 5%, the moduli of compacted glass turned out to be significantly higher than that of ordinary glass. For the bulk modulus, this difference was 7%, and for the shear modulus, 30% (Fig 1). During heating before devitrification, the elastic characteristics approached each other, completely coinciding immediately before T_g . In the liquid, of course, there were no differences. Thus, we have shown that, by changing the production protocol, it is possible to design glasses with desired properties.

The study was supported by the Russian Science Foundation, scientific project No. 22-22-00530.

References

- I. V. Danilov, E. L. Gromnitskaya and V. V. Brazhkin, *J. Phys. Chem. B*, 2016, **120**, 30, 7593– 7597
A. G. Lyapin, E. L. Gromnitskaya, I. V. Danilov and V. V. Brazhkin, *RSC Adv.*, 2017, **7**, 33278- 33284.

Structural transformations in Type II Multiferroic and Probable Topological Nontrivial Insulator $MnSb_2Se_4$ under High Pressure

Anjana Joseph^{1,2}*, Rahul Kumar^{1,2}, A. Sundaresan^{1,2}, Chandrabhas Narayana^{1,2}

Chemistry and Physics of Materials Unit, Jawaharlal Nehru Centre for Advanced Scientific Research, Jakkur, 560064, Bangalore, India

School of Advanced Materials, Jawaharlal Nehru Centre for Advanced Scientific Research, Jakkur, 560064, Bangalore, India

Keywords: High pressure, Raman spectroscopy, Synchrotron X-Ray Diffraction

*e-mail: anjana@jncasr.ac.in

The electronic, magnetic, and topological characteristics of transition metal chalcogenides in the family AB_2X_4 (where A = Fe, Mn; B = Sb, Bi; and X = S, Se, Te) has attracted the researchers after the recent experimental observation of Quantum Anomalous Hall Effect (QAHE) in $MnBi_2Te_4$ [1-3]. Recently, spin-induced multiferroicity was experimentally established in $MnSb_2S_4$ (space group: $C2/m$) [3]. According to reports on isostructural compounds, $MnSb_2Se_4$ is a type II multiferroic with strong magneto-electric coupling and it undergoes a long-range antiferromagnetic ordering at $T_N = 22.5$ K whereas $MnSb_2Te_4$ has a rhombohedral structure with a ferromagnetic

ground state [4-5]. Recent studies on layered MnSb₂Se₄ ($R\bar{3}m$: $E_g = 258.3$ meV) based on first-principle calculations predicted that MnSb₂Se₄ could be easily converted into Weyl semimetal by applying a pressure ~ 0.85 GPa and to a 3D anti-ferromagnetic topological insulator at ~ 2.45 GPa [6]. Here we report a detailed high pressure Raman Spectroscopy and synchrotron X-ray diffraction studies (XPRESS beamline, ELETTRA) on polycrystalline MnSb₂Se₄ till 9 GPa exploring the topological and structural transitions. All measurements were carried out using Diamond Anvil Cell. The analysis of Raman spectra and the Rietveld refinement of XRD pattern reveals that it crystallises in C2/m monoclinic phase at ambient conditions. Under pressure the material shows some intriguing Raman mode behaviour, with some Raman modes softening under high pressure and some others hardening along with the clear structural transition visible after

2.5 GPa. Pressure evolution of Raman modes and their full width at half maximum (FWHM) show slope changes at ~ 1.5 GPa and ~ 2.5 GPa. The synchrotron XRD results show two structural transitions at ~ 2.5 GPa and at ~ 5 GPa with the coexistence of phases over some pressure ranges. The structural transformations are reversible, as evidenced by the appearance of the C2/m phase Raman spectra after the pressure is released. The results are analysed in connection with the recent theoretical predictions by Zhang et.al.

References:

- Y. Deng, Y. Yu, M. Z. Shi, Z. Guo, Z. Xu, J. Wang, X. H. Chen, Y. Zhang, *Science* **367**, 6480 (2020)
H. Sun, B. Xia, Z. Chen, Y. Zhang, P. Liu, Q. Yao, H. Tang, Y. Zhao, H. Xu, and Q. Liu, *Phys. Rev. Lett.* **123**, 096401 (2019).
C. De, N. V. Ter-Oganessian, A. Sundaresan, *Phys. Rev. B* **98**, (17)174430 (2018)
R. Kumar and A. Sundaresan, *Materials Research Bulletin* **145**, 111569 (2022)
T. Murakami, Y. Nambu, T. Koretsune, G. Xiangyu, T. Yamamoto, C. M. Brown, H. Kageyama, *Phys. Rev. B* **100**, (2019)
H. Zhang, W. Yang, Y. Wang, and X. Xu, *Phys. Rev. B* **103**, 094433 (2021)

Compressibility of chemical compounds

Andrzej Katrusiak

*Department of Materials Chemistry, Faculty of Chemistry, Adam Mickiewicz University, Uniwersytetu
Poznańskiego 8, 61-614 Poznan, Poland*

Compressibility and thermal expansion belong to the most basic properties of all matter. The description of these properties can be connected with the foundations of thermodynamics and of all materials sciences. The compressibility and thermal expansion of solids have the

form of tensors, which reflect the symmetry, crystal structure, chemical composition and cohesion forces. Traditionally, compressibility is the inverse of the hardness of solid materials and it is considered a static property related to equilibrated systems. The hardness, bulk modulus, Young modulus, and Poisson's ratio, clearly depend not only on the material itself, but also on the mode of applying the stress. In recent decades, owing to the ingenious inventions of high-pressure devices, particularly the diamond anvil cell, as well as spectacular improvements in the measuring equipment, such as powerful radiation sources, area detectors, diffractometry, computational hardware and software, the compressibility measurements have significantly increased in numbers and precision and they have expanded to all fields of materials sciences. Compressibility continues to be the most basic macroscopic property, but at the same time, it provides increasingly more refined characteristics pertaining to the microscopic structure. This poses new questions regarding the validity of the compressibility calculations, which in traditional solid-state physics could be performed just for the monotonic compression regions of a given chemical compound. Presently, gradual chemical changes induced in chemical compounds have been observed for specific phases, without distinct phase transitions. For example, a gradual conformation change can occur in a given compound, or a charge-transfer complex gradually changes the rate of the electron transfers between the neutral and ionic states, which is reflected in the crystal compression. Other examples of possible transformations and the measurement techniques affecting the compressibility determination will be discussed [1-6].

1. Roszak K, Katrusiak A. *High-pressure and environment effects in selenourea and its labile crystal field around molecules. Acta Crystallogr. B77, 2021,449–455.*
2. Cai W. et al. *Giant Negative Area Compressibility Tunable in a Soft Porous Framework Material. J. Am. Chem. Soc., vol. 137, 2015, 9296–9301.*
3. P. A. Guńka et al., "Compressed Arsenolite As₄O₆ and Its Helium Clathrate As₄O₆·2He," *Cryst. Growth Des.*, 15, 2015, 3740–3745.
4. Zakharov B. A. et al. *The role of fluids in high-pressure polymorphism of drugs: different behaviour of b-chlorpropamide in different inert gas and liquid media. RSC Adv. 6, 2016, 92629–92637.*
5. Bhattacharyya S. et al., "Dynamic Resolution of Piezosensitivity in Single Crystals of π -Conjugated Molecules," *Chem. Eur. J.* 25, 2019, 6092–6097.
6. Collings I.E., Hanfland M. *Effect of synchrotron X-ray radiation damage on phase transitions in coordination polymers at high pressure. Acta Cryst. B78, 2022,100-106*

Universal Hydrogen Bond Symmetrisation Dynamics under extreme Conditions

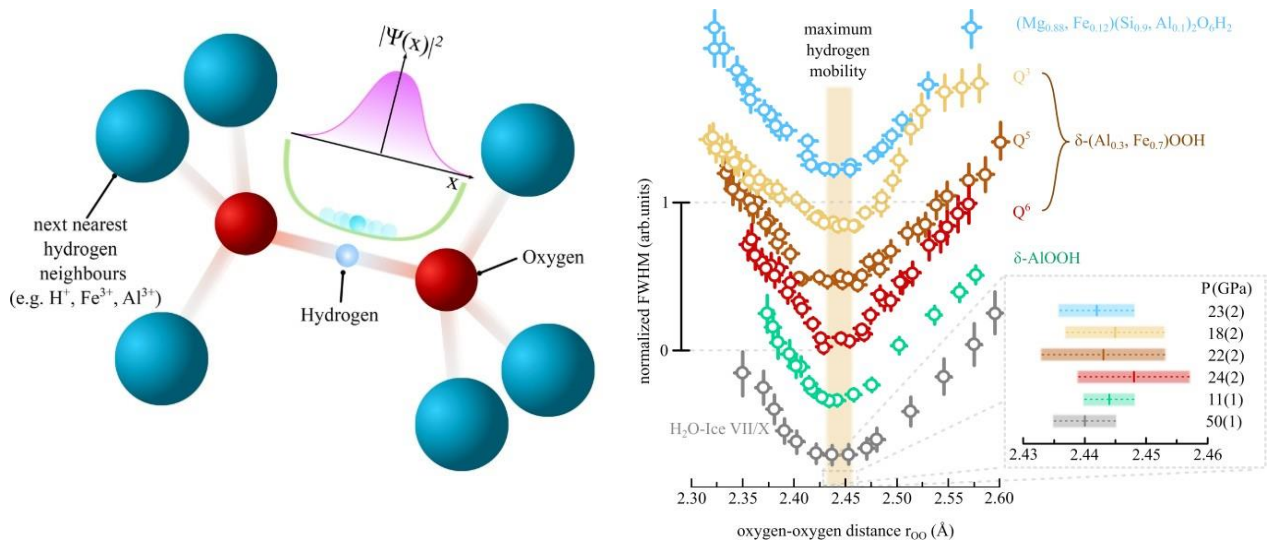
Thomas Meier, Florian Trybel, Saiana Khandarkhaeva, Dominique Laniel, Takayuki Ishii, Alena Aslandukova, Natalia Dubrovinskaia & Leonid Dubrovinsky

The experimental study of hydrogen-bonds and their symmetrization under extreme conditions is predominantly driven by diffraction methods, despite challenges of localising or probing the hydrogen subsystems directly. Until recently, H-bond symmetrization has been addressed in terms of either nuclear quantum effects, spin crossovers or direct structural transitions; often leading to contradictory interpretations when combined. Here, we present high-resolution in-situ $^1\text{H-NMR}$ experiments in

diamond anvil cells investigating a range of systems containing linear $\text{O-H}\cdots\text{O}$ units at pressure ranges of up to 90 GPa covering their respective H-bond symmetrization. We found pronounced minima in the

pressure dependence of the NMR resonance line-widths associated with a maximum in hydrogen mobility, precursor to a localisation of hydrogen atoms. These minima, independent of the chemical environment of the $\text{O-H}\cdots\text{O}$ unit, can be found in a narrow range of oxygen oxygen distances between

2.44 and 2.45 Å, leading to an average critical oxygen-oxygen distance of 2,443(1) Å.



References:

- Meier, T., Trybel, F., Khandarkhaeva, S., Laniel, D., Ishii, T., Aslandukova, A., Dubrovinskaia, N., & Dubrovinsky, L. (2022). Structural independence of hydrogen-bond symmetrisation dynamics at extreme pressure conditions. *Nature Communications*, 13(1), 1–8.
- Meier, T., Aslandukova, A., Trybel, F., Laniel, D., Ishii, T., Khandarkhaeva, S., Dubrovinskaia, N., & Dubrovinsky, L. (2021). In situ high-pressure nuclear magnetic resonance crystallography in one and two dimensions. *Matter and Radiation at Extremes*, 6(6), 068402.
- Trybel, F., Meier, T., Wang, B., & Steinle-Neumann, G. (2021). Absence of proton tunneling during the hydrogen-bond symmetrization in delta-AlOOH. *Physical Review B*, 104(10), 104311.
- Trybel, F., Cosacchi, M., Meier, T., Axt, V. M., & Steinle-Neumann, G. (2020). Proton dynamics in high-pressure ice-VII from density functional theory. *Physical Review B*, 102(18), 184310.
- Meier, T., Petitgirard, S., Khandarkhaeva, S., & Dubrovinsky, L. (2018). Observation of nuclear quantum effects and hydrogen bond symmetrisation in high pressure ice. *Nature Communications*, 9(1), 2766.

Stability of the tetragonal phase of BaZrO₃ under high pressure

Constance Toulouse¹, Danila Amoroso², Robert Oliva¹, Cong Xin^{3,4}, Pierre Bouvier⁵, Pierre Fertey⁶, Philippe Veber⁷, Mario Maglione³, Philippe Ghosez², Jens Kreisel¹, and Mael Guennou¹

¹University of Luxembourg, Luxembourg

²Université de Liège, Belgium

³Institut de Chimie de la Matière Condensée de Bordeaux, France

⁴Luxembourg Institute of Science and Technology (LIST), Luxembourg

⁵Institut Néel CNRS, Grenoble, France

⁶Synchrotron SOLEIL, Gif-sur-Yvette, France

⁷Institut Lumière Matière CNRS, Villeurbanne, France

We revisit the high-pressure behavior of BaZrO₃ by a combination of first-principle calculations, Raman spectroscopy and x-ray diffraction under high pressure. We confirm experimentally the cubic-to-tetragonal transition at 10 GPa and find no evidence for any other phase transition up to 45 GPa, the highest pressures investigated, at variance with past reports. Contradictions in past reports of Raman spectroscopy experiments in particular are explained based on the specifics of the competing phases. We reinvestigate phase stability with density functional theory considering not only the known tetragonal (I4/mcm) phase but also other potential antiferrodistortive candidates. This shows that the tetragonal phase becomes progressively more stable upon increasing pressure as compared to phases with more complex tilt systems. The possibility for a second transition to another tilted phase at higher pressures, and in particular to the very common orthorhombic Pnma structure, is therefore ruled out.

High-pressure and high-temperature chemistry of phosphorus and nitrogen: synthesis and characterization of α - and γ -P₃N₅

Matteo Ceppatelli^{*,a,b}, Demetrio Scelta^{a,b}, Manuel Serrano-Ruiz^a, Kamil Dziubek^a, Fernando Izquierdo-Ruiz^{c,d}, J. Manuel Recio^c, Gaston Garbarino^e, Volodymyr Svitlyk^e, Mohamed Mezouar^e, Maurizio Peruzzini^a, Roberto Bini^{a,b,f}

^aICCOM-CNR, Institute of Chemistry of OrganoMetallic Compounds, National Research Council of Italy, I-50019 Sesto Fiorentino, Firenze, Italy

^bLENS, European Laboratory for Non-linear Spectroscopy, I-50019 Sesto, Fiorentino, Firenze (Italy)

^cMalta-Consolider Team and Departamento de Química física y Analítica, Universidad de Oviedo, 33006 Oviedo, Spain

^dDepartment of Chemistry and Chemical Engineering, Chalmers University of Technology, Gothenburg 412 96, Sweden

^eESRF, European Synchrotron Radiation Facility, 38000 Grenoble, France

^fDipartimento di Chimica "Ugo Schiff", Università degli Studi di Firenze, I-50019 Sesto Fiorentino, Firenze, Italy

*corresponding author: matteo.ceppatelli@iccom.cnr.it and ceppa@lens.unifi.it

Due to the high stability of the N_2 molecule, the direct chemical reactivity between phosphorus and nitrogen requires challenging pressure and temperature conditions and has remained essentially unexplored so far. While crystalline α - P_3N_5 was obtained in 1997 using chemical precursors [1] and γ - P_3N_5 in 2001 by high-temperature compression of α - P_3N_5 [2], the synthesis of γ - P_3N_5 from the reaction of phosphorus and nitrogen at high pressure and high temperature, firstly reported during the 2018 EHPRG Meeting [3] and the 2019 IUCr-ECA high-pressure workshop [4], has been published only recently [5,6]. In this study the direct chemical reactivity between phosphorus and nitrogen was induced under high-pressure and high-temperature conditions (9.1 GPa, 2000-2500 K), generated by a laser-heated Diamond Anvil Cell, and studied by synchrotron X-ray diffraction, Raman spectroscopy and DFT calculations. α - P_3N_5 and γ - P_3N_5 were identified as reaction products. The structural parameters and vibrational frequencies of γ - P_3N_5 were characterized during room temperature compression and decompression to ambient conditions, determining the equation of state of the material up to 32.6 GPa and providing insight about the lattice dynamics of the unit cell during compression, which essentially proceeds through the rotation of the PN_5 square pyramids and the distortion of the PN_4 tetrahedra. While the identification of α - P_3N_5 demonstrates for the first time the direct synthesis of this phosphorus nitride polymorph from the elements, its detection in the outer regions of the laser-heated area suggests α - P_3N_5 as an intermediate step in the progressive nitridation of phosphorus towards the formation of γ - P_3N_5 , with increasing coordination number of P by N from 4 to 5. No evidence of a higher-pressure phase transition was observed, questioning the existence of predicted structures containing octahedral hexa-coordinated P atoms in the investigated pressure range.

References

- [1] Horstmann, S. et al. *Angew. Chem. Int. Ed.* 1997, 36, 1873-1875.
- [2] Landskron, K. et al. *Angew. Chem. Int. Ed.* 2001, 40, 2643-2645.
- [3] Ceppatelli, M. et al. 56th EHPRG Meeting, 02-07/09/2018 Aveiro, Portugal.
- [4] Scelta, D. et al. IUCr-ECA High-Pressure Workshop, 13–17/08/2019, Wien, Austria.
- [5] Niwa, K. et al. *J. Raman Spectrosc.* 2021, 52, 1064-1072.
- [6] Ceppatelli, M. et al. *Inorg. Chem.* 2022 doi:10.1021/acs.inorgchem.2c01190.

Acknowledgements

PHOSFUN (ERC-Advanced Grant 670173), Deep Carbon Observatory (DCO), GreenPhos-alta pressione (CNR), HP-PHOTOCHEM (FCRF), PRIN-2017-KFY7XF-FERMAT (MUR), ESRF, AEI (PGC18-094814-B-C22, RED2018-102612-T), FICYT and FEDER (AYUD/2021/51036, AYUD/2021/58773).

Acoustic wave velocities in Mars' mantle minerals.

Caroline Bollinger, Frédéric Béjina, Misha Bystricky, Pascal Munsch.

With the successful landing of a seismometer (SEIS) at the surface of Mars (Mars InSight mission), the interior structure of the red planet is now better constrained. However, these advances raise further questions as other teleseismic events are still being recorded and mineralogical models of the interior of Mars are debated.

Mineral physics experiments conducted at high temperature and pressure (HT/HP) are essential to accurately measure the physical properties of the materials that potentially constitute the Martian mantle. These properties, for example the thermoelastic parameters of possible mantle mineral phases, are needed to interpret the seismic data and construct accurate models of mineralogical composition and structure of the martian upper mantle. The inversion of seismic and geodetic data depends on density, seismic velocities and rheology, properties themselves related to the presence of mineral phases at equilibrium, liquidus and solidus curves, equations of state, thermoelastic and viscoelastic properties of the constituent materials at Martian P, T conditions.

We present here preliminary results on the elastic properties measured in representative minerals from Mars' mantle. The experiments were carried out on synthetic aggregates (olivine and pyroxenes, $\text{Fe}/(\text{Fe}+\text{Mg}) = 0.25$) under HP-HT (from room PT conditions up to 12 GPa and 1200°C) in a large volume press on a synchrotron light line (APS, Chicago, USA). Equations of state and sound wave velocities were determined by coupled synchrotron X-ray diffraction and ultrasonic interferometry. Implications for the mineralogical composition of the upper mantle of Mars will be discussed.

High-pressure tuning of $d-d$ electronic transitions and bandgap in cobalt iodate, $\text{Co}(\text{IO}_3)_2$

A. Liang,¹ F. Rodríguez,² P. Rodríguez-Hernandez,³ A. Muñoz,³ R. Turnbull^{1,*} and D. Errandonea¹

¹ *Departamento de Física Aplicada—ICMUV, Universitat de València, MALTA Consolider Team, Edificio de Investigación, c/ Dr. Moliner 50, 46100 Burjassot, Valencia, Spain*

² *DCITIMAC, MALTA Consolider Team, Facultad de Ciencias, Universidad de Cantabria, 39005 Santander, Spain*

³ *Departamento de Física and Instituto de Materiales y Nanotecnología, MALTA Consolider Team, Universidad de La Laguna, 38206 La Laguna, Tenerife, Spain*

* Presenting author

High pressure optical absorption measurements on $\text{Co}(\text{IO}_3)_2$ allow simultaneous observation of the optical bandgap energy and the $d-d$ electronic transitions associated with associated with Co^{2+} . In this work we combine high-pressure optical-absorption, X-ray diffraction and density functional theory calculations to show that changes in the bandgap energy and $d-d$ electronic transitions are closely related to subtle structural changes related to the crystal field, ultimately yielding a non-linear pressure-evolution of the bandgap and enhancement of the symmetry of CoO_6 octahedra. The enhanced symmetry has a strong influence on the optical absorption spectra, thereby revealing a structural phase transition at 7.3 GPa. Changes in the $d-d$ transition energies also support the existence of such a phase transition.

High-pressure polymerisation of CS_2 : “Bridgman’s black” revisited

S. Klotz^{a,1}, B. Baptiste^a, T. Hattori^b, S.M. Feng^c, Ch. Jin^c, K. Béneut^a, J.M. Guigner^a, I. Estève^a

^a*Institut de Minéralogie, de Physique des Matériaux et de Cosmochimie (IMPMC), CNRS UMR7590, Sorbonne Université, 4 Place Jussieu, 75252 Paris, France*

^b*J-PARC Center, Japan Atomic Energy Agency, 2-4 Shirakata, Tokai, Ibaraki 319-1195, Japan*

^c*Institute of Physics, Chinese Academy of Sciences (IOPCAS), School of Physics, University of Chinese Academy of Sciences(UCAS), Beijing 100190, China*

It is known since decades that carbon disulphide (CS_2) transforms under pressure of a few GPa and under moderate high temperatures irreversibly into a polymeric 3-dimensional solid (“Bridgman black”) with complex structure containing multiple-types of C-C, C-S and S-S bonds [1-5]. Here we show that by compression at 300 K to ~ 7 GPa using large-volume Paris-Edinburgh devices, an instantaneous reaction leads to a mixture of pure sulphur and a well-defined compound with stoichiometry close to C_2S . The availability of macroscopic sample quantities enables an in-depth characterisation of the reaction product by applying a variety of techniques, in particular x-ray and neutron diffraction, Raman scattering, infrared absorption, density and resistivity measurements [6]. We find that this material is fundamentally different to Bridgman black and consists of sulphur bonded to sp^2 graphite layers of nanometric dimension, with some similarity to graphene oxide. The compound is a semiconductor with a gap of 45 meV and a conductivity 13 orders of magnitude higher than found in the 3D C-S polymer known so far. The material can be easily produced in cm^3 quantity and may have technological applications.

[1] P.W. Bridgman, *Proc. Amer. Acad. Arts Sci.* **74**, 399-424 (1942).

[2] B. Ochiai, & T. Endo, *Prog. Polym. Sci.* **30**, 183-215 (2005).

[3] E. Whalley, *Can. J. Chem.* **38**, 2105 (1960).

[4] E.G. Butcher, M. Alsop, J.A. Weston & H.A. Gebbie, *Nature* **199**, 756 (1963).

[5] W.S. Chan & A.K. Jonscher, *Phys. stat. sol.* **32**, 749 (1969).

[6] S. Klotz, B. Baptiste, T. Hattori, S.M. Feng, Ch. Jin, K. Béneut, J.M. Guigner, I. Estève, *Carbon* **185**, 491 (2021)

Melting curve of indium at high pressure measured by picosecond acoustics

Simon Ayrinhac^{1*}, Michel Gauthier¹, Marc Morand¹, Yiuri Garino¹, Silvia Boccato¹, Frédéric Decremps¹, Paraskevas Parisiades¹, Philippe Rosier^{1,2}, Nicki C. Siersch¹, Abderraouf Seghour¹, and Daniele Antonangeli¹

¹*Institut de Minéralogie de Physique des Matériaux et de Cosmochimie (IMPMC), Sorbonne Université, CNRS UMR 7590, Muséum National d'Histoire Naturelle, 4 Place Jussieu, F-75005 Paris, France*

²*Laboratoire de Physique des 2 Infinis Irène Joliot-Curie (IJCLab), Université Paris-Saclay, CNRS UMR 9012, 91405 Orsay, France*

Keywords: picosecond acoustics technique, phase diagram, melting line, indium

*e-mail: simon.ayrinhac@sorbonne-universite.fr

Picosecond acoustics (PA) is a time-resolved optical pump-probe technique based on reflectivity measurements used to study the propagation of acoustic waves in a large variety of samples [1, 2]. When associated with resistively heated diamond anvil cell (hDAC), it allows very accurate determination of thermoelastic properties including melting curves and phase diagrams [3, 6]. With such experiments it is possible to simultaneously measure pressure and temperature, transit time or surface phonon imaging, and to deduce the physical state of the sample (liquid or solid) as demonstrated thereafter on indium.

Indeed, although the melting temperature T_M^0 of In is very well known at ambient pressure [4], its melting curve above few GPa measured by several authors using different techniques shows significant discrepancies (see [5] and Figure 1).

In this work, particular care is devoted to the p-T metrology. The accuracy and consistency of the p-T measurements are checked with two *in-situ* calibrants (chromium-doped corundum, $\alpha\text{-Al}_2\text{O}_3\text{:Cr}^{3+}$ and samarium-doped strontium tetraborate, $\text{SrB}_4\text{O}_7\text{:Sm}^{2+}$) in addition to a thermocouple glued on the rear side of the diamond.

The melting curve is determined using two methods: first with the observation of a discontinuity in the sound velocity upon increasing or decreasing of the pressure at constant temperature [6], second monitoring the p-T liquid and solid phases equilibrium conditions.

The latter is usually applied to transparent samples [7, 8], but despite the nontransparency of In, PA technique allows to finely probe its thermodynamical state [3]. Finally, the experimental melting curve is well-fitted [3] up to 6 GPa by a Simon-Glatzel curve

$$T_M(p) = T_{ref} \left(\frac{p - p_{ref}}{a} + 1 \right)^{1/c}$$

where $a=4.61(11)$ GPa, $c=1.792(34)$, $p_{ref} = 0$ GPa, and $T_{ref} = T_M^0 = 429.74850(34)$ K [4].

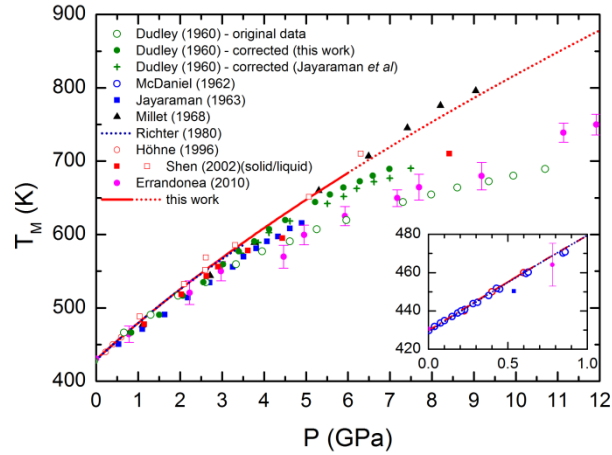


Figure 1. The In melting curve determined using picosecond acoustics (red line), extrapolated above 6 GPa (red dotted line) and compared with the literature data.

1. F. Decremps et al, *Ultrasonics*, 56 129 (2015)
2. S. Boccatto et al, *Phys. Chem. Miner.*, 49(6) 1 (2022)
3. S. Ayrinhac et al, *Phys. Rev. Mat.*, 6(6) 063403 (2022)
4. H. Preston-Thomas, *Metrologia*, 27 3 (1990)
5. D. Errandonea, *J. Appl. Phys.* 108, 033517 (2010)
6. S. Ayrinhac et al, *J. Phys.: Condens. Matter*, 27 275103 (2015)
7. F. Datchi et al, *Phys. Rev. B*, 61 6535 (2000)
8. V. M. Giordano et al, *J. Chem. Phys.*, 125 054504 (2006)

Formation and stability of dense methane-hydrogen compounds

Umberto Luca Ranieri^{1,2}, Lewis J. Conway³, Mary-Ellen Donnelly¹, Huixin Hu¹, Mengnan Wang¹, Philip Dalladay-Simpson¹, Miriam Peña-Alvarez³, Eugene Gregoryanz^{1,3,4}, Andreas Hermann³, Ross T. Howie^{1,3}

¹Center for High Pressure Science and Technology Advanced Research, 1690 Cailun Road, Shanghai, 201203, China

²Dipartimento di Fisica, Università di Roma La Sapienza, Piazzale Aldo Moro 5, 00185 Rome, Italy ³Centre for Science at Extreme Conditions and The School of Physics and Astronomy, The University of Edinburgh, Peter Guthrie Tait Road, Edinburgh, United Kingdom

⁴Key Laboratory of Materials Physics, Institute of Solid State Physics, CAS, Hefei, China

In the outer Solar System, methane and hydrogen are the most common molecules aside from water, so their interaction in extreme conditions is important for understanding the evolution and interior dynamics of Neptune and Uranus, for example. For the past 25 years, some methane-hydrogen inclusion compounds have been known to form below 10 GPa [1]. Their Raman signatures have also appeared at higher pressures in various experimental studies investigating hydrocarbons at deep-Earth conditions or synthesizing high-temperature superconducting hydrides, but were never formally identified.

Through a series of x-ray diffraction and Raman spectroscopy diamond anvil cell experiments, combined with density functional theory calculations, we have systematically investigated the dense CH₄-H₂ binary system at high pressure and room temperature [2]. We find that in CH₄-rich mixtures, tetragonal (CH₄)₂H₂ forms above 4.6 GPa. In H₂-rich mixtures, we observe the formation of hexagonal CH₄(H₂)₂ above 5 GPa, before partially transforming into monoclinic (CH₄)₃(H₂)₂₅ at 10-15 GPa. The three compounds persist over a remarkably broad pressure regime, exceeding 160 GPa. We do not observe CH₄H₂ and CH₄(H₂)₄, which have been previously claimed [1].

(CH₄)₂H₂ shares its Al₂Cu-type structure with (H₂S)₂H₂ and (CH₄)_x(H₂S)_{2-x}(H₂) [3] and exhibits extreme hardening of the H₂ intramolecular vibrational mode with pressure. CH₄(H₂)₂ has the structure of the hexagonal Laves phase of MgZn₂, which is also formed at high pressure by Ar(H₂)₂ [4]. (CH₄)₃(H₂)₂₅, which has been previously observed by Raman in the literature but has been wrongly identified as CH₄(H₂)₂, represents a unique composition and is the first stoichiometric compound to surpass 50 wt% H₂. It has a methane sublattice similar to that of the Xenon atoms in Xe(H₂)₈ [5] and holds a vast amount of molecular hydrogen.

It is likely that methane can retain its molecular character to much more extreme conditions than previously considered by forming such host-guest compounds with hydrogen. From a planetary context, the formation of methane-hydrogen compounds could influence critical

properties of planetary matter, such as thermal conductivities and viscosities. We estimate that the melting temperatures of each compound are substantially different from either methane or hydrogen. From a materials science context, $(\text{CH}_4)_2\text{H}_2$ exhibits an extremely high H_2 intramolecular vibrational frequency combined with a high Debye temperature, both of which are promising ingredients for high- T_c superconductivity. Moreover, if these compounds can form at low pressures (for example by adjusting the temperature), they have the potential for use in hydrogen storage.

M. Somayazulu et al., Science 271, 1400–1402 (1996)

U. Ranieri et al., Phys. Rev. Lett. 128, 215702 (2022)

[3] *E. Bykova et al., Phys. Rev. B 103, L140105 (2021)* [4] *C. Ji et al., PNAS 114, 3596–3600 (2017)*

[5] *M. Somayazulu et al., Nature Chem. 2, 50–53 (2010)*

Synthesis of van der Waals Ga_2S_3 structures under high pressure

Samuel Gallego Parra

New van der Waals (vdW) materials with novel properties are expected to be synthesised to face technological challenges. One of them requires abundant, non-toxic elements as constituents and green synthesis. These requirements are difficult to meet, basically due to the presence of rare-earth, toxic elements (Bi, As, Sb, Te...). Furthermore, these vdW materials have own the capacity of tailoring their properties, such as strong dipole moment, piezoelectricity and pyroelectricity are being demanded. In this way, ferroelectric-to-paraelectric phase transition (PT) can be driven by high temperature (HT) or varying composition.

We are witnessing the A_2X_3 (A=Al, Ga, In; X=S, Se, Te) compounds being studied to find ferroelectric and paraelectric vdW materials. Among all these compounds, only In_2Se_3 exhibits these structures experimentally: $\alpha\text{-In}_2\text{Se}_3$ (space group (s.g.) $R\bar{3}m$, hexagonal, No. 160, Z=3, non-centrosymmetric), stable at room temperature (RT), and $\beta\text{-In}_2\text{Se}_3$ (s.g. $R\bar{3}m$, hexagonal, No. 160, Z=3, centrosymmetric), observed at HT [1-3]. For the rest of this family, a few theoretical works have highlighted possibilities for obtaining such vdW structures and switching them via increasing/decreasing temperature. More precisely, $\alpha\text{-In}_2\text{Se}_3$ -like structure is dynamically stable for the all family at RT [4], unlike the $\beta\text{-In}_2\text{Se}_3$ - like structure [5]. However, this structure becomes stable above the theoretical T_c calculated, following a tendency of $\text{Al}_2\text{X}_3 > \text{Ga}_2\text{X}_3 > \text{In}_2\text{X}_3$ [4].

When it comes under extreme conditions, such as high pressure, related to both structures, α - In_2Se_3 undergoes a PT to β - In_2Se_3 at above 10-12 GPa, after transforming into β' - In_2Se_3 at 1 GPa [6]. Among this family of compounds, just α' - Ga_2S_3 happens to turn into β - In_2Se_3 -like structure (β' - Ga_2S_3) at about 16 GPa [7]. Evidence of such PT has been stressed in subsequent works [8, 9]. What is more unexpected, after this α' - β' PT on Ga_2S_3 , two other polymorphs have been synthesized upon decreasing pressure, at 9.0 and 3.0 GPa, respectively [8]. However, further information about the nature of both polymorphs was not given.

In this work, we have confirmed this β' - Ga_2S_3 under HP via XRD and Raman measurements, joint theoretical simulations. Upon decreasing pressure, α - In_2Se_3 -like structure matches quite well with the 1st polymorph observed at 9.0 GPa (ϕ - Ga_2S_3). Raman signatures and pressure dependence of structural parameters have allowed us to discern such β' - ϕ PT. The 2nd polymorph below 1.0 GPa has been identified with a disordered zincblende (γ - Ga_2S_3). To complement our results, we discuss the relation between the PTs of both Ga_2X_3 and AGa_2X_4 compounds.

[1] J. Ye et al., *J. Appl. Phys.* 1998, **37**, 4264-4271.

[2] K. Osamura et al., *J. Phys. Soc. Jpn.* 1966, **21**, 1848-1848.

[3] G. Han et al., *Small* 2014, **10**, 2747-2765.

[4] J. Liu et al., *2D Mat.* 2019, **6**, 025001.

Y.-T. Huang et al., *Appl. Phys. Rev.* 2021, **8**, 031413.

R. Vilaplana et al., *Inorg. Chem.* 2018, **57**, 8241-8252. [7] X. Lai et al., *J. Appl. Phys.* 2014, **116**, 193507.

[8] L. Yang et al., *J. Mater. Chem. C* 2021, **9**, 2912-2918.

[9] S. Gallego-Parra et al., *Phys. Chem. Chem. Phys.* 2021, **23**, 6841-6862.

Elasticity and the post-stishovite transition of eclogitic stishovite: Insights from in-situ XRD and ultrasonic interferometry

A. Rosenthal^{1,2*}, W. A. Crichton¹, A. R. Thomson³, J. P. Brodholt³

¹ID06-LVP, ESRF - The European Synchrotron

²Research School of Earth Sciences, The Australian National University

³Department of Earth Sciences, University College London

*anja.rosenthal@esrf.fr

Al-bearing stishovite and, later, post-stishovite are among the chief hydrogen-bearing phases in subducted oceanic crust (eclogite) at lower mantle conditions¹, being able to carry up to ~0.3 wt. % of H₂O¹⁻⁴. H₂O-bearing Al-stishovite was recently suggested to cause seismic discontinuities and heterogeneities in the deep Earth's lower mantle depths at ~1000 km depth⁵.

The incorporation of Al into stishovite leads to significant changes to its phase diagram and ability to take up H₂O^{5,6}. For instance, it halves the pressure required for its rutile- to CaCl₂-type transformation, which exhibits significant elastic softening and may be seismically observable^{5,6}.

A range of defective stishovite samples were synthesized between 15-32 GPa at ~1200 °C from glasses using 10/5, 10/4 and 7/3 multianvil assemblies. Recovered samples were double-polished (~0.5 mm thick) and quantitatively analysed by EPMA. Combined in-situ X-ray diffraction and ultrasonic interferometry, using 10/4 and 7/3 geometries, were conducted at ID06-LVP of the ESRF to ~32 GPa and 1800 K. In highly defective samples the onset of the transition to post-stishovite was accompanied by significant softening of shear wave velocities V_S . Therefore, the effect of Al- and H₂O-defects on the acoustic velocities of stishovite and an estimate of the role of defects in controlling the transformation pressure to the post-stishovite phase were assessed.

This study provides density and sound velocity measurements and thus, enable better experimental constraints of bulk elastic properties and their P and T derivatives of Al-H₂O-bearing stishovite at mantle-relevant P, T. This study extends information essential to the interpretation of the seismic observables and contribute to more complete modelling of subducted oceanic crustal material (i. e. eclogitic bodies) inside the Earth's deep mantle.

The study is supported by MSCA-IF 898169 'ELASTIC' to AR.

[1] Litasov et al (2007) *EPSL* **262**, 620-634

[2] Irifune & Ringwood (1993) *EPSL* **117**, 101-110

[3] Litasov & Ohtani (2005) *PEPI* **150**, 239-263

[4] Ono et al (2001) *EPSL* **190**, 57-63

[5] Lakshatanov et al (2007) *PNAS* **104**, 34, 13588-13590

[6] Lakshatanov et al (2005) *Phys Chem Miner* **32**, 466-470

VIPA-based Brillouin spectroscopy: a new tool for exploring the thermodynamics of warm dense molecular system

A. Forestier^{1,2}, G. Weck^{1,2}, F. Datchi³, P. Loubeyre^{1,2}

¹CEA, DAM, DIF, 91297 Arpajon Cedex, France

²Université Paris-Saclay, CEA, Laboratoire Matière en Conditions Extrêmes (LMCE), 91680 Bruyères-le-Châtel, France

³Institut de Minéralogie, de Physique des Matériaux et de Cosmochimie (IMPIC), Sorbonne Université, CNRS UMR 7590, 4 place Jussieu, 75005 Paris, France

Exploring the properties of simple molecular systems (essentially composed of C, H, N, O elements) at extreme pressures and temperatures ($P = 0 - 200$ GPa, $T = 1000 - 5000$ K) is of great interest both for fundamental physics and to model planetary interiors [1]. Ab-initio calculations have predicted rich phase diagrams with possibilities of interesting phenomena, like first order fluid-fluid transition, high protonic conduction in superionic states and rearrangement of molecular bonds [1,2]. Hitherto, measurements under these extreme conditions were mainly performed in dynamical, laser-induced shock studies. Thanks to recent developments of adapted sample confinements and optimized spectroscopic diagnostics, static experiments using diamond anvil cells (DAC) can now offer a detailed microscopic picture of these warm dense molecular systems, allowing direct comparison with ab-initio predictions and model refinements.

In this talk, we will show that in-situ Brillouin spectroscopy in the laser heated DAC is a powerful tool for probing these warm dense planetary interior states. Brillouin measurements provide sound velocities versus pressure and temperature. The fluid equation of state is obtained through thermodynamic integration [3], and sound velocity discontinuities are signature of phase transitions, such as melting.

Up to now, Brillouin measurements in DACs were almost exclusively performed using the Tandem Fabry-Perot (TFP) instrument. Based on the temporal scan of tunable Fabry-Perot etalons, spectrum acquisition typically takes a few minutes to a few hours, which is a severe drawback for laser heating experiments, in which one wishes to maintain stable temperatures and avoid chemical reactions or anvil breakage.

We have implemented a new approach for high-pressure Brillouin spectroscopy using a hyperfine spectrometer, which is based on the dispersion of the scattered light from a VIPA (Virtually Imaged Phased Array). The VIPA allows spectrum dispersion in space such as it can be recorded over a 2-dimensional CMOS sensor, allowing a drastic speed up in measurement time with respect to the TFP. We have implemented our hyperfine spectrometer along with the TFP interferometer on the same optical bench such as comparison in terms of signal-to-noise ratio, precision and spectral response could be performed [4].

We will illustrate the capabilities of the new technique by showing the first Brillouin measurements on nitrogen melting at high pressure. Brillouin spectra of excellent quality

could be recorded in 1 minute or less at conditions up to ~90 GPa and ~2000 K. Comparison with melting curves obtained via other experimental techniques [5] shows a good agreement.

VIPA-Brillouin spectroscopy has the potential to become an important platform to investigate the properties of warm dense molecular systems.

[1] Redmer et al. *Icarus* **211**, n°1, 798 (2011)

[2] Boates & Bonev, *Phys. Rev. Lett.* **102**, n°1, 015701 (2009)

[3] Ninet et al. *J. Chem. Phys.* **153**, n°11, 114503 (2020)

[4] Forestier et al. (2022, submitted)

[5] Weck et al. *Phys. Rev. Lett.* **119**, n°23 (2017)

High-pressure behavior of monoclinic $(\text{Eu}_{1-x}\text{Yb}_x)_2\text{O}_3$ solid solution: a spectroscopic study

M. T. Candela^{1,3}, F. Aguado^{2,3}, J. A. González^{2,3}, R. Valiente^{1,3}

¹ Applied Physics Department. University of Cantabria. Avda. Los Castros 48, 39005- Santander. Spain

² CITIMAC Department. University of Cantabria. Avda. Los Castros 48, 39005- Santander. Spain

³ Nanomedicine Group. IDIVAL. Avda. Cardenal Herrera Oria, 39011- Santander. Spain

Email: candelamt@unican.es

Materials based on rare-earth (RE) ions have attracted a lot of attention in the last decades due to their numerous applications in different fields (optics, electronics, biomedicine, etc). Among the RE-based systems, RE_2O_3 sesquioxides present interesting physical and chemical properties, such as low phonon energies or high- chemical stability. Eu_2O_3 and Yb_2O_3 belong to the RE_2O_3 family, and the former is commonly employed as an activator of RE-based phosphors due to the bright red luminescence of Eu^{3+} while the latter is an interesting compound for gate dielectric applications due to its high-k value [1,2]. Moreover, $(\text{Eu}_{1-x}\text{Yb}_x)_2\text{O}_3$ phosphors have been found to present interesting characteristics at ambient conditions since through energy transfer processes between Eu^{3+} and Yb^{3+} ions it is possible to obtain simultaneous visible (Eu^{3+}) and NIR (Yb^{3+}) emission upon Eu^{3+} excitation. [3]

At ambient conditions both Eu_2O_3 and Yb_2O_3 crystallize in the cubic bixbyite-type structure, commonly denoted as C-type (s.g. *Ia-3*), which is the characteristic phase of RE_2O_3 formed by small and middle sized RE ions. Eu_2O_3 can also crystallize in the monoclinic B-type structure (s.g. *C2/m*) after thermal treatments at temperatures above

~1050 °C. Meanwhile, RE₂O₃ formed by large RE ions exist in the hexagonal A-type conformation (s.g. *P-3m1*).

The high-pressure behavior of RE₂O₃ has been extensively studied by several research groups, however most of the studies have focused on the characterization of C-type polymorph over the B-type one. Moreover, the effect of pressure on RE₂O₃ impurified with other RE' ions in significant amounts has been scarcely studied under pressure although effects on phase sequence and transition pressures have been reported [4,5].

In this work, we study the high-pressure behavior of the monoclinic (Eu_{1-x}Yb_x)₂O₃ solid solutions prepared by the sol-gel Pechini method. The pressure evolution of these compounds has been determined by spectroscopic techniques, including Raman and Eu³⁺ photoluminescence measurements in the 0-15 GPa pressure range. Also, the high- pressure behavior of this compound has been compared to that of other RE₂O₃.

References

- [1] H. E. A. Mohamed et al. *J. Opt. Soc. Am. A*, 37 (11), C73, (2020).
- [2] T. Pan and W. Huang. *Appl. Surf. Sci.*, 255, 4979–4982, (2009).
- [3] M. T. Candela et al. *J. Alloys Compd.*, 921, 166043, (2022).
- [4] K. A. Irshad, et al. *J. Alloys Compd.*, 725, 911–915, (2017).
- [5] K. A. Irshad et al. *Sci. Rep.*, 10(1), 1–9 (2020).

Correlation between spectroscopic and mechanical properties of gold nanocrystals under pressure

Camino Martín-Sánchez^{1*}, Ana Sánchez-Iglesias², Paul Mulvaney³, Luis M. Liz- Marzán^{2,4} and Fernando Rodríguez¹

¹MALTA Consolider, University of Cantabria, Facultad de Ciencias, Santander 39005, Spain

²CIC biomaGUNE and CIBER-BBN, Donostia- San Sebastián 20014, Spain ³ARC Centre of Excellence in Exciton Science, Victoria 3010, Australia ⁴Ikerbasque, Basque Foundation for Science, Bilbao 48013, Spain

*e-mail: martinsc@unican.es

In the last ten years, there has been significant progress in the use of metallic nanoparticles for sensing in pressure experiments [1-9]. Particularly, those methods based on optical spectroscopy are very attractive, since they exploit the high sensitivity of surface plasmonic resonances (SPR) in metal nanoparticles (NP).

Under a hydrostatic load, it is assumed that the NP compresses isotropically, thus retaining their shape under pressure. Nonetheless, under non-hydrostatic conditions the stresses along the different axes of the nanoparticles differ, inducing changes in the NP morphology. These effects have been directly observed using optical absorption spectroscopy measurements on gold nanorods (AuNR), the SPR and absorption cross-section of which show an abnormal behavior above the pressure transmitting medium solidification pressure [5,6]. Nevertheless, such spectroscopic anomaly has not been directly observed so far in measurements on gold nanospheres (AuNS) [8]. The different behavior of AuNRs and AuNSs under nonhydrostatic conditions has been attributed to either NP aggregation and/or NP deformation. However, to the best of our knowledge, there has not been any experimental evidence supporting this hypothesis yet.

In this work, we investigate the effects of non-hydrostatic pressure on the morphology and stability of AuNR and AuNS in methanol-ethanol 4:1 by means of optical absorption spectroscopy and transmission electron microscopy at pressures of up to 23 and 30 GPa, respectively. We demonstrate that solvent solidification and associated non-hydrostatic stresses have a negligible effect on the shape and size of AuNS. On the contrary, while AuNR maintained their initial morphology in the hydrostatic pressure range, the uniaxial stress components induced under non-hydrostatic conditions have a shearing effect on the AuNR, breaking them into smaller particles.

References

- [1] Y. Bao et al. *J. Appl. Phys.* **2014**, *115*, 223503.
[2] Y. Bao et al. *Appl. Phys. Lett.* **2015**, *107*, 201909. [3] X. Gu et al. *Phys. Rev. Lett.* **2018**, *121*, 056102.
[4] F. Medeghini et al. *ACS Nano* **2018**, *12*, 10310–10316.
C. Martín-Sánchez et al. *ACS Nano* **2019**, *13*, 498-504.
C. Martín-Sánchez et al. *J. Phys. Chem. Lett.* **2019**, *10*, 1587–1593.
M. Runowski et al. *Nanoscale* **2019**, *11*, 8718–8726.
C. Martín-Sánchez et al. *J. Phys. Chem. C* **2020**, *124*, 8978–8983.
[9] K. A. Harkins et al. *J. Phys. Chem. C* **2021**, *125*, 27747–27752
-

High Pressure Topological transition of 1T-TiSe₂

Janaky Sunil

High Pressure Topological transition of 1T-TiSe₂: Topological insulators (TIs) are a family of materials that have received a lot of attention in condensed matter physics. TIs exhibit conducting gapless surface states while having an insulating electronic band gap in their bulk due to strong spin-orbit coupling (SOC) [1, 2]. When strain or alloying are applied to certain materials, a topologically trivial phase of the pristine sample can be transformed into a topologically nontrivial phase. This is in generally called topological quantum phase transition (TQPT). TQPT is the adiabatic band inversion that takes place at the time reversal invariant momenta point, with parity shift (odd/even), resulting in an isostructural second-order transition. The topological invariant Z_2 undergoes a shift through this process, going from $Z_2 = 0$ (normal insulator) to $Z_2 = 1$ (TI) [1, 3, 4]. In this context, the layered transition metal dichalcogenide, titanium diselenide (TiSe₂) has been studied using high-pressure Raman spectroscopy and X-ray diffraction (XRD). TiSe₂ has been the subject of much investigation for more than 30 years due to a variety of unique electrical characteristics, including charge density wave (CDW) and superconductivity [5, 6]. Zhu et al. [7] has predicted the topological trivial to nontrivial transition at about 2.7-2.8GPa and a nontrivial to trivial transition at around 3.2-4.2GPa 1T-TiSe₂. Our decision to conduct high-pressure Raman spectroscopy and XRD experiments on 1T-TiSe₂ was heavily influenced by this intriguing theoretical prediction of many topological transitions. Studies using high pressure Raman spectroscopy on 1T-TiSe₂ were conducted up to 20.5GPa. We observe three transitions at 2.5GPa, 6.0GPa, and 15GPa based on anomalies in phonon linewidth (lifetime) and phonon frequency of A_{1g} mode. These observed anomalies (induced from unusual electron-phonon coupling) closely match two topologically nontrivial and trivial transitions predicted by the theoretical work. The trigonal (1T) phase of 1T-TiSe₂ is stable up to a pressure of around 15GPa, beyond which it transitions structurally as evidenced by the emergence of new Raman modes. Up to around 19GPa, the 1T and the new high-pressure phase coexist. This assumption about the structural phase transition was further substantiated using High-pressure XRD.

Most of the results are published in “V Rajaji et al 2019 J. Phys.: Condens. Matter 31 165401”

References:

1. Hassan M Z and Kane C L, *Rev. Mod. Phys.* 82 3045 (2010).
2. Qi X L and Zhang S C, *Rev. Mod. Phys.* 83 1057 (2011).
3. M. S. Bahrany, B. J. Yang, R. Arita, and N. Nagaosa, *Nat. Commun.* 3, 679 (2012).
4. W. Liu, X. Peng, C. Tang, L. Sun, K. Zhang, and J. Zhong, *Phys. Rev. B* 84, 245105 (2011).
5. Zunger A and Freeman A J, *Phys. Rev. B* 17 1839 (1978).
6. J Kusmartseva A F, Sipos B, Berger H, Forró L and Tutiš E, *Phys. Rev. Lett.* 103 236401 (2009).
7. Zhu Z, Cheng Y and Schwingenschlögl U, *Sci. Rep.* 4 4025 (2014).

Pressure-induced transitions in the $[\text{Ru}_2\text{Cl}(\text{Dp-AniF})_4]$ molecular unit

Almudena Inchausti,¹ Miriam Peña-Álvarez,² Camino Martín-Sánchez,³ Fernando Rodríguez,³ Jesús Antonio González,³ Valentín García-Baonza,¹ Mercedes Taravillo¹ and Álvaro Lobato¹

¹MALTA-Consolider Team, Dpto. de Química Física, Facultad de Ciencias Químicas, Universidad Complutense, 28040 Madrid, Spain, almuinch@uclm.es

²Centre for Science at Extreme Conditions and School of Physics and Astronomy, The University of Edinburgh, Peter Guthrie Tait Road, Edinburgh, United Kingdom

³MALTA-Consolider Team, Dpto. De Ciencias de la Tierra y Física de la Materia Condensada, Universidad de Cantabria, 39005 Santander, Spain

The search for molecular materials with tuneable magnetic properties continues to be on the agenda. Although most of these molecules are based on first-row transition-metal ions, 4d and 5d metallic ions are attracting much attention due to their several advantages, including a large spin-orbit coupling and remarkable zero-field splitting. [1] Among the great number of possible candidates, metal-metal bonded complexes have been proposed as important precursors for multifunctional magnetic materials. Unfortunately, most of these compounds don't present any unpaired electrons, although there are some exceptions, highlighting Ru_2^{5+} systems.

Mixed-valence diruthenium paddlewheel-type compounds show interesting features due to a quasi-degeneracy of their π^* (d_{xz} - d_{xz} ; d_{yz} - d_{yz}) and δ^* (d_{xy} - d_{xy}) orbitals, and most of the known species present three unpaired electrons in their ground state ($\pi^*\delta^*$)³. [2] However, their metal-metal bond is strongly dependent on the ligand field, which leads to a borderline stability between $S = 3/2$ and $S = 1/2$ states. Although many efforts are being employed on understanding these effects, only few studies focused on the mechanisms governing the structural distortions of these compounds under pressure, and their effects on the Ru-Ru bond and associated properties.

In this work, we present our studies in the $[\text{Ru}_2\text{Cl}(\text{Dp-AniF})_4]$ ($\text{Dp-AniF} = \text{N,N}'\text{-bis}(4\text{-metoxyphenyl})\text{formamidinate}$) under pressure. This Ru_2^{5+} compound has been chosen due to its sensitivity to external stimuli, as it presents a small spin crossover when decreasing temperature. [3] For this compound, we have observed two transitions below 5 GPa, in accordance to a previous work related to the mixed metal quantum ferromagnet $[\text{Ru}_2(\text{O}_2\text{CMe})_4]_3[\text{Cr}(\text{CN})_6]$. [4] By means of Raman and optical spectroscopy measurements in a diamond anvil cell, we provide insight into the structural and electronic modifications of the diruthenium bond under pressure.

[1] X.Y. Wang *et al.* *Chem. Soc. Rev.*, 2011, 40, 3213-3238.

[2] F. Cotton et al. *Multiple Bonds Between Metal Atoms*; Eds.; Springer Science and Business Media, Inc.: New York, 2005.

[3] P. Angaridis et al. *JACS*, 2005, 127, 14, 5008-2009.

[4] K. R. O'Neal et al. *Phys. Rev. B*, 2014, 90, 104301.

Moderate Pressure Pasteurisation at Room Temperature on endogenous and inoculated microorganisms of fish soup as a novel nonthermal food pasteurisation methodology

Lemos A.T.¹, Martins, A.P.¹, Delgadillo I.¹, Saraiva J.A.¹

¹ LAQV-REQUIMTE, Department of Chemistry, University of Aveiro, 3810-193 Aveiro, Portugal

Corresponding author: jorgesaraiva@ua.pt and alvarotomaz@ua.pt

Background: Recently, several studies showed the capacity of hyperbaric storage (HS) at room temperature (RT) to inactivate microorganisms at pressures usually between 75-100 MPa [1]. These findings led us to use a light higher pressure, between 125-250 MPa, to enhance microbial inactivation as a new nonthermal pasteurisation approach, also at RT, to achieve at least 5.0 log units reduction in bacterial vegetative pathogens, tentatively called moderate pressure pasteurisation (MPP) [2]. This way, foods would be pasteurised and stored almost simultaneously, which represents a great advantage on reduction of deteriorative effects of thermal treatment on food quality properties. After MPP, the foods could be preserved at refrigeration (RF) or by HS/RT. Thus, MPP would occur at RT, what is an advanced feature for a pasteurisation process and additionally, if MPP was followed by HS preservation, it would be a *quasi*-energetically costless process, since energy (in a minor amount) would be only needed to compress the pressure vessel [2].

Methods: So, to test MPP on a ready-to-eat (RTE) fish soup, different pressure levels between 125-250 MPa, up to 24 h, at naturally variable uncontrolled room temperature (≈ 20 °C) was carried out and the effect on endogenous (*Pseudomonas* spp. and total aerobic mesophiles) and inoculated microorganisms (a surrogate *Listeria innocua* and a pathogenic *Salmonella enterica*) was observed, followed by storage at RF or under HS/RT at 75 MPa. Additionally, the main chemical properties were investigated namely, pH, total soluble solids and colour.

Results: MPP (150-250 MPa, 12-24 h) caused a significant reduction of microbial counts, either endogenous or pathogenic microorganisms, of at least 3.0 and 4.0 log CFU/g for *Pseudomonas* spp. and total aerobic mesophiles, respectively while 4.0 and 6.9 log CFU/g reduction was obtained for *Salmonella enterica* (MPP; 6 h) and *Listeria innocua* (MPP; 24 h), respectively. Additionally, after MPP (post-MPP), RF samples showed microbial development over 8.5 log

CFU/g, mainly after 21 days, contrarily to post-MPP at 75 MPa/RT, where microbial inactivation reaching the detection limit (< 1.0 log CFU/g). Accordingly, for MPP (200 MPa, 12-24 h), the pH, total soluble solids and colour of fish soup was equal or even better under post-MPP/75 MPa than post-MPP/RF.

Conclusions: Overall, the present work opens the possibility of using MPP (125-250 MPa) at RT as an interesting methodology for food pasteurisation, followed by food preservation by HS mainly at 75 MPa/RT, resulting in enhanced safety and extended shelf-life compared to RF, as a novel *quasi*-energetically costless moderate food pasteurisation and storage (MPPS) methodology.

Acknowledgements: Thanks are due to the University of Aveiro and FCT/MCT for the financial support for LAQV-REQUIMTE (UIDB/50006/2020) through national funds and, where applicable, co-financed by the FEDER, within the PT2020 Partnership Agreement and for supporting the PhD grant of Álvaro T. Lemos (SFRH/BD/129848/2017) and PhD grant of Ana P. Martins (SFRH/BD/146369/2019).

References:

1. M.D. Santos, L.G. Fidalgo, C.A. Pinto, R.V. Duarte, Á.T. Lemos, I. Delgadillo, J.A. Saraiva, *Crit. Rev. Food Sci. Nutr* 61 (2020).
2. Á.T. Lemos, A.P. Martins, I. Delgadillo, J.A. Saraiva, *Food Microbiol* 105 (2022).

Germination and inactivation of *Byssochlamys nivea* ascospores under hyperbaric storage - dependence on thermal and nonthermal pre-activation steps

Carlos A. Pinto¹, Maria Holovicova², Miroslav Habán³, Marta Habanova³, Jorge A. Saraiva¹

¹LAQV-REQUIMTE, Chemistry Department, University of Aveiro, Campus Universitario de Santiago, 3810-193 Aveiro, Portugal

²AgroBioTech Research Centre, Slovak University of Agriculture in Nitra, Tr. A. Hlinku 2, Nitra, 949 76, Slovakia

³Institute of Nutrition and Genomics, Faculty of Agrobiological and Food Resources, Slovak University of Agriculture in Nitra, 949 76 Nitra, Slovakia

Backgrounds: Hyperbaric storage (food storage under pressure, HS) is being studied as a replacement or complement of the traditional refrigeration processes, considering the energetic savings attained by HS (energy is only used during the quick compression/decompression phases of the pressure vessel) and no energy is needed to keep the product under pressure. This methodology makes use of hydrostatic pressures (up to 150

MPa) to hurdle microbial development and inhibit deteriorative reactions in foods and can be performed at room temperatures (RT)¹. Considering that, generally, pasteurized acidic foods are to be kept under refrigeration, due to the possible presence of specific fungi spores, such as those from *Byssochlamys nivea*, that are quite resistant to thermal and nonthermal pasteurization procedures, and can produce mycotoxins (patulin), novel methodologies to destroy spores are of utmost interest, particularly those with milder impacts on food quality².

Objectives: This work aimed evaluating the effectiveness of HS/RT to control the development of *B. nivea* ascospores in commercial apple juice (pH 3.70) and the impact of pre-ascospore activation procedures by thermal (70 and 80 °C for 30 seconds) and HPP (600 MPa, 3 minutes, RT). Thus, samples were processed in the aforesaid conditions and placed under HS conditions (25-150 MPa) for 30 days at uncontrolled RT (20-25 °C), and at atmospheric pressure at RT and under refrigeration (unprocessed samples were also placed at the same aforesaid conditions). The microbiological analyses were made in potato dextrose agar.

Results: The results showed that there was a clear dependence on the activation methodology on the ability of HS to control the germination of *B. nivea* ascospores. Unprocessed samples and samples processed at 70 °C for 30 sec. evolved quite similarly under HS conditions, wherein neither ascospore germination nor inactivation was observed. A different scenario was observed for samples processed at 80 °C for 30 sec and 600 MPa/3 min, wherein not only ascospore inhibition was observed (25-50 MPa) but also ascospore inactivation (75-150 MPa) of more than 3 log units of for both cases (initial load of 5.17 log CFU/mL). Differently, conventional refrigeration only inhibited ascospore development, being a possible threat for food safety due to possible germination after the 30 days of the study and mycotoxins production.

Conclusion: A fully nonthermal process, HS with a previous HPP treatment (600 MPa/3 min) resulted in at least more than 3 log units of *B. nivea* ascospores inactivation along storage, while this ascospore cannot be inactivated by thermal pasteurization or HPP, resulting in enhanced food safety, with the added advantage of being performed at uncontrolled RT, thus allowing considerable energetic savings and milder effects on foods.

Acknowledgements: Thanks are due to the University of Aveiro and FCT/MCT for the financial support to the LAQV-REQUIMTE research Unit (UIDB/50006/2020) through national funds and, where applicable, co-financed by the FEDER, within the PT2020 Partnership Agreement. Carlos A. Pinto also acknowledges FCT/MCT for the PhD grant reference SFRH/BD/137036/2018. The authors also acknowledge the Operational Programme Integrated Infrastructure, for the project: Long-term strategic research of prevention, intervention and mechanisms of obesity and its comorbidities, IMTS: 313011V344, co-financed by the European Regional Development Fund”.

References:

1. Santos et al. (2021). *Crit. Rev. Food. Sci. Nutr.*, 61(12), 2078-2089.
2. Pinto et al (2020). *Compr. Rev. Food Sci.*, 19(2), 553-573.

Unravelling the mechanisms of adaptation to high pressure in proteins

Antonino CALIÒ¹, Philippe OGER¹, Judith PETERS^{2,3,4}

¹Univ Lyon, UCBL, INSA Lyon, CNRS, MAP UMR 5240, 69622 Villeurbanne, France

²Institut Laue Langevin, Grenoble, France

³Univ Grenoble Alpes, CNRS, LiPhy, Grenoble, France

⁴Institut Universitaire de France, Paris, France

Background: The adaptation of proteins to high pressure is still an open debate, but understanding this mechanism could shed light on the origins of life^{1,2}, lead to a better understanding of protein dynamics, and deliver new tools to engineer pressure-resistant enzymes for biotechnological purposes. While the thermodynamic and dynamical properties of model proteins under pressure have been extensively studied with different techniques³⁻⁶, the evolutionary aspects of their adaptation have not received much attention.

Disentangling the contributions of pressure adaptation from those of another kind of adaptation, such as high or low temperature, is a difficult task and, in fact, genomic studies were not able to determine a clear pattern among the order of Thermococcales.

Methods: Recent experiments by our group (by Elastic and Quasi-elastic Incoherent Neutron Scattering, EINS and QENS) focused on pressure adaptation by studying whole cells of two closely related species (*Thermococcus barophilus*, Tba, and *Thermococcus kodakarensis*, Tko) that grow at the same optimal temperature (85°C) but differ only for the optimum pressure (400 bar for Tba, 1 bar for Tko), and they highlighted the differences in the dynamics of the two organisms' proteomes⁷⁻⁹.

To take this investigation to the molecular level, we now studied the protein *Phosphomannose Isomerase* and the *Ribosomal protein S24e* (with EINS, 2-D Nuclear Magnetic Resonance (NMR) Spectroscopy and X-ray crystallography) from the two organisms.

Results: Our results evidence that the substitutions of amino acids enhancing pressure stability are those in the hydrophobic core, which eliminate cavities, and those on the surface, which modulate the interaction of the proteins with the surrounding water layer and give them the right flexibility to perform their function under high pressure.

Conclusion: We observed that pressure adaptation involves the decoupling of protein-water dynamics and the elimination of cavities in the protein core. This is achieved by rearranging the charged residues on the protein surface and using bulkier hydrophobic residues in the core.

References

- ¹W. Martin *et al.*, *Nature Reviews Microbiology* **6**, 805–814 (2008).
²S. Miller *et al.*, *Nature* **334**, 609-611 (1988).
³S.A. Hawley, *Biochemistry* **10**, 2436-2442 (1971).
⁴C. Royer, *BBA – Protein Structure and Molecular Enzymology* **1595**, 201-209 (2002).
⁵L. Meinhold *et al.*, *PNAS* **104**, 17261-17265 (2007).
⁶F. Librizzi *et al.*, *Scientific Reports* **8**, 2037 (2018).
⁷N. Martinez *et al.*, *Scientific Reports* **6**, 32816 (2016).
⁸M. Golub *et al.*, *Langmuir* **34**, 10419-10425 (2018).
⁹M. Salvador-Castell *et al.*, *Soft Matter* **15**, 8381-8391 (2019).

Multi-technical methodological approaches for the study of liquids under extreme conditions of pressure and temperature

Silvia Boccato¹, Raffaella Torchio², Guillaume Morard³, Yiuri Garino¹, Sakura Pascarelli⁴, Daniele Antonangeli¹

¹*Institut de Minéralogie de Physique des Matériaux et de Cosmochimie (IMPMC), Sorbonne Université, CNRS UMR 7590, Muséum National d'Histoire Naturelle, 4 Place Jussieu, F-75005 Paris, France*

²*ESRF-European Synchrotron Radiation Facility, Grenoble, France*

³*Université Grenoble Alpes, Université Savoie Mont Blanc, CNRS, IRD, Université Gustave-Eiffel, ISTERre, Grenoble, France*

⁴*European XFEL, Holzkoppel 4, 22869 Schenefeld, Germany*

Being able to analyse the structure of a liquid as a function of pressure and temperature allows to deduce the compressibility and the thermal expansion, as well as to identify liquid-liquid phase transitions. Accessing the density of the liquid of materials constituting planetary cores (coupled with the study of melting curves and the determination of the density of the corresponding solid) allows to better constrain the differentiation process of a planet from the magma ocean and to understand its crystallization regime.

In this context X-ray diffraction (XRD) and X-ray absorption spectroscopy (XAS) are routinely used techniques to directly explore the atomic structure of materials under extreme conditions of pressure and temperature. When performed in a synchrotron, these two probing techniques coupled with a diamond anvil cell (DAC) and with a laser heating (LH) system allow to probe properties of materials at pressures of few Mbar and temperatures of

thousands of kelvin. XRD and XAS are both bulk techniques that allow to follow in-situ structural changes, are sensitive to the local structure of a liquid and allow to determine its compressibility.

The detection of the solid-liquid phase transition with XRD is possible with the appearance of the liquid diffuse scattering and the disappearance of the solid peaks associated to the solid sample^{1,2}. Moreover, the liquid diffuse scattering signal can be analysed to obtain structural information. A recently developed software for the analysis of X-ray diffuse scattering signal, Amorpheus³, will be here presented. Amorpheus is open-source, free and easy-to-use and it allows to perform a customizable analysis of a large amount of liquid and amorphous data.

XAS is as well a suitable technique for the detection of melting⁴ and the structural and electronic information contained in the XANES (X-ray absorption near edge structure) can be employed to determine in-situ the composition of a binary alloy⁵. Taking as example Fe-C and Fe-O, we show that chemical migrations induced by the temperature gradients can now be tracked in-situ, with direct consequences in high pressure studies of laser heated binary systems. Finally, the analytical solutions proposed to determine the compressibility of liquids under extreme conditions⁶ (where the data quality loss is significant) will be shown.

This work sets the bases for future high pressure studies with both fundamental and planetary implications.

[1] G. Morard et al., *Phys Chem Minerals* (2011) 38:767–776

[2] S. Anzellini et al., *Science* (2013) 340:464-466

[3] S. Boccatto et al., *High Press Res* (2022) 42:69-93

[4] S. Boccatto et al., *J Geophys Res Solid Earth* (2017) 122:9921-9930

[5] S. Boccatto et al., *Sci Rep* (2020) 10:11663

[6] S. Boccatto et al., *Phys Rev B* (2019) 100:180101

Room-Temperature Superionic Conduction in Complex Transition Metal Hydrides with High Hydrogen Coordination

Shigeyuki Takagi

Institute for Materials Research, Tohoku University, Sendai 980-85177, Japan

E-mail: shigeyuki.takagi.c5@tohoku.ac.jp

Solid-state materials containing rotatable polyanions, such as $B_{12}H_{12}^{2-}$,¹⁾ constitute a peculiar class of ionic conductors due to their unique transport behavior, where rotating polyanions

promote phase transitions to disordered phases with several orders of magnitude enhancement in cation conductivities. A major drawback is the high temperature required to activate rotation and thereby low conductivities at room temperature.

In this study, I adopted a novel approach to reduce the transition temperature based on the use of homoleptic transition metal hydride complexes, wherein hydrogen is the sole ligand species, covalently binding to single transition metals, as a new class of rotatable polyanions. The motivation for this choice is that, unlike other polyanions, the rotation only requires small displacements of highly mobile hydrogen and could therefore be expected to occur with low activation energy. The high mobility of hydrogen is also expected to thermodynamically favor the cation conducting high-temperature phase because the resulting high degree of orientational disorder enhances the entropic contribution to the free energy, thereby further suppressing the phase transition temperature.

I found that MoH_9^{3-} in an existing material $\text{Li}_5\text{MoH}_{11}$ exhibits “pseudorotation” with remarkably low activation energy of a few meV. This motion yields a large entropic contribution of 19.1 J/mol·K, significantly stabilizing the lithium ion conducting high-temperature phase below room temperature. The room-temperature lithium ion conductivity reaches $7.9 \times 10^{-2} \text{ S cm}^{-1}$,²⁾ which is more than three times greater than the highest value of $2.5 \times 10^{-2} \text{ S cm}^{-1}$ previously reported for $\text{Li}_{9.54}\text{Si}_{1.74}\text{P}_{1.44}\text{S}_{11.7}\text{Cl}_{0.3}$.³⁾ The detailed mechanism of the pseudorotation will be discussed in the presentation.

References:

- T. J. Udovic, M. Matsuo, A. Unemoto, N. Verdal, V. Stavila, A. V. Skripov, J. J. Rush, H. Takamura, and S. Orimo, Chem. Commun. 50, 3750-3752 (2014).*
S. Takagi, T. Ikeshoji, S. Sato, S. Orimo, Appl. Phys. Lett. 116, 173901 (2020).
Y. Kato, S. Hori, T. Saito, K. Suzuki, M. Hirayama, A. Mitsui, M. Yonemura, H. Iba, and R. Kanno, Nature Energy 1, 16030 (2016).

High-pressure synthesis of aluminum-iron alloy hydride

Hiroyuki Saitoh

National Institute for Quantum Science and Technology

saito.hiroyuki@gst.go.jp

We have been searching for new classes of hydrides consisting only of metals with low affinity for hydrogen by using the high-pressure hydrogenation technique. Aluminum is a lightweight and inexpensive metal, which is ideal if it can be used as a raw material for

hydrogen storage materials. However, it is also known that aluminum and its alloys have very low affinity for hydrogen. Recently, we reported that an alloy consisting only of aluminum and iron, earth-abundant metals with low hydrogen affinity, can form hydrides under high temperature and high pressure and that the resulting hydrides may be thermodynamically stable even at near ambient pressure. If the synthesis pressure of this hydride can be lowered, it may be used as a practical hydrogen storage material.

The starting materials was $\text{Al}_{13}\text{Fe}_4$ alloy prepared by an arc furnace. The obtained ingot was crushed into disk shape 1 mm in diameter and 0.4 mm in height. The disk-shaped sample was set in a sample capsule made of boron nitride and located in a cubic pressure medium along with graphite heater, internal hydrogen source (NH_3BH_3), and hydrogen sealing capsule. The internal hydrogen source evolve hydrogen at high pressure, and the evolved hydrogen was confined in the hydrogen sealing capsule. In this way, we hydrogenated alloys under high pressure and high temperature.

High pressure and high temperature were generated using a cubic-type multi-anvil press. The sample was pressurized to 9 GPa at room temperature and heated to 750 °C at approximately constant pressure of 9 GPa. The sample was immersed in fluid hydrogen to form its hydride. The sample was then cooled to room temperature and depressurized to ambient pressure. The hydrogenation process of the sample was monitored by an in-situ synchrotron radiation X-ray diffraction measurement system installed on beamline BL14B1, SPring-8.

No structural phase transition took place during pressurization at room temperature. When the sample was heated to around 600°C, internal hydrogen source evolved hydrogen and the sample was immersed in fluid hydrogen. At the same time as the hydrogen evolution, the peaks intensities from $\text{Al}_{13}\text{Fe}_4$ began decreasing and new Bragg peaks began to appear. The former was vanished approximately 5 min after the sample was heated to 750 °C. The newly appeared Bragg peaks were indexed by a unit cell of a novel hydride, Al_3FeH_4 . In this way, we find hydrogenation pressure-temperature conditions of $\text{Al}_{13}\text{Fe}_4$ alloy under high pressure and high temperature by using in situ synchrotron radiation x-ray diffraction technique. The obtained Al_3FeH_4 retained its crystal structure during the process of cooling to room temperature and decompression to ambient pressure, and could be recovered at ambient conditions. This work was supported by JSPS KAKENHI Grant-in-Aid for Scientific Research on Innovative Areas “Hydrogenomics” (Nos. JP18H05513 and JP18H05518) as well as JSPS KAKENHI (No. JP22H01821) and grants from the Inter-University Cooperative Research Program of the Institute for Materials Research, Tohoku University (Proposal Nos. 20K0022, 202012-RDKGE-0066, and 202112-RDKGE-0025).

The rich structural landscape induced by pressure in multifunctional FeVO₄

J. Gonzalez-Platas¹, S. Lopez-Moreno², E. Bandiello³, M. Bettinelli⁴, and D. Errandonea^{3,*}

¹*Departamento de Física, Instituto Universitario de Estudios Avanzados en Física Atómica, Molecular y Fotónica (IUDEA), Universidad de La Laguna, Spain*

²*CONACYT, Division de Materiales Avanzados, Instituto Potosino de Investigación Científica y Tecnológica (IPICYT), Mexico*

³*Departamento de Física Aplicada, ICMUV, Universidad de Valencia, Spain*

⁴*Luminescent Materials Laboratory, Department of Biotechnology, University of Verona, Italy*

*Presenting author: daniel.errandonea@uv.es

Currently, there is an increase in the requirement of materials suitable for green technologies. These include energy-storage devices, sustainable and nonconventional energy sources, low-consuming electronics, and information-storage appliances. FeVO₄ has many interesting electronic and magnetic properties, which make it suitable for these applications. Consequently, FeVO₄ is being considered as a dream material for developing multiple noncontaminant technologies. FeVO₄ is a multiferroic material, considered for the development of next-generation memory devices. The thermal and electrical conductivity, mechanical strength, chemical stability, and electronic band gap of FeVO₄ also make it suitable for the development of electrodes of low-cost energy storage devices, such as supercapacitors. They also make it a promising anode material for potassium-ion batteries.

We have studied the high-pressure behavior of FeVO₄ by means of single-crystal X-ray diffraction (XRD) and density functional theory (DFT) calculations. We have also performed high-pressure optical-absorption measurements to characterize the band gap. We have found that the structural sequence of FeVO₄ is different from that previously assumed. We have determined that FeVO₄, under compression (at room temperature), first transforms at 2.11(4) GPa from the ambient-pressure triclinic structure (FeVO₄-I) to a second previously unknown triclinic structure (FeVO₄-I'), which experiences a subsequent phase transition at 4.80(4) GPa to a monoclinic structure (FeVO₄-II'). Single-crystal XRD has enabled these novel findings as well as an accurate determination of the crystal structure of FeVO₄ polymorphs under high-pressure conditions. The crystal structure of all polymorphs has been accurately solved at all measured pressures. The pressure dependence of the unit-cell parameters and polyhedral coordination have been obtained and are discussed. The room-temperature equation of state and the principal axes of the isothermal compressibility tensor of FeVO₄-I and FeVO₄-I' have also been determined. The structural phase transition observed here between these two triclinic structures at 2.11(4) GPa implies abrupt coordination polyhedra modifications, including coordination number changes. DFT calculations support the conclusions extracted from our experiments. The structural changes induce substantial changes in the optical properties of FeVO₄ including a band-gap collapse. According to our

DFT calculations, these phenomena are related to contribution of iron d-electrons to the bottom of the conduction band. In this presentation, results will be discussed and systematically compared with other orthovanadates.

Interplay between proton dynamics and Fe valence fluctuation in $\text{Fe}_3(\text{PO}_4)_2(\text{OH})_2$

G. Hearne¹, V. Ranieri², P. Hermet², J. Haines², O. Cambon², J.L. Bantignies³,
P. Fertey⁴, T. Stuerzer⁵, M. Poienar⁶, J. Rouquette²

¹Department of Physics, University of Johannesburg PO Box 524, Auckland Park 2006, Johannesburg, South Africa

²ICGM, Université de Montpellier, CNRS, ENSCM, 34095 Montpellier, France ³L2C, Université de Montpellier, CNRS, 34095 Montpellier, France ⁴Synchrotron Soleil, L'Orme des Merisiers, Saint-Aubin, BP 48, 91192 Gif-sur-Yvette Cedex, France

⁵Bruker AXS GmbH, Ostliche Rheinbruckenstrasse 49, Karlsruhe D-76187, Germany

⁶National Institute for Research and Development in Electrochemistry and Condensed Matter, Renewable Energies - Photovoltaic Laboratory, Str. Dr. A. Paunescu Podeanu, nr.144, 300569, Timisoara, Timis, Romania

Pressure dependence of mixed-valence barbosolite $\text{Fe}^{2+}\text{Fe}^{3+}_2(\text{PO}_4)_2(\text{OH})_2$ is investigated based on a combination of single crystal X-ray diffraction, DFT calculations, infrared and Mössbauer spectroscopy to determine how the change in H-bonding, i.e. $\text{O}-\text{H}\cdots\text{O}$, may influence $\text{Fe}^{2+}\rightarrow(\text{OH})^-$

$\rightarrow\text{Fe}^{3+}$ intervalence electron transfer and vice-versa.

Recently, the original $P2_1/n$ space group of barbosolite was questioned as n -glide plane reflection conditions ($h0l:h+l=2n$) were found to be violated based on TEM and single crystal X-ray diffraction. A doubled unit-cell barbosolite structure in the $P2_1$ space group, i.e. along the c axis, was proposed[1]. However, subsequent analysis reveals that such reflections thought to be attributable to the doubled unit-cell, are in fact due to a non-merohedral twinning with a 90° rotation angle. The barbosolite structure is clearly still centrosymmetric with the $P2_1/n$ space-group as either suggested by the cumulative probability distribution curves and the use of a polar twinning law in the $P2_1$ space group solution. Moreover, contrary to what was originally proposed, the presence of an additional non-stoichiometric iron statistically connects the face sharing FeO_6 octahedra trimers, i.e. $\text{Fe}^{2+}-\text{Fe}^{3+}-\text{Fe}^{2+}$, to form infinite chains along $\langle 110 \rangle$ as observed in the lipscombite-like structure[2]. Based on DFT calculations, hydrogen atoms are located in the

octahedral volume of this additional non-stoichiometric atom iron site and forms a hydrogen bond O–H···O between the (OH)⁻ common vertex of three octahedra and one of the oxygens of a PO₄ group, i.e. as part of Fe–O–H···O–P structural sequences. This means that the FeO₆ octahedral trimers are either connected by a hydrogen bond or by this non-stoichiometric iron site.

Pressure triggers proton delocalization involving a *P21/n-Cc* phase transition in a $2a \times 2b \times c$ supercell at ~5 GPa in hydrogen bonds of the Fe–O–H···O–P structural segments. Hydrogen bond reinforcement and anticipated proton dynamics, discerned by IR spectroscopy and symmetrization of lattice parameters, impact on the crystal field at proximate Fe cations. This triggers dynamical minority-spin electron exchange along Fe²⁺–L–Fe³⁺ pathways (ligand *L* = O or (OH)⁻ of shared octahedral faces), discerned by ⁵⁷Fe Mössbauer spectroscopy at 10–30 GPa. The pressure response of these mixed-valence hydroxy phosphates exemplify the interplay between proton (THz) and electron (MHz) dynamics on two disparate time scales in the same condensed phase. This is of widespread relevance to charge dynamics in hydrogen bonded systems (e.g., biomolecular complexes and planetary interiors).

M. Poienar et al., J. Solid State Chem., 287 (2020).

I. Vencato et al., American Mineralogist, 74 (1989) 456-460.

General relationship between the bandgap energy and iodine-oxygen bond distance in metal iodates

Akun Liang,^{1,*} Robin Turnbull,¹ Placida Rodríguez-Hernandez,² Alfonso Muñoz,² M Jasmin,³ Lan-Ting Shi,⁴ and Daniel Errandonea¹

¹*Departamento de Física Aplicada -ICMUV-MALTA Consolider Team, Universitat de València, c/Dr. Moliner 50, Burjassot (Valencia) 46100, Spain. E-mail: akun2.liang@uv.es*

²*Departamento de Física and Instituto de Materiales y Nanotecnología, MALTA Consolider Team, Universidad de La Laguna, La Laguna 38206, Tenerife, Spain*

³*TKM College of Arts and Science, Kollam, Kerala 691005, India*

⁴*College of Physics, Sichuan University, Chengdu 610065, China*

The search for the next generation nonlinear optical (NLO) materials has driven the synthesis and characterization of numerous new metal iodates [1,2]. An ideal NLO crystal should have: a high laser damage threshold (LDT), an excellent thermal stability, a wide transparency window which means a wide bandgap energy, and a large second-harmonic generation response (SHG) [3]. A two-step investigation has been implemented to determine the relationship between the bandgap energy and the iodine-oxygen bond distance in metal iodate materials, by the means of high-pressure optical absorption

experiment and density functional theory (DFT) calculations. Firstly, we utilised high pressure conditions on Mg and Zn iodates to correlate the pressure- induced changes in bandgap energy with changes in the iodine-oxygen bond distances. On both cases, the bandgap energy shows a nonlinear decrease under compression. The nonlinear behaviour is a consequence of the interplay between the pressure- induced increase of the first nearest neighbour iodine-oxygen bonds, which favours a narrowing of the bandgap, and the decrease of the second nearest neighbour iodine- oxygen bonds, which favours an opening of the bandgap. The inverse correlation between the bandgap energy and the iodine-oxygen bond distance is confirmed in the second part of the investigation by collating and comparing the bandgap energies and corresponding average iodine-oxygen bond distances of the metal iodates reported in the literature. In the comparison, only non-transition and closed-shelled transition metals were included, without regard for their chemical formula, crystal structure or stoichiometry. The partial filled $3d$ orbital of transition metal will contribute to the valence band maxima (VBM) or conduction band minima (CBM) in the electronic structure and narrow the bandgap [4], so transition-metal iodates have been ruled out in this study.

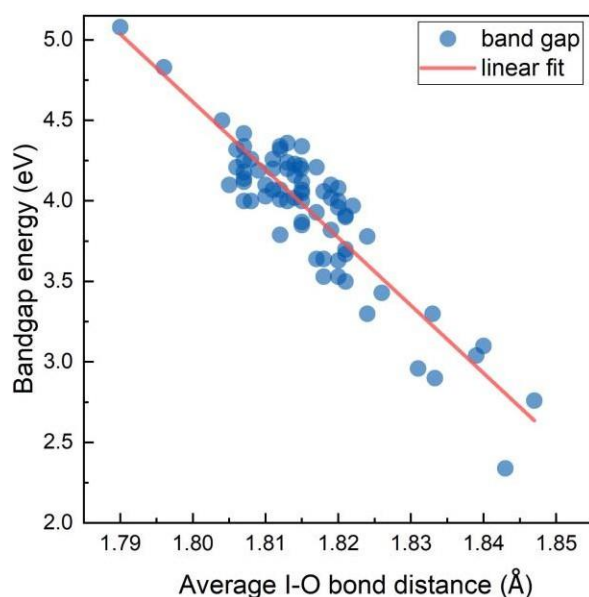


Figure 1. Collated bandgap energy and average I-O bond distances of 71 different metal iodates as found in the literature.

References:

1. H. Fan, G. Peng, C. Lin, K. Chen, S. Yang, and N. Ye, *Inorg. Chem.* **59**, 7376 (2020).
2. H. Jo, H. G. Kim, H. R. Byun, J. I. Jang, and K. M. Ok, *J. Solid State Chem.* **282**, 121120 (2020).
3. F. F. Mao, C. L. Hu, J. Chen, B. L. Wu, and J. G. Mao, *Inorg. Chem.* **58**, 3982 (2019).
4. A. Liang, P. Rodriguez-Hernandez, A. Munoz, S. Raman, A. Segura, and D. Errandonea, *Inorg. Chem. Front.* **8**, 4780 (2021).

Pressure induced emission enhancement and bandgap narrowing: experimental investigations and first principles theoretical simulations on the model halide perovskite Cs₃Sb₂Br₉

DEBABRATA SAMANTA

Introduction

The search for energy-efficient materials has gained momentum in recent times, to use with green and renewable energy sources. The Cs₃Sb₂Br₉ crystal is a superior candidate for solar cells owing to its outstanding photovoltaic properties [1, 2]. It is important to analyse and understand the fundamental interactions and the correlation between the structure and the electronic properties. The phase stability of bulk Cs₃Sb₂Br₉ under pressure, which is important during applications, remains unexplored. Therefore, we have focused on structural, optical, and electronic properties of bulk Cs₃Sb₂Br₉ crystal under pressure.

Methods

Crystalline powder of Cs₃Sb₂Br₉ is prepared by acid precipitation method [3]. High pressure experiments are carried out using a piston-cylinder type diamond anvil cell (DAC) of culet size 300 μm . High-pressure Raman scattering and PL measurements are carried out using the Raman spectrometer (Monovista from SI GmBH) in the backscattering geometry. 532 nm and 488nm laser lines are used to excite the sample for Raman and PL experiments, respectively. x-ray diffraction (XRD) experiments are performed at the XPRESS beamline in the Elettra synchrotron radiation source. First-principles density functional theory (DFT) calculations are performed using a plane-wave basis set as implemented in the QUANTUM ESPRESSO [4, 5] software.

Results

We have investigated an electronic transition associated with direct-to-indirect bandgap transition around 3 GPa from both experiments and first-principle DFT calculations (Fig. 1). High-pressure Raman measurements show a broad minimum in linewidth of A_{1g} and E_g modes at around 3 GPa due to unusual electron-phonon coupling. A larger compression along the basal plane compared to the prismatic plane leads to a micro- structural change in the trigonal lattice, as evidenced from XRD analysis. Self-trapped exciton manifests itself in the photoluminescence spectra through below bandgap broadband emission and the emission gets enhanced under pressure (Fig. 2). Intriguingly, a 27.5%

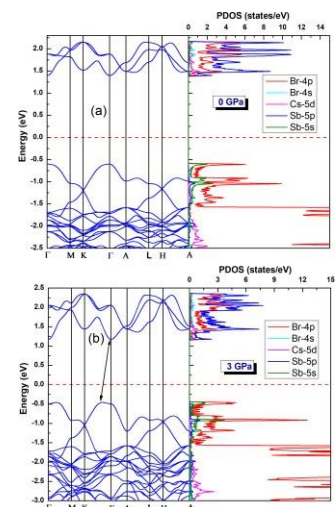


Figure 1

narrowing of the bandgap is estimated by the first-principles calculations within the GGA to an electronic exchange and correlation functional.

Conclusions

The work not only provides a relationship between optical properties and structural evolution of the Cs₃Sb₂Br₉ under pressure but also shows an effective way for achieving high optical response by tuning interatomic distances without changing the material composition. We also believe that this work will influence further research to understand the peculiarity of property- structure relation of the lead-free halide perovskites.

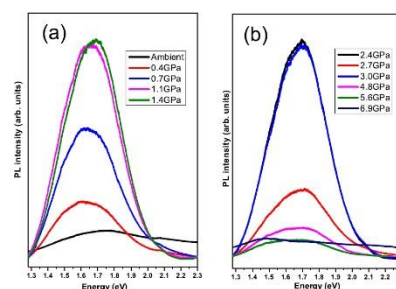


Figure 2

References

1. L. Zhang et al., *Angew. Chem. Int.* 57, 11213 (2018)
2. P. Liu et al., *Adv. Opt. Mater.* 8 2001072 (2020)
3. D. Samanta et al., *J. Phys. Chem. C.* 125, 6, 3432-3440 (2021)
- P. Giannozzi et al., *J. Phys.: Condens. Matter* 21, 395502 (2009)
- P. Giannozzi et al., *J. Phys.: Condens. Matter* 29, 465901 (2017)
6. D. Samanta et al., *Phys. Rev. B* 105, 104103 (2020)

Pressure driven Phase Transition in NdNiO₃ Nanostructures

Raktima Basu¹, Debabrata Samanta¹, Mrinmay Sahu¹, and Goutam Dev Mukherjee¹

¹National Centre for High Pressure Studies and Department of Physical Sciences, Indian Institute of Science Education and Research Kolkata, Mohanpur Campus, Mohanpur 741246, Nadia, West Bengal, India.

*Corresponding author: goutamdev@iiserkol.ac.in

Objective

Metal to insulator transition (MIT) accompanied by structural distortions in NdNiO₃ (NNO) attracted significant attention in recent years [1]. NNO undergoes a first-order structural transition from orthorhombic to monoclinic phase along with the metal to insulator transition at ~200K [2]. The transition temperature depend strongly on Ni-O-Ni bond angle and Ni-O bond length; and therefore, a strain is anticipated to play a major role in the phase-transition.

The phase-transition with strain in nanostructured NNO (1D, therefore free from any external strain) is thus be explored through XRD and Raman spectroscopic measurements varying the pressure hydrostatically.

Method

The nanostructured NNO were synthesized by solid-state route. The pressure-dependent Raman studies were carried out using 532 nm source and the XRD pattern were collected at DESY with X-ray beam having wavelength of 0.2904 Å. The sample was placed inside the central hole of diameter 100 micron of rhenium gasket pre-indented to a thickness of about 30 microns. A small Ruby sphere was loaded along with the sample, which acted as pressure marker.

Results

The XRD pattern (fig. 1a) matches with the reported orthorhombic structure of NNO (ICSD #111149). Fig. 1c shows the pressure evolution of the diffraction pattern of the sample up to 35 GPa. A new Bragg line is observed to evolve above ~15 GPa (shown by the arrow). The XRD pattern above 15 GPa (fig. 1b) matches with the monoclinic structure of NNO (ICSD #164826).

The Raman spectra for the nanostructured NNO are reported for the first time (fig. 2), which resembles with its 2D counterparts except from the broad nature of the mode frequencies. The most prominent changes are the following: (i) The very intense Raman modes at ~ 303, 407, and 865 cm^{-1} strongly decrease in intensity above 15 GPa, indicating presence of metallicity in the system. (ii) The Raman peaks between 500 to 800 cm^{-1} harden and undergo a strong broadening and increase in intensity. The broad Raman mode at ~650 cm^{-1} is reported to be originated due to octahedron breathing [3], which strongly depends on charge disproportion of nickel ion ($\text{Ni}^{3+\delta}$ and $\text{Ni}^{3-\delta}$). The charge transfer ' δ ' modifies the Ni-O interaction, and thereby the vibrational frequency. The increase in intensity and strong broadening of this vibrational mode indicates an increase in ' δ ' with increase in pressure.

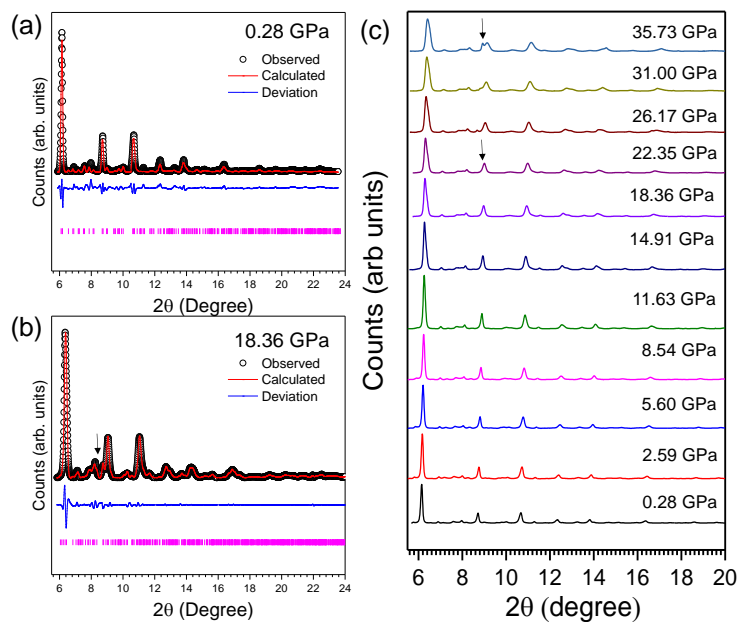


Fig. 1. Refined XRD patterns of NdNiO₃ nanostructures at (a) ambient pressure and (b) at 18 GPa. (c) XRD patterns of the sample as a function of pressure.

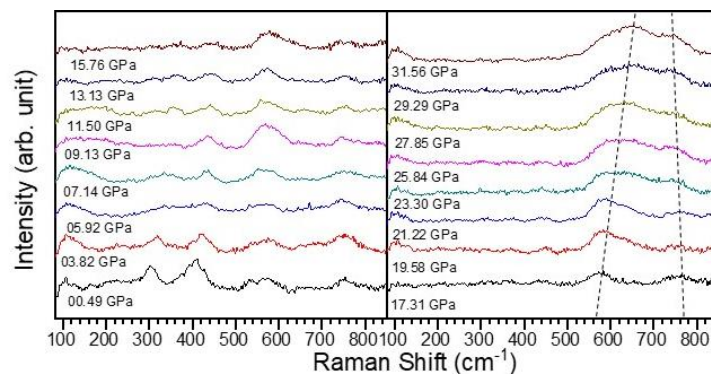


Fig. 2. Raman spectra as a function of pressure of pristine NdNiO₃.

Conclusion

We report the pressure driven phase transition in NdNiO₃ nanostructures. The high-pressure Raman and XRD studies reveal that the nanostructures undergo a structural transition from orthorhombic to monoclinic due to charge disproportion under pressure resembling the temperature induced structural transition.

References

1. S. Middey, et al., *Annu. Rev. Mater. Res.* 46, 305 (2016).
2. M. Zaghrioui, et al., *J. Magn. Magn. Mater.* 211, 238 (2000).
3. M. Zaghrioui, et al., *Phys. Rev. B* 64, 081102 (2001).

Preparation of Confined, Low-Dimensional Boron Nitride in the 1-D Pores of Siliceous Zeolites under High Pressure, High Temperature Conditions

Damian Paliwoda[†], Marco Fabbiani[†], Mélanie Wynn[‡], Frederico Alabarse^{||}, Anja Rosenthal[□], Wilson Crichton[□], Leszek Konczewicz[▲], Michal Bockowski[■], David Maurin[▲], Thierry Michel[▲], Umit B. Demirci[§], Jérôme Rouquette[†], Patrick Hermet[†], Francesco di Renzo[†], Arie van der Lee[§], Guillaume Cassabois[▲], Samuel Bernard[‡], Julien Haines^{*†}

[†] ICGM, CNRS, Université de Montpellier, ENSCM, Montpellier, France.

^{||} Elettra Sincrotrone Trieste, Trieste, Italy ESRF, Grenoble, France

[□] [▲] Laboratoire Charles Coulomb, UMR 5221 CNRS, Université de Montpellier, Montpellier, France.

Institute of High-Pressure Physics, Polish Academy of Sciences, Sokolowska 29/37 01-142 Warsaw, Poland

[§] IEM, UMR 5635 (CNRS-ENSCM-UM), Université de Montpellier, Montpellier, France.

[‡] CNRS, IRCER, UMR 7315, University of Limoges, F-87000 Limoges, France

Low dimensional boron nitride chains were prepared in the one-dimensional pores of the siliceous zeolites TON and MTW by the infiltration followed by the dehydrocoupling and pyrolysis of ammonia borane under high pressure, high temperature conditions. High-

pressure x-ray diffraction in a diamond anvil cell and in a large volume, multianvil device was used to follow in situ these different steps in order to determine the optimal conditions for this process. Based on these results, millimeter-sized samples of BN/TON and BN/MTW were synthesized. Characteristic B-N stretching vibrations of low-dimensional BN were observed by infrared and Raman spectroscopies. The crystal structures were determined using a combination of x-ray diffraction and density functional theory with one and two one-dimensional zig-zag (BN)_x chains per pore in BN/TON and BN/MTW, respectively. These 1-D BN chains potentially have interesting photoluminescence properties in the far ultraviolet region of the electromagnetic spectrum.

Resolving puzzles of the deep-focus earthquake mechanism based on plastic strain-induced olivine-spinel transformation and transformation-induced plasticity

Valery I. Levitas

Iowa State University, Departments of Aerospace Engineering and Mechanical Engineering, Ames, Iowa 50011, U.S.A.

Ames Laboratory, Division of Materials Science and Engineering, Ames, IA, USA

e-mail: vlevitas@iastate.edu

Deep-focus earthquakes that occur at 350–700 km, where pressure is 12-23 GPa and temperature is 900-2000 K, are generally assumed to be caused by olivine-spinel phase transformation (PT) in a metastable subducted olivine. However, there are many existing puzzles:

- (a) What are the reasons and mechanisms for jump from geological strain rates 10^{-17} – $10^{-15} s^{-1}$ to seismic strain rates 10 – $10^3 s^{-1}$?
- (b) How does metastable olivine, which does not completely transform to spinel for over the million years, suddenly transform during seconds?
- (c) How to connect shear-dominated seismic signals with volume-change dominated transformation strain during PT?

We proved [1] that plastic flow alone cannot lead to localized in mm-scale band heating, that is why PT is required. We introduced a combination of several novel concepts that resolve the above puzzles quantitatively [1]. In the previous papers, pressure- and stress-induced PTs were considered as a mechanism for initiation of the shear instability. However, these PTs occur during plastic flow, i.e., they should be revisited as plastic strain-induced PT produced by defects with strong stress concentrators, like dislocation pileups [2,3]. This

necessitates nucleation of nanosize regions with limited or absent growth, which explains nanosize structure of the transformed regions. Rate of PTs is determined by rate of plastic deformations, and in thin shear band it can be many orders of magnitude faster than pressure-induced PTs. Strain-induced PTs may occur at much lower pressure and temperature than expected from the phase diagram and may involve unusual PTs not observed without plasticity. We found an analytical 3D solution for coupled deformation-transformation-heating in a shear band. This solution predicts conditions for severe (singular) transformation-induced plasticity (TRIP). TRIP occurs due to internal stresses caused by volume change during the PT combined with external stresses. Since PT causes TRIP, which (like traditional plasticity) promotes strain-induced PT, it in turn promotes TRIP, and so on, there is a self-blown-up deformation-transformation-heating process due to positive thermomechanochemical feedback between TRIP and strain-induced phase transformation. This process leads to temperature in a band, above which the self-blown-up shear-heating process in the shear band occurs after finishing the PT. Relatively small shear strain in laboratory experiment ($\gamma = 43$ vs. $\gamma = 10^6$ in nature) is because the temperature cannot grow due to several orders of magnitude thinner shear band. Our findings change the main concepts in studying the initiation of the deep-focus earthquakes and PTs during plastic flow in geophysics in general.

[1] V.I. Levitas, *Resolving puzzles of the phase-transformation-based mechanism of the deep-focus earthquake*. <http://arxiv.org/abs/2110.10862> (2021).

[2] Levitas, V.I. (2004) *High-pressure mechanochemistry: conceptual multiscale theory and interpretation of experiments*. *Physical Review B*, 70, 184118.

[3] Levitas V.I. (2019) *High-Pressure Phase Transformations under Severe Plastic Deformation by Torsion in Rotational Anvils*. *Material Transactions*, 60, 1294-1301.

Accurate Crystal Structure of Ice VI from X-Ray Diffraction with HAR

Michał L. Chodkiewicz¹, Roman Gajda¹, Krzysztof Woźniak¹

¹*Biological and Chemical Research Centre, Department of Chemistry, University of Warsaw, Żwirki i Wigury 101, Warszawa, 02-089, Poland.*

kwozniak@chem.uw.edu.pl

Background. Water is an essential chemical compound for living organisms, and twenty of its different crystal solid forms (ices) are known. Still, there are many fundamental problems with these structures such as establishing the correct positions and thermal motions of

hydrogen atoms. The list of ice structures is not yet complete as DFT calculations have suggested existence for additional as of yet unknown phases. In many ice structures, neither neutron diffraction nor DFT calculations nor X-ray diffraction methods can easily solve the problem of hydrogen atom disorder or accurately determine their atomic displacement parameters.

Methods. We applied a new way of refinement of single crystal high pressure X-ray synchrotron and laboratory data called Hirshfeld Atom Refinement. This method utilizes aspherical atomic scattering factors and is especially effective in the case of refinement of crystals of H-rich compounds.

Results. Here we present accurate crystal structures of H₂O, D₂O and mixed (50%H₂O/50%D₂O) ice VI obtained by Hirshfeld Atom Refinement (HAR) against high pressure single crystal synchrotron and laboratory X-ray diffraction data. It was possible to obtain O-H bond lengths and anisotropic atomic displacement parameters for disordered hydrogen atoms which are in good agreement with the corresponding results of single crystal neutron diffraction data.

Conclusions. Our results show that Hirshfeld atom refinement against X-ray diffraction data is a tool which can compete with neutron diffraction in detailed studies of polymorphic forms of ice and crystals of other hydrogen rich compounds. As neutron diffraction is relatively expensive, requires larger crystals which might be difficult to obtain, and access to neutron facilities is restricted, cheaper and more accessible X-ray measurements combined with HAR can facilitate the verification of the existing ice polymorphs and the quest for the new ones.

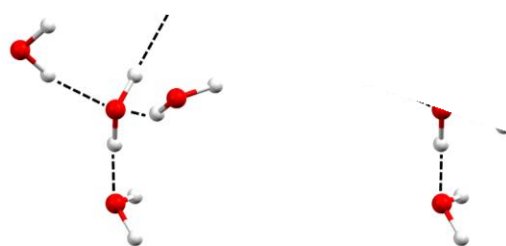


Fig. 1. Examples of water clusters considered.

References

[1] M. L. Chodkiewicz, R. Gajda, B. Lavina, S. Tkachev, V. B. Prakapenka, P. Dera, K. Woźniak, *Accurate crystal structure of ice VI from X-ray diffraction with Hirshfeld Atom Refinement*, IUCRJ, 2022, Submitted

Acknowledgements: Financial support of this work by the National Science Centre, Poland, through OPUS 21 grant number DEC-2021/41/B/ST4/03010 is gratefully acknowledged. The work was accomplished at the TEAM TECH Core Facility for crystallographic and biophysical

research to support the development of medicinal products sponsored by the Foundation for Polish Science (FNP). The synchrotron radiation experiments were performed at the APS (Proposal No. GUP-71134) and DESY (Proposal I-20200083 EC).

Rough diamond anvil: Critical microstructure, pressure-dependent yield surface of perfect plasticity, record low pressure for strain-induced α - ω transformation in Zr, and combined strain and time-controlled kinetics

F. Lin¹, V.I. Levitas^{1,2,3}, K.K. Pandey⁴, S. Yesudhas¹, C. Park⁵

¹*Department of Aerospace Engineering, Iowa State University, Ames, Iowa 50011, USA*

²*Department of Mechanical Engineering, Iowa State University, Ames, Iowa 50011, USA*

³*Ames Laboratory, U.S. Department of Energy, Iowa State University, Ames, Iowa 50011, USA*

⁴*High Pressure & Synchrotron Radiation Physics Division, Bhabha Atomic Research Centre, Mumbai 400085, India*

⁵*HPCAT, X-ray Science Division, Argonne National Laboratory, Argonne, Illinois 60439, USA*

Pressure dependence of yield strength is of great interest to material science and the geoscience community since processes involving high pressure, plastic deformation, and phase transformation (PT) are common in material synthesis and geodynamic activities. However, an easy and robust method for such measurement is lacking. This study introduces new rough diamond anvils (rDA), which drastically change the plastic flow, microstructure, and PT. Maximum friction equal to the yield strength in shear is achieved, which allows us to determine the pressure dependence of the yield strength. The first in-situ deformation experiment with rDA in DAC was performed on a heavily pre-deformed (after strain hardening saturation) commercial Zr sample to study the strain-induced PT kinetics, microstructure evolution, and yield strength of ω -Zr. Radial distribution of pressure, crystallite size, dislocation densities in phases, and phase volume fractions, all averaged over sample thickness, were measured with synchrotron diffraction in axial geometry. Sample thickness was measured using x-ray absorption. Different contact friction conditions at the sample-culet interface leads to various steady microstructures and the minimum pressure for strain-induced PT and PT kinetics. Steady microstructure in terms of constant crystallite size and dislocation density, which are independent of pressure, plastic strain and strain path, and crystallite size of α -Zr is reached immediately after completing α - ω PT. A record minimum pressure (0.67 GPa) for α - ω PT of Zr was identified, which is 9 times lower than under hydrostatic condition (6.0 GPa), 5.1 times lower than phase equilibrium pressure (3.4 GPa), and twice lower than the minimum pressure for strain-induced PT with traditional smooth diamond anvils (1.36 GPa). Such pressure is independent of plastic strain and

pressure-strain paths. While usually, the kinetics of strain-induced PT depends on plastic strain only, and time is not a parameter, here we found that the volume fraction of ω -Zr changes in time at fixed strain. Kinetics fitting also shows that the rate of PT is independent of the volume fraction of ω -Zr compared with a typical smooth diamond anvil experiment, which is due to a limited number of nuclei growth without interaction. Pressure distribution, crystallite size, and dislocation density evolution indicate that ω -Zr reached steady microstructure and behaves like perfectly plastic and isotropic with a plastic strain and strain path-independent yield surface of perfect plasticity immediately after PT, with the yield strength of ω -Zr $\sigma_y = 1.24 + 0.0965 p$ (GPa). Crystallite size and dislocation density evolution in ω -Zr during α - ω PT depend solely on the volume fraction of ω -Zr and are independent of plastic strain and its path and pressure. RDA allows us to in situ determine laws of plastic flow, microstructure, and PT evolution under high pressure and bring up new directions for microstructure formation and material synthesis via PT.

The behavior of simple molecule of bromine under high pressure high temperature conditions

O. Ibragimova, I. Chuvashova

Florida International University, Department of Chemistry and Biochemistry

The high-density fewer atoms' propellants are the most preferred for the aero-space industry because of its significant amount of heat impute and low mass. Although the high-density hydrogen is the best candidate for this role, its production and further study are complicated. Halogens, such as chlorine and bromine, have similar electron structure and could be used to study the behavior of simple molecules as they have similar molecular dissociation and metallization behavior.

Despite the fact that there are numerous studies devoted to the behavior of halogens under high pressure, no one has reported yet about high pressure high temperature phase transitions. Moreover, most of the publication are devoted to iodine which is not so high-reactive and volitive as bromine and chlorine, but has the lowest pressure (~ 15 GPa) for the first phase transition. Upon solidification halogens have the molecular orthorhombic structure (space group *Cmca*) that converts into atomic face-centered-cubic structure (*Immm*) with pressure increase. It is well-known that the laser heating of sample during the compression will help us to overcome the energy barrier of phase transition for elemental molecular compounds.

In this work bromine was studied at pressure range 5 GPa – 128 GPa by X-ray diffraction in a diamond anvil cell. The sample was heated up to 2700K after each pressure was reached. During the experiments we observed two irreversible phase transitions for bromine: at 15 GPa and 21 GPa. It is important to note that both of them happened while the sample was heated. The first phase transition was the recombination from orthorhombic $Cmca$ to monoclinic $C2/m$ structure. It didn't lead to a full transformation, so as a result we had a mixture of $Cmca$ and $C2/m$ after the heating. When we increased pressure further, during heating bromine converted partially into fcc structure $Immm$ and after the sample was cooled to ambient temperature, we recorded the presence of two phases: $Cmca$ and $Immm$. The current phase mixture with graduate prevalence of $Immm$ structure was observed until 96 GPa, when during the heating all remaining $Cmca$ converted to $Immm$.

To sum up, in this work we compressed bromine up to 128 GPa with laser heating. We observed several phase transitions and showed that bromine transition from molecular to monoatomic state goes through $C2/m$ phase which was not observed previously in the literature.

Strain-Induced Phase Transformations under High Pressure: Four-Scale Theory, Experiments, and Phenomena

Valery I. Levitas

*Iowa State University, Departments of Aerospace Engineering and Mechanical Engineering, Ames, Iowa, U.S.A.
Ames Laboratory, Division of Materials Science and Engineering, Ames, IA, USA*

vlevitas@iastate.edu

During compression in diamond anvil cell (DAC), materials undergo large plastic deformations, which cause growth of pressure and various phase transformations (PTs). Importantly, these PTs should be treated as strain-induced PTs under high pressure rather than pressure-induced PTs. Pressure- and stress-induced PTs occur by nucleation at pre-existing defects (e.g., dislocations) below the yield strength. Strain-induced PTs occur by nucleation at new defects generated during plastic flow. Strain-induced PTs require completely different thermodynamic and kinetic treatment and experimental characterization [1-3]. Superposition of plastic shear on high pressure in rotational DAC (RDAC) leads to numerous mechanochemical phenomena, including reducing PT pressure by one to two orders of magnitude and the appearance of new phases [1-6]. Thus, plastic shear reduced graphite-diamond PT pressure from 70 GPa to 0.7 GPa [5]. In situ XRD experiments [6] provide the

evolution of distributions of pressure and concentration of high-pressure phases, crystallite size, and sample thickness profile. PTs in Zr, BN, graphite, and Si are discussed. Four-scale theory was developed, and corresponding simulations were performed. Molecular dynamic [7,8] and first-principle [9] simulations were used to determine PT criteria under six components of stress tensor. At the nanoscale and microscale, nucleation at various evolving dislocation configurations was studied utilizing developed nanoscale [10,11] and scale-free [12] phase-field approaches. The possibility of reducing PT pressure by more than an order of magnitude due to stress concentration at the shear-generated dislocation pileups is proven. Strain-controlled kinetic equation was derived and utilized in the large-strain macroscopic theory for coupled PTs and plasticity. At the macroscale, the behavior of the sample in DAC/RDAC is studied using the finite element approach [13,14]. Various experimental effects are reproduced. The first experimental calibration and confirmation of the strain-controlled kinetics [1] were obtained for α - ω PT in Zr [6]. The obtained results offer a new fundamental understanding of strain-induced PTs under high pressure in DAC/RDAC and methods of controlling PTs and searching for new high-pressure phases and phenomena.

V.I. Levitas, *Phys Rev. B*, **70**, 184118 (2004).

V.I. Levitas, *Journal of Physics: Condensed Matter*, **30**, 163001 (2018).

V.I. Levitas, *Material Transactions*, **60**, 1294-1301 (2019).

C. Ji, V.I. Levitas, H. Zhu, J. Chaudhuri, A. Marathe, Y. Ma, *PNAS*, **109**, 191088 (2012).

Y. Gao, Y. Ma, Q. An, V.I. Levitas, Y. Zhang, B. Feng, J. Chaudhuri, W.A. Goddard III, *Carbon*, **146**, 364 (2019).

K. K. Pandey, V. I. Levitas. *Acta Materialia*, **196**, 338-346 (2020).

V.I. Levitas, H. Chen, L. Xiong, *Phys. Rev. Lett.*, **118**, 025701 (2017).

V.I. Levitas, H. Chen, L. Xiong, *Phys. Rev. B*, **96**, 054118 (2017).

N.A. Zarkevich, H. Chen, V.I. Levitas, D.D. Johnson, *Phys. Rev. Lett.*, **121**, 165701 (2018).

V.I. Levitas, M. Javanbakht, *Nanoscale*, **6**, 162 (2014).

M. Javanbakht, V.I. Levitas, *Phys. Rev. B*, **94**, (2016) 214104.

V.I. Levitas, S.E. Esfahani, I. Ghamarian, *Phys. Rev. Lett.*, **121**, 205701 (2018).

B. Feng, V.I. Levitas, *International Journal of Plasticity*, **96**, 156-181 (2017).

B. Feng, V.I. Levitas, W. Li, *International Journal of Plasticity*, **113**, 236-254 (2019).

An exploratory study of polymeric matter under high pressure

M. S. Klippel^{a*}; M. T. Orlando^b and M. F. Martins^a

^aLaboratory of Combustion and Combustible - PPGEM. ^bHigh Pressure Laboratory - Physics Department. Federal University of Espirito Santo, 514 Fernando Ferrari Av., Vitoria 29075-910, Brazil.

*Corresponding author e-mail: miriam.klippel@edu.ufes.br

The consequences of all the plastic discarded in inappropriate places still impose suffering on the planet. Pyrolysis can be a technique used to convert plastic waste into valuable products. However, due to insufficient heat transfer in pyrolytic reactors, it is possible to produce polymeric matter with a less molecular weight and low commercial value. This study investigated the influence of the high-pressure piston- cylinder cell (5 or 10 kbar at room temperature) on polymeric material to produce a value- added product. X-ray diffraction analysis (XRD) were carried out before and after the pressure treatments. All samples showed a predominance of amorphous structure. The results reveals that the increase in pressure indicate a reduction in the material's amorphous phase, suggesting that higher pressure may increase the crystalline phase of the polymeric material.

Experimental and theoretical study of β -As₂Te₃ under hydrostatic pressure

R. Vilaplana,^{1*} S. Gallego-Parra,² E. Lora da Silva,^{3,2} D. Martínez-García,⁴ G. Delaizir,⁵ A. Muñoz,⁶ P. Rodríguez-Hernández, V. P. Cuenca-Gotor,² J. A. Sans,² C. Popescu,⁷ A. Piarristeguy,⁸ and F. J. Manjón²

¹ Centro de Tecnologías Físicas: Acústica, Materiales y Astrofísica, MALTA Consolider Team, Universitat Politècnica de València, 46022 Valencia, Spain

²Institute of Physics for Advanced Materials, Nanotechnology and Photonics, Department of Physics and Astronomy, Faculty of Sciences, University of Porto, 4169-007 Porto, Portugal

³Instituto de Diseño para la Fabricación y Producción Automatizada, MALTA Consolider Team, Universitat Politècnica de València, 46022 Valencia, Spain

⁴Departamento de Física Aplicada – ICMUV, MALTA Consolider Team, Universitat de València, Burjassot, Spain

⁵ Institut de Recherche sur les Céramiques (IRCER), UMR CNRS 7315, Centre Européen de la Céramique, 87068 Limoges, France

⁶Departamento de Física, Instituto de Materiales y Nanotecnología, MALTA Consolider Team, Universidad de La Laguna, Tenerife, Spain

⁷ALBA-CELLS, Cerdanyola, E-08290 Barcelona, Spain

⁸ICGM, Univ Montpellier, CNRS, ENSCM, Montpellier, France

* Corresponding author e-mail: rovilap@fis.upv.es

We report a joint experimental and theoretical high-pressure structural and vibrational study of β -As₂Te₃; a polymorph of As₂Te₃ with tetradymite (*R-3m*) structure. This polymorph is isostructural with β -Bi₂Se₃, β -Sb₂Te₃, and β -Bi₂Te₃, which are topological insulators (TIs) at ambient conditions, and excellent thermoelectric materials near room temperature. It has been recently predicted that β -As₂Te₃ has an ultra-low lattice thermal conductivity at room pressure [1,2] and that it must undergo a pressure-induced topological quantum phase

transition (TQPT) around 2 GPa from a trivial semiconductor to a 3D topological Dirac semimetal with a single Dirac cone at the Γ point [2]. Moreover, it has been predicted that this compound is a TI above 2 GPa, whose bandgap increases above that pressure and decreases above 4 GPa leading to a metallization above 6 GPa [2].

Two types of samples have been characterized by angle-dispersive synchrotron powder X-ray diffraction and Raman scattering measurements under hydrostatic conditions with the help of *ab initio* calculations. One sample was synthesized at high pressure and high temperature conditions with a Paris-Edinburg cell and the other by the melt-quenching technique.

We provide the pressure dependence of the experimental and theoretical lattice parameters and unit-cell volume of β -As₂Te₃ as well as its zero-pressure axial compressibilities and bulk modulus that have been compared with isostructural sesquichalcogenides. A strong anisotropic compression is observed with a large decrease of the *c* lattice parameter up to 2 GPa and a minimum of the *c/a* ratio around 6.5 GPa. We have also provided the pressure dependence of the experimental and theoretical frequencies of the Raman-active modes of β -As₂Te₃ as well as their Grüneisen parameters, and linewidths. Again, changes in intensities and linewidths have been found near 2 and 6 GPa, respectively. All the changes in structural and vibrational parameters occurring at 2.0(2) and 6.0(5) GPa in β -As₂Te₃ suggest the presence of two isostructural phase transitions (IPTs) of electronic origin. The 1st IPT is related to the pressure-induced TQPT recently proposed to occur near 2 GPa that transforms β -As₂Te₃ from a trivial semiconductor to a 3D topological Dirac semimetal, unlike isostructural sesquichalcogenides. The 2nd IPT is related to the minimum observed in the *c/a* ratio and is also coincident with the closing of the bandgap, as recently proposed. Therefore, we ascribe this IPT to a pressure-induced insulator-metal transition. We have also identified by Le Bail analysis the onset of two first-order PT around 10 GPa and the onset of a 2nd PT around \sim 17.9 GPa. We have tentatively proposed that the 1st HP phase of β -As₂Te₃ has monoclinic *C2/m* structure. The recovery of both α -As₂Te₃ and β -As₂Te₃ on decreasing pressure from 18 GPa evidences the competitiveness of both polymorphs near room conditions. Additionally, we have found a high anharmonic behavior of the two Raman-active modes with lowest frequency in β -As₂Te₃ that is related to its already reported ultra-low lattice thermal conductivity. Moreover, we have studied the similarities of β -As₂Te₃ with α -Sb₂Te₃, and α -Bi₂Te₃, thus providing insights of the origin of the ultra-low lattice thermal conductivity values in these compounds in relation to the unconventional chemical bonds present in these isostructural materials.

[1] da Silva, E. L.; Leonardo, A.; Yang, T.; Santos, M.; Vilaplana, R.; Gallego-Parra, S.; Bergara, A.; Manjón, F. β -As₂Te₃: Pressure-induced three-dimensional Dirac semimetal with ultralow room-pressure lattice thermal conductivity. *J Physical Review B* **2021**, *104*, 024103.

[2] Vaney, J. B.; Crivello, J. C.; Morin, C.; Delaizir, G.; Carreaud, J.; Piarristeguy, A.; Monnier, J.; Alleno, E.; Pradel, A.; Lopes, E. B. Electronic structure, low-temperature transport and thermodynamic properties of polymorphic β -As₂Te₃. *RSC advances* **2016**, *6*, 52048-52057.

Kinetics of plastic strain induced $\alpha \rightarrow \omega$ phase transition in Zr_{2.5}Nb alloy

K. K. Pandey^{1*}, H. K. Poswal¹, Himani Bansal¹, Valery I. Levitas^{2,3}, Vivekanand Dubey⁴ and S. Roychowdhury⁴

¹High Pressure & Synchrotron Radiation Physics Division, Bhabha Atomic Research Centre, Mumbai-400085, India

²Iowa State University, Departments of Aerospace Engineering and Mechanical Engineering, Ames, Iowa 50011, U.S.A.

³Ames Laboratory, Division of Materials Science and Engineering, Ames, IA, USA

⁴Materials Processing and Corrosion Engineering Division, Bhabha Atomic Research Centre, Mumbai-400085, India

*kkpandey@barc.gov.in

Zr, being relatively transparent to neutrons, is an important material for nuclear reactors. Alloying with Nb significantly improves its mechanical and corrosion resistance properties and make it a suitable structural material for nuclear reactors [1-3]. It has been shown that in case of pure Zr, severe plastic straining can bring down the $\alpha \rightarrow \omega$ phase transition pressure by nearly a factor of 4.5 as compared to hydrostatic compression [4]. Nb, being a β phase stabiliser, is expected to further reduce the transition pressure if we consider Usikov/Zilbershtein pathway [5] of transformation through intermediate β phase. In fact, some high pressure torsion (HPT) studies show presence of $\beta + \omega$ phases after HPT treatment [6,7]. Hence, to study the effect of Nb alloying on the kinetics of $\alpha \rightarrow \omega$ phase transition in Zr, we carried out a systematic in situ study on Zr_{2.5}Nb alloy under severe plastic straining. For these studies, thin Zr_{2.5}Nb alloy sheets (~ 150 μ m thick) were prepared through cold rolling from initial ~ 4 mm thick sheet down to ~ 300 μ m (to obtain saturated hardness in sample) and subsequent polishing. For in situ studies, these sheets were subjected to severe plastic straining in diamond anvil cell under different load conditions. At each load condition, diffraction patterns were recorded across anvil entire culet (200 μ m diameter) in steps of 10 μ m. The measurements were carried out at BL-11 [8] at Indus-2 synchrotron source with micro-focused X-rays ($\lambda = 0.5509 \text{ \AA}$; FWHM ~ 8 μ m). We also carried out high-pressure experiments on Zr_{2.5}Nb alloy under hydrostatic loading. Our studies show only irreversible $\alpha \rightarrow \omega$ phase transition in both the cases. We did not observe any significant presence of β phase at ambient conditions as well as at high pressures, detectable through XRD measurements. Our hydrostatic high-pressure studies show an increase of ~ 2 GPa in $\alpha \rightarrow \omega$ phase transition pressure in Zr_{2.5}Nb alloy to 7.4 GPa as compared to pure Zr. Under plastic straining $\alpha \rightarrow \omega$ phase transition initiates at ~ 2.3 GPa which is ~ 1 GPa higher than that in case of pure Zr. The theoretically predicted plastic strain- controlled kinetic equation [9] was quantified for the $\alpha \rightarrow \omega$ phase transition pressure in Zr_{2.5}Nb alloy and found to be slower than that in case of pure Zr. We also estimated pressure dependent elastic properties and

yield strengths of both the phases of Zr. Such studies help establish methodology for material investigations under any complex load-shear pathways.

References

- R. Krishnan and M. K. Asundi, *Proc. Indian Acad. Sci. (Engg. Sci.)* 4, 1, 41-56 (1981).
N. M. Beskorovainyi, B. A. Kalin, P. A. Platonov, and I. I. Chernov. *Structural materials for nuclear reactors, Energoatomisdat, Moscow*, (1995).
[3] L. B. Zuev, B. S. Semukhin and S. Y. Zavodchikov, *Mater. Lett.*, 57, 1015–1020 (2005).
K. K. Pandey and V. I. Levitas; *ActaMat.* 196, 338-346 (2020)
M. P. Usikov, V. A. Zilbershtein, *Phys. Stat. Sol. (A)* 19, 53 (1973).
Alexander P. Zhilyaev, Alfred V. Sharafutdinov and M. Teresa Perez-Prado, *Advanced Engineering Materials*, 12, No. 8 (2010).
Boris B. Straumal, Alena S. Gornakova, Olga B. Fabrichnaya, Mario J. Kriegel, Andrey A. Mazilkin, B. Baretzky, A. M. Gusak and S. V. Dobatkin, *High Temp. Mater. Proc.*, Vol. 31, 339–350 (2012).
[8] K. K. Pandey et al. *Pramana* 880 (4), 607-619 (2013).
[9] V. I. Levitas, *Physical Review B* 70, 184118 (2004).
-

Record Low Transformation Pressure and New Phase Transformation Sequence in Nano-Si under Plastic Compression

Sorb Yesudhas^{1*}, Feng Lin¹, Krishan Kumar Pandey², Jesse Smith³ and Valery I. Levitas^{1*}

¹Department of Aerospace Engineering, Iowa State University, Ames, Iowa, 50011 USA ²High Pressure & Synchrotron Radiation Physics Division, Bhabha Atomic Research Center, Mumbai 400085, India

³HPCAT, X-ray Science Division, Advanced Photon Source, Argonne National Laboratory, Lemont, IL 60439 USA

*Corresponding author: sorbya@iastate.edu, vlevitas@iastate.edu

There is a significant difference between phase transformations (PTs) under hydrostatic compression (pressure-induced PTs) and plastic strain-induced PTs that occur during plastic flow under compression without pressure transmitting medium (PTM) [1,2]. Since the pressure-induced PTs start due to the nucleation at pre-existing defects and the plastic strain-induced PTs occur at new defects that appear during plastic flow, the materials exhibit very different behavior under plastic compression. The compression of samples under plastic strain not only reduces the PTs pressures drastically but also provides a new avenue to explore hidden phases, which cannot be obtained under hydrostatic compression. The plastic strain-induced PTs require completely different experimental characterization and thermodynamic and kinetic description.

High-pressure synchrotron X-ray diffraction (HPXRD) studies were conducted on 100 nm size Si powder loaded in Cu gaskets under compression without any PTM. The HPXRD studies were carried out at 16-ID-B beamline at HPCAT, Advanced Photon Source, Argonne, with X-ray wavelength, $\lambda = 0.4066 \text{ \AA}$. The XRD patterns were collected along two diameters

of the culet with a step size of 10 μm under varying loads and anvil rotation angles. Pressure at each point of the sample in each phase was determined using equations of state of Si phases obtained using He PTM. The XRD patterns were refined using GSAS II software to extract the lattice parameters, volume fractions of phases, and texture by the Rietveld refinement method. High-pressure synchrotron XRD studies on 100 nm Si under hydrostatic compression exhibit the following phase

transformation sequence: Si-I (S.G: $Fd\bar{3}m$) to Si-II (S.G: $I4_1/amd$) to Si-XI (S.G: $Imma$) and Si-V (S.G: $P6/mmm$) below 30 GPa. The plastic strain-induced PTs show different PT sequences: Si-I to Si-II to Si-III (S.G: $Ia\bar{3}$) to Si-XI, and Si-V below 30 GPa. The Si-I to Si-II transition pressure of 100 nm Si is observed to be reduced drastically from 16 GPa to 0.5 GPa by a factor of 32. The distribution of lattice parameters and volume fractions of Si phases were calculated along the sample diameter. In contrast to hydrostatic compression, the Si-I, Si-II, and Si-XI phases are coexisting in a wide range of pressures under plastic compression.

Acknowledgments

We thank National Science Foundation (CMMI-1536925 & DMR-1904830).

References

- V. I. Levitas, Material Transactions, 60, 1294 (2019).*
V. I. Levitas, Physical Review B, 70, 184118 (2004).

Far Infrared Study of Pressure-Tunable Fano Resonance and Metallization Transition in semiconducting Transition Metal Dichalcogenides

Elena Stellino

Background

Transition Metal Dichalcogenides (TMDs) are 2D crystals that exhibit a graphene-like structure, with strong intra-layer covalent bonds and weak van der Waals (vdW) forces between planes.

The application of pressure provides an effective way to modulate the interaction between adjacent layers, allowing getting a deeper insight into the fundamental physics of these materials and paving the way for new technological applications. Pressure-dependent studies have found that most of semiconducting TMDs undergo a pressure-induced transition toward a metallic state [1,2,3,4].

However, a certain ambiguity still exists in the determination of the metallization pressure and in the explanation of the microscopic origin of the transition.

Methods

In our work, we address the unsolved mechanism of the metallic transition in TMDs studying, by synchrotron-based far-infrared (FIR) spectroscopy, the pressure-induced changes in the optical response of MoTe₂, MoS₂, WS₂. We found that the FIR spectrum provides us with two descriptors indicating the onset of the metallic behaviour and the origin of the free carriers formed in the process. The first one is the absorbance spectral weight (SW), whose abrupt increase under pressure can be related to the increase in the carrier density. The second one is the Fano lineshape of the E_{1u} vibrational mode, symptomatic of the coupling between the phonon and a continuum of electronic transitions with comparable energies. These transitions cannot originate from a valence-to-conduction-band excitation, which is too energetic for the phonon to couple with, but they reasonably occur from doping levels in the proximity of the conduction band. The evolution of the phonon profiles gives us a unique benchmark to evaluate the response of these doping states to the applied pressure and represents the first case of pressure-tunable Fano resonance reported for TMD semiconductors.

Results and conclusion

In all the considered samples, the SW and the Fano asymmetry parameter remain almost constant below the metallization threshold. Then, as the SW increases, we observe an abrupt symmetrization in the E_{1u} peak.

Our idea is that the metallic behaviour observed in the considered crystals arises from the pressure-induced reduction of the energy separation between conduction band and doping levels. As this separation goes to zero, the free carrier density increases and no more direct electronic transitions from inter-band states are available for the phonon to couple with, suppressing the electron-phonon coupling mechanism of the Fano resonance. Interestingly, this process is completely uncorrelated with the closure of the *standard* band-gap, which occurs at higher pressures, as reported by near infrared measurements from the literature [4].

Our results shed light on the key role played by intrinsic defects in the TMD electronic response under pressure, allowing us to frame a coherent scenario for the metallization process in this class of semiconductors.

References

- [1] Zhao *et al.*, *Phys. Rev. B* 99, 024111, 2018
- [2] Nayak *et al.*, *Nat. Commun.* 5, 3731, 2014
- [3] Nayak *et al.*, *ACS Nano*, 9, 9, 9117–9123, 2015
- [4] Brotons-Gisbert *et al.*, *Phys. Rev. Materials* 2, 054602, 2018

Understanding the behaviour of spin crossover materials for barocaloric applications: (P,T) phase diagrams

P. Rosa^{1*}, M. Marchivie¹, P. Guionneau¹, B. Vignolle¹, J.-P. Itié²

¹ICMCB, Bordeaux Institute of Condensed Matter Chemistry, CNRS-University of Bordeaux, Pessac, France

²Synchrotron SOLEIL, L'Orme des Merisiers Saint-Aubin, Gif-sur-Yvette, France

Keywords: spin crossover, phase diagrams, barocalorics

*e-mail: patrick.rosa@icmcb.cnrs.fr

Climate change preoccupations motivates researching alternatives to energy-intensive vapor-compression thermodynamic machines, which use gases with tremendous greenhouse effect and are of limited thermodynamic efficiency. Roughly 3 billion systems (refrigeration, air-conditioning, heat pumps) consume roughly about 1/6th of the whole global electricity production, with greenhouse gas emissions equivalent to the whole EU emissions.^[1] The mechanocaloric effect, which refers to adiabatic temperature changes induced by stress or pressure, is one of the most promising energy-saving new technology for cooling systems. Mechanocaloric research produced in the last decade highly performing materials, overcoming easily electrocaloric and magnetocaloric materials.^[2] Most interestingly, mechanocaloric materials use non-critical, cheap, abundant and non-toxic elements. In 2016 a milestone paper identified molecular Spin CrossOver (SCO) complexes as showing promising mechanocaloric potential.^[3] Following papers evidenced large to colossal barocaloric effects around the SCO temperatures,^[4] which were reviewed recently in a very favourable light as compared to other materials being investigated.^[5] Indeed SCO corresponds to a stimulus-induced ($T, P, \text{light}, \dots$) electronic configuration change, leading to a switch of optical/magnetic/electronic/structural properties concomitant with configurational, magnetic and phonon entropy changes^[6] that may be sensitive to very small pressure perturbations of a few kilobars or even less.

Understanding the properties of such systems is crucial for the design of improved systems. To do so it is most informative to cross data gathered from structural determinations under varied conditions (temperature, light irradiation or pressure) and properties determination under similar conditions (magnetism, spectroscopy, ...). We will present studies on two spin crossover complexes. SCO compounds show a change of spin state under application of such external stimuli, change that goes together with modification of the population of molecular orbitals, with anti-bonding orbitals corresponding to longer metal-ligand bond lengths being populated in the High Spin (HS) state. Pressure is thus naturally one of the relevant thermodynamic constraints to consider: in SCO materials based on Fe^{2+} (d^6) ions, it usually favors the diamagnetic low-spin (LS) state, which has a lower volume than the paramagnetic HS state. Diffraction studies, on single crystals or polycrystalline powder, are a powerful tool to study and understand the nature of the species observed when combining pressure and temperature changes, allowing the mapping of the phase diagram of those complexes.

- [1] D. Coulomb et al., *IIR Inf.* **2017**, 17.
[2] L. Mañosa et al. *Appl. Phys. Lett.* **2020**, 116, 050501.
[3] K. G. Sandeman *APL Mater.* **2016**, 4, 1.
[4] P. J. Von Ranke *Appl. Phys. Lett.* **2017**, 110, 18. P. J. Von Ranke et al. *Phys. Rev. B* **2018**, 98, 224408. S. P. Vallone et al. *Adv. Mater.* **2019**, 31, 1.
[5] P. Loveras, J.-L. Tamarit *MRS Energy&Sustainability* **2021**, 8, 3.
[6] W. Nicolazzi et al., *Comptes Rendus Chim.* **2018**, 21, 1060.
-

Boron and Nitrogen Dopants Enhanced Stability of Diamane Induced by High Pressure

Caoping Niu^{1,2}, Xianlong Wang^{1,2,*}

¹*Institute of Solid State Physics, Hefei Institutes of Physical Science, Chinese Academy of Science, Hefei 230031, China*

²*University of Science and Technology of China, Hefei 230026, China*

*Email: xlwang@theory.issp.ac.cn

Formation of sp^3 bonds between bi-layer graphene could give rise to a single-layer diamond, named as diamane. Diamane is expected to be a new carbon based 2D material with excellent properties, which combines the characteristics of both graphene and diamond. However, diamane synthesized through high-pressure methods cannot be maintained under ambient conditions. Based on first-principles methods, we studied the structural stability and electronic properties of B-doped, N-doped and B-N-codoped cubic and hexagonal diamane. B atom tends to stay at internal substitutional site, while N atom tends to stay at external substitutional site without H saturation. More importantly, the doped N atom in B-N co-doped diamane tends to be passivated by H because of the reduced stability of a lone pair of electrons affected by the B dopant. The bandgap of doped diamane is adjustable, depending on the distribution of doped atoms, which can be potentially applied to two-dimensional electronic devices. The B dopant, N dopant, and B-N co-dopant can reduce the FE and promote synthesis of diamane. Diamane containing a vertical B-N bond has the lowest FE, while the FE of diamane doped with N atoms is not sensitive to the distribution of the N dopant, which may be easy to achieve experimentally. This work provides a way for high-pressure synthesis of diamane, which maybe stable at ambient pressure.

Key Words: First-principles; Diamane; Dopants

Reference:

C. Niu, Y. Cheng, K. Yang, J. Zhang, H. Zhang, Z. Zeng, and X. Wang*, *Boron-dopant enhanced stability of diamane with tunable band gap*, *J. Phys.: Condens. Matter*, 32, 135503 (2020)

C. Niu, J. Zhang*, H. Zhang, J. Zhao, W. Xia, Z. Zeng, and X. Wang*, *Configuration stability and electronic properties of diamane with boron and nitrogen dopants*, *Phys. Rev. B*, 105, 174106 (2022)

High pressure Raman study of ternary tin dichalcogenides, $\text{SnS}_x\text{Se}_{2-x}$

N. Sorogas^{1,*}, A.N. Anagnostopoulos¹, K. Papagelis¹, D. Christofilos², and J. Arvanitidis¹

¹Physics Department, Aristotle University of Thessaloniki, 54124 Thessaloniki, Greece

²School of Chemical Engineering and Laboratory of Physics, Faculty of Engineering, Aristotle University of Thessaloniki, 54124 Thessaloniki, Greece

Tin-based chalcogenides are promising candidates for various applications in thermoelectrics, photodetectors, gas sensors, supercapacitors, solar cells and electrocatalysts, owing to their important electronic, optical and thermal properties [1]. Semiconducting SnS_2 and SnSe_2 dichalcogenides and their alloys usually crystallize in the hexagonal CdI_2 -type crystal structure, in which the covalently bonded S(Se)-Sn-S(Se) layers are stacked through van der Waals interactions, having thus anisotropic properties and permitting new two-dimensional systems by mechanical exfoliation [2]. Upon pressure application, they undergo significant changes in their structural and electronic properties, exhibiting new superconducting, charge density wave or topologically non-trivial phases [3]. In this work, the hydrostatic pressure response of the phonon modes of ternary $\text{SnS}_x\text{Se}_{2-x}$ ($x=0.6,0.8,1$) alloys, grown by the Bridgman technique [2], has been studied by means of Raman spectroscopy (LabRAM-HR spectrometer, $\lambda_{\text{exc}}=514$ nm). High pressure (up to 8 GPa) was generated using a gas membrane-type diamond anvil cell and the 4:1 methanol-ethanol mixture was used as the pressure transmitting medium.

Owing to the two-mode behaviour of the E_g and A_{1g} modes in the ternary dichalcogenide alloys [4], four Raman bands are observed at ambient conditions and the frequency evolution of the three $\{E_g(\text{SnSe}_2\text{-like}), A_{1g}(\text{SnSe}_2\text{-like})$ and $A_{1g}(\text{SnS}_2\text{-like})\}$ was followed with pressure. Upon pressure application, all Raman peaks shift quasi-linearly to higher frequencies due to the volume reduction and the bond stiffening. The pressure coefficient of the $A_{1g}(\text{SnS}_2\text{-like})$ peak frequency increases gradually from 3.60 to 3.93 $\text{cm}^{-1}\text{GPa}^{-1}$ with increasing S content, x . These values are compatible with those reported in the literature for the binary SnS_2 [5]. At the same time, the pressure coefficient of the $A_{1g}(\text{SnSe}_2\text{-like})$ peak frequency decreases from

3.08 to 2.72 $\text{cm}^{-1}\text{GPa}^{-1}$ with x , being always larger than that observed for the binary SnSe_2 [5]. Furthermore, despite the strong covalent bonding in the ab plane compared to the weak van der Waals interactions along the c -axis, the in-plane $E_g(\text{SnSe}_2\text{-like})$ mode exhibits larger pressure coefficient than those of the A_{1g} modes along the c -axis in all the studied alloys. The Grüneisen parameters were deduced for the $A_{1g}(\text{SnS}_2\text{-like})$: 0.35, 0.34, 0.36 and the $A_{1g}(\text{SnSe}_2\text{-like})$ mode: 0.44, 0.41, 0.37 for $x=0.6, 0.8$ and 1, respectively. These values suggest the stronger Sn-S interaction along the c -axis compared to the Sn-Se one in the ternary alloys, compatible with the decrease of the lattice constants on going from SnSe_2 to SnS_2 [6].

References

- [1] M. Kumar et al., *AIP Adv.* **11**, 025040 (2021).
M.M. Gospodinov et al., *Mater. Res. Bull.* **38**, 177 (2003).
G.P. Kafle et al., *J. Mater. Chem. C* **8**, 16404 (2020).
[4] V.G. Hadjiev et al., *Phys. Rev. B* **87**, 104302 (2013).
S.V. Bhatt et al., *Solid State Commun.* **201**, 54 (2015).
F.A.S. Al-Alamy and A.A. Balchin, *J. Cryst. Growth* **38**, 221 (1977).

*nsorogka@physics.auth.gr

Structural and electronic phase transitions in $\text{Zr}_{1.03}\text{Se}_2$ at high pressure

Bishnupada Ghosh, Mrinmay Sahu, Debabrata Samanta, Pinku Saha, Anshuman Mondal and Goutam Dev Mukherjee

National Center for High Pressure Studies, Indian Institute of Science Education and Research Kolkata

Backgrounds: Transition-metal dichalcogenides (TMDs) have been intensively studied over the past decades and have attracted huge attention for many applications in optoelectronic materials, data storage devices, sensors, spintronics, etc. [1, 2]. ZrSe_2 and HfSe_2 semiconductors have band gap values similar to silicon ranging from 0.9 to 1.2 eV, and can be a suitable replacement in the field of electronic devices [3]. The effect of strain on the structural and electronic properties of these materials is a matter of concern nowadays. Here we have studied the structural as well as electronic properties of $\text{Zr}_{1.03}\text{Se}_2$ at high pressures.

Methods: A piston cylinder-type diamond anvil cell having a 300 μm culet diameter is used to generate high pressure. We have performed high-pressure XRD measurements on $\text{Zr}_{1.03}\text{Se}_2$ up to 30.9 GPa at the ELETTRA synchrotron center, using an X-ray having a wavelength of 0.4957

Å. We have also carried out Raman spectroscopic measurements up to 34.1 GPa using a micro Raman facility, using 532 nm laser as the excitation source. To know how the electronic properties evolve with pressure, low temperature resistivity measurements using four probe technique at ambient as well as selected high-pressure points are performed. A closed cycle cryostat is used to vary the sample temperature from room temperature to 22K.

Results and Conclusions: The ambient XRD pattern is indexed to a 1T structure. The high pressure XRD study (Fig.1) shows a gradual structural phase transition from the ambient 1T phase to a monoclinic phase starting at 5.9 GPa and completing at around 14.8 GPa. Above 14.8 GPa the structure remains monoclinic up to the highest pressure of this study. In the intermediate pressure region, a mixed phase exists. The Raman spectra also show the appearance of new Raman modes above 5.9 GPa, which may be due to the change in symmetry associated with the structural transition.

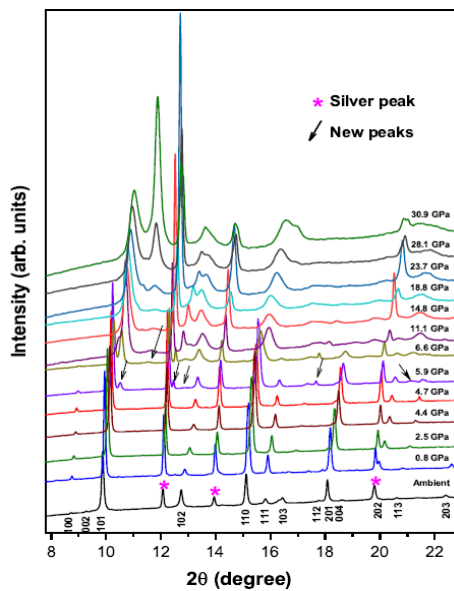


Fig1: Pressure evolution of XRD patterns of $Zr_{1.03}Se_2$

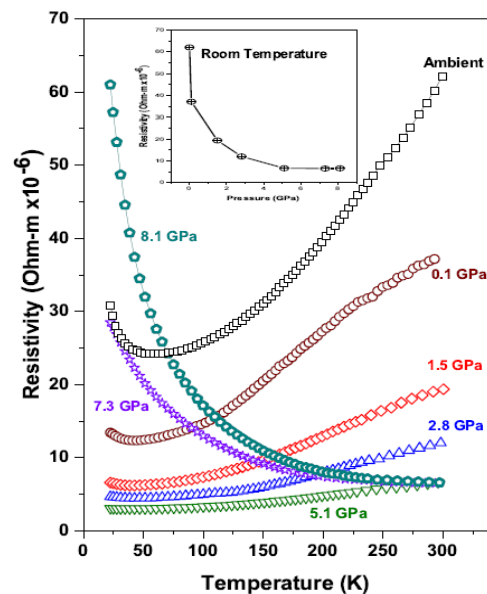


Fig2: Low T resistivity of $Zr_{1.03}Se_2$ at selected high pressure points

$ZrSe_2$ is reported as an indirect band gap semiconductor. The temperature variation of resistivity of $Zr_{1.03}Se_2$ (Fig.2) reveals a metallic character at ambient pressure due to the presence of excess Zr in the sample. At low temperatures, the $\rho(T)$ shows an upturn indicating a possibility of the Kondo effect resulting from the magnetic impurities associated with excess Zr. Above 5.1 GPa, the temperature-dependent resistivity data show that in the mixed phase, a small band gap opens in the sample resulting in a pressure-induced metal to semiconductor transition.

Reference:

[1] S. U. Rehman and Z. Ding, *Phys. Chem. Chem. Phys.* 20, 16604 (2018).

[2] Q. Song, H. Wang, X. Pan, X. Xu, Y. Wang, Y. Li, F. Song, X. Wan, Y. Ye, and L. Dai, *Sci. Rep.* 7, 1 (2017).

[3] M. Salavati, *Front. Struct. Civ. Eng.* 13, 486 (2019).

Evidence of Si-II to Si-I reversible phase transformation and retaining of Si-II under ambient pressure after plastic shear under pressure

Sorb Yesudhas^{1*}, Feng Lin¹, Krishan Kumar Pandey², Maddury Somayazulu³ and Valery I. Levitas^{1*}

¹Department of Aerospace Engineering, Iowa State University, Ames, Iowa, 50011 USA ²High Pressure & Synchrotron Radiation Physics Division, Bhabha Atomic Research Center, Mumbai 400085, India

³HPCAT, X-ray Science Division, Advanced Photon Source, Argonne National Laboratory, Lemont, IL 60439 USA

*Corresponding author: sorbya@iastate.edu, vlevitas@iastate.edu

Silicon exhibits a complex phase transformation sequence under compression and decompression. With compression, Si adopts the following phase transformations (PTs) sequence: Si-I (cubic, S.G: $Fd\bar{3}m$), Si-II (tetragonal, S.G: $I41/amd$), Si-XI (orthorhombic, S.G: $Imma$), and Si-V (hexagonal, S.G: $P6/mmm$) below 30 GPa. Upon decompression, depending on the decompression rates, it exhibits different phase transformation paths. Upon slow decompression, Si stabilizes in Si-III (S.G: $Ia\bar{3}$) phase via an intermediate high-pressure Si-XII (S.G: $R\bar{3}$) phase. Reversibility of the Si-I and Si-II phases has never been achieved before and is remaining to be a longstanding puzzle. Also, the reverse phase transformation from high pressure never resulted in residual Si-II. Since the pressure-induced PTs appear due to the nucleation at pre-existing defects whereas the strain-induced PTs happen because of nucleation at new defects that appear during plastic flow, therefore, the materials exhibit very different behavior under plastic compression. The plastic strain-induced PTs differ qualitatively from pressure- and stress-induced transformations and require completely different experimental characterization and thermodynamic and kinetic description [1,2]. High-pressure synchrotron X-ray diffraction (HPXRD) studies were conducted on 100 nm size Si powder loaded in Cu gaskets under compression without any PTM. The HPXRD studies were carried out at 16-ID-B beamline at HPCAT, Advanced Photon Source, Argonne, with X-ray wavelength, $\lambda = 0.4066 \text{ \AA}$. The XRD patterns were collected along the sample radius under the continuous rotation of one of the anvils at the rate of 60 minutes per rotation. Pressure at each point of the sample in each phase was determined using equations of state of Si phases obtained using He PTM.

Initially, the sample was pressurized up to 0.5 GPa and shear was developed on the sample by continuous anvil rotation until a significant proportion of Si-II was achieved. The XRD

pattern collected along the pressure-released sample showed a complete reversible phase transformation from Si-II to Si-I. In another run, the sample was pressurized up to the initiation of the Si-II phase transformation at 1.6 GPa. The shear was developed on the sample up to 5.6 GPa. A coexistence of Si-I, Si-II, and Si-III phases was achieved, and the pressure was released to the ambient pressure. The XRD patterns of the pressure-released sample show the coexistence of Si-I and Si-III phases. Interestingly, in some regions, Si-I and Si-II phase coexistence was achieved, i.e., Si-II was retained as a metastable phase at ambient pressure.

Acknowledgments

We thank National Science Foundation (CMMI-1536925 & DMR-1904830).

References

- V. I. Levitas, *Material Transactions*, **60**, 1294 (2019).
V. I. Levitas, *Physical Review B*, **70**, 184118 (2004).

Microstructural evolution across $\alpha \rightarrow \omega$ phase transition in Zr under hydrostatic compression

K. K. Pandey^{1*}, Valery I. Levitas^{2,3#}, Changyong Park⁴, and Guoyin Shen⁴

¹High Pressure & Synchrotron Radiation Physics Division, Bhabha Atomic Research Centre, Mumbai-400085, India

²Iowa State University, Departments of Aerospace Engineering and Mechanical Engineering, Ames, Iowa 50011, U.S.A.

³Ames Laboratory, Division of Materials Science and Engineering, Ames, IA, USA

⁴High Pressure Collaborative Access Team, X-ray Science Division, Argonne National Laboratory, Argonne, IL, 60439 USA

*kkpandey@barc.gov.in; #vlevitas@iastate.edu

Pressure-induced phase transformations (PTs) are initiated by nucleation at pre-existing defects (e.g., dislocations) below the yield [1-3], which implies a key role of initial microstructure in the evolution of high-pressure PTs. This becomes particularly important for metallic systems, for which non-directional metallic bonding character makes them more prone to such defects under various mechanical processing treatments used for sample preparation. This could be one of the reasons for large scatter in PT initiation pressure in same material by different researchers [4-7]. The effect of initial microstructure and its

evolution across the $\beta\beta\beta$ phase transition in commercially pure Zr under hydrostatic compression has been studied using in situ x-ray diffraction measurements. Two samples were studied: strongly plastically pre-deformed Zr with saturated hardness and annealed. Phase transformation $\beta\beta\beta$ initiates at higher pressure for annealed sample, i.e., pre-straining promotes nucleation by producing more and stronger stress concentrators (various dislocation configurations, twins, etc). With PT progress, promoting effect of prestraining reduces with crossover to suppressing. This suggests that pre-straining suppresses growth by producing more obstacles (dislocation forest, point defects, domain and grain boundaries) for interface propagation. The crystal domain size reduces and microstrain and dislocation density increase during loading of both β and $\beta\beta$ phases in the single-phase regions. For β phase, domain size are much lower for prestrained Zr, while microstrain and dislocation density are much larger. At the same time, they do not differ much in β -Zr, implying that microstructure is not inherited during PT. This may happen if moving $\beta\beta\beta$ interfaces sweep away the entire microstructure (domains and dislocations) in the β phase and new domains and dislocations are formed in the β -Zr. A simple model for the initiation of the PT involving microstrain and for the growth stage is suggested. The obtained results initiate the experimental basis for future predictive structural models for the pressure-induced PTs, and combined pressure- and strain-induced PTs.

References

- V. I. Levitas, *Physical Review B* 70, 184118 (2004).
V. I. Levitas, *Journal of Physics: Condensed Matter*, 30, 163001 (2018).
V. I. Levitas, *Material Transactions*, 60, 1294-1301 (2019).
[4] A. P. Zhilyaev et al., *Mat. Sci. Eng. A*, 528, 3496-3505 (2011).
N. Velisavljevic et al., *J. Phys.: Condens. Matter* 23, 125402 (2011).
M. T. Perez-Prado and A. P. Zhilyaev, *PRL*, 102, 175504 (2009).
B. Srinivasarao, A. P. Zhilyaev and M. T. Perez-Prado, *Scr. Mat.*, 65, 241-244 (2011).